HEI
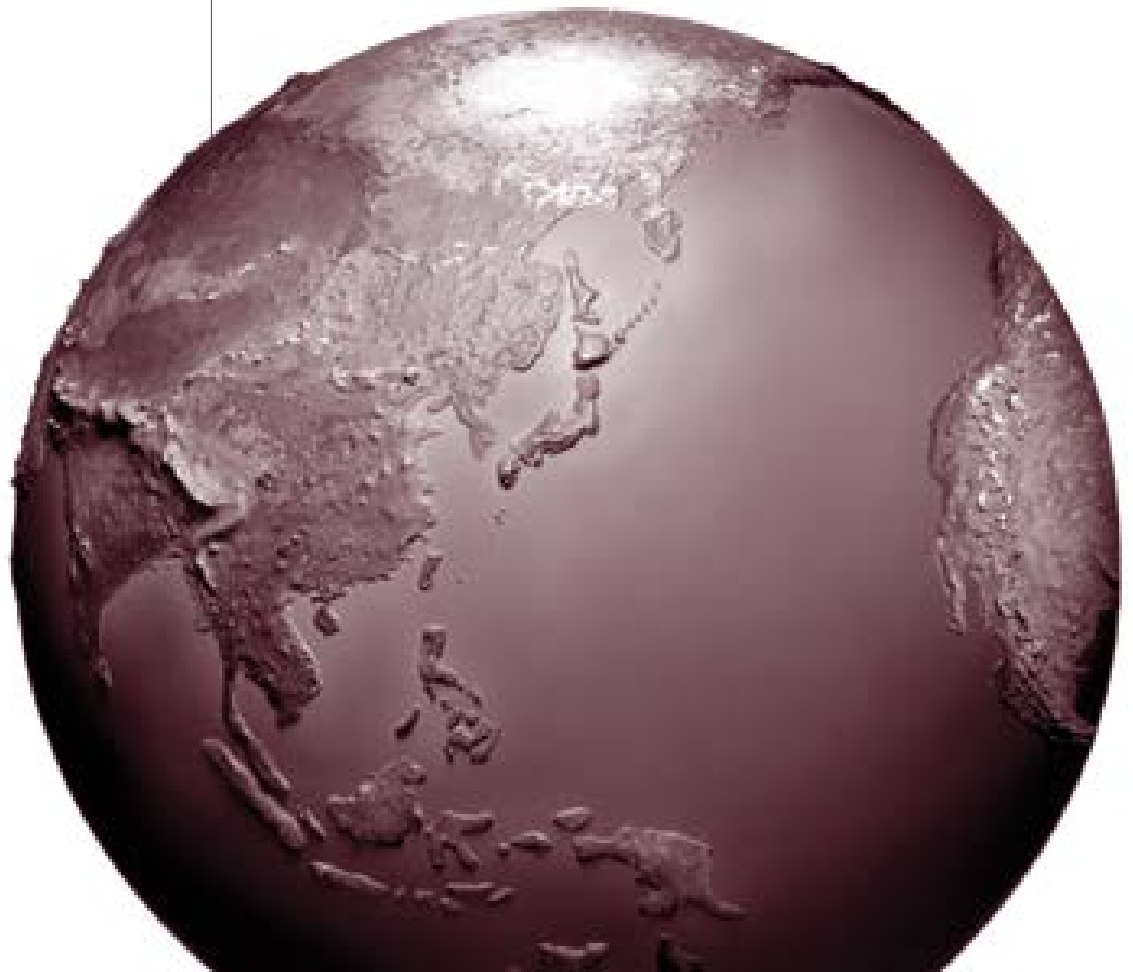
HEALTH EFFECTS INSTITUTE

December 2019

Impacts of Shipping on Air Pollutant Emissions, Air Quality, and Health in the Yangtze River Delta and Shanghai, China

Yan Zhang, Junlan Feng, Cong Liu, Junri Zhao, Weichun Ma, Cheng Huang, Jingyu An, Yin Shen, Qingyan Fu, Shuxiao Wang, Dian Ding, Wangqi Ge, Freda Fung, Kethural Manokaran, Allison P. Patton, Katherine D. Walker, and Haidong Kan

Impacts of Shipping on Air Pollutant Emissions, Air Quality, and Health in the Yangtze River Delta and Shanghai, China

Yan Zhang, Junlan Feng, Cong Liu, Junri Zhao, Weichun Ma, Cheng Huang, Jingyu An, Yin Shen, Qingyan Fu, Shuxiao Wang, Dian Ding, Wangqi Ge, Freda Fung, Kethural Manokaran, Allison P. Patton, Katherine D. Walker, and Haidong Kan

Special Report 22

Health Effects Institute

Boston, Massachusetts

Trusted Science • Cleaner Air • Better Health

CONTENTS

ABOUT HEI

The Health Effects Institute is a nonprofit corporation chartered in 1980 as an independent research organization to provide high-quality, impartial, and relevant science on the effects of air pollution on health. To accomplish its mission, the institute

- Identifies the highest-priority areas for health effects research;

- Competitively funds and oversees research projects;

- Provides intensive independent review of HEI-supported studies and related research;

- Integrates HEI's research results with those of other institutions into broader evaluations; and

- Communicates the results of HEI's research and analyses to public and private decision makers.

HEI typically receives balanced funding from the U.S. Environmental Protection Agency and the worldwide motor vehicle industry. Frequently, other public and private organizations in the United States and around the world also support major projects or research programs. HEI has funded more than 340 research projects in North America, Europe, Asia, and Latin America, the results of which have informed decisions regarding carbon monoxide, air toxics, nitrogen oxides, diesel exhaust, ozone, particulate matter, and other pollutants. These results have appeared in more than 260 comprehensive reports published by HEI, as well as in more than 1,000 articles in the peer-reviewed literature.

HEI's independent Board of Directors consists of leaders in science and policy who are committed to fostering the public–private partnership that is central to the organization. For this report, the draft final report was reviewed by independent external peer reviewers, who were selected by HEI for their expertise.

All project results are widely disseminated through HEI's website (*www.healtheffects.org*), printed reports, newsletters and other publications, annual conferences, and presentations to legislative bodies and public agencies.

CONTRIBUTORS

PEER REVIEWERS

Simon Ng, *Director, Policy and Research, Business Environment Council, Hong Kong, China*

Hugo Denier van der Gon, *Senior Scientist, Climate, Air and Sustainability, TNO (Netherlands Organisation for Applied Scientific Research), Utrecht, The Netherlands*

Yuxuan Wang, *Assistant Professor, Department of Earth and Atmospheric Sciences, The University of Houston, Texas, U.S.A.*

Tze-wai Wong, *Adjunct Professor, Division of Occupational and Environmental Health, The Jockey Club School of Public Health and Primary Care, The Chinese University of Hong Kong, China*

HEI PROJECT STAFF

Katherine D. Walker, *Principal Scientist*

Allison P. Patton, *Staff Scientist*

Kethural Manokaran, *Research Assistant*

Lee Ann Adelsheim, *Research Assistant*

Kathryn Liziewski, *Research Assistant*

Eleanne van Vliet, *Staff Scientist (peer review management)*

Hilary Selby Polk, *Managing Editor*

Mary K. Brennan, *Consulting Editor*

Hope Green, *Editorial Project Manager*

Fred Howe, *Proofreader*

Ruth E. Shaw, *Compositor*

EXECUTIVE SUMMARY

Impacts of Shipping on Air Pollutant Emissions, Air Quality, and Health in the Yangtze River Delta and Shanghai, China

Yan Zhang[1], Junlan Feng[1], Cong Liu[1], Junri Zhao[1], Weichun Ma[1], Cheng Huang[2], Jingyu An[2], Yin Shen[3], Qingyan Fu[3], Shuxiao Wang[4], Dian Ding[4], Wangqi Ge[5], Freda Fung[6], Kethural Manokaran[7], Allison P. Patton[7], Katherine D. Walker[7], and Haidong Kan[1]

[1]Fudan University, Shanghai, China; [2]Shanghai Academy of Environmental Science, China; [3]Shanghai Environmental Monitoring Center, China; [4]Tsinghua University, Beijing, China; [5]Shanghai Urban-Rural Construction and Transportation Development Research Institute, China; [6]Natural Resources Defense Council, Hong Kong, China; [7]Health Effects Institute, Boston, Massachusetts, United States of America

---

What This Study Adds

- This study provides a comprehensive and detailed spatial analysis of the impacts of shipping and related activities on air quality and health of the populations of the Yangtze River Delta (9-km resolution) and the city of Shanghai (1-km resolution).

- It examines emissions and health effects in a baseline year (2015, before implementation of China's domestic emissions control areas [DECAs]*) and under three future emissions control scenarios (2030).

- Both the baseline and future analyses showed the importance for air quality and human health of controlling emissions from shipping and related activities that occur close to population centers, in particular from coastal or international ships entering inland waterways of Shanghai.

- In the Yangtze River Delta in 2015, shipping-related exposures to $PM_{2.5}$ contributed to about 3,600 premature deaths from stroke, chronic obstructive pulmonary disease, ischemic heart disease, and lung cancer combined, and to 270,000 hospital admissions from all causes. About a third of these deaths were in Shanghai.

- The analysis of the current policy scenario identified clear health benefits of full compliance with the current China DECA policies; the number of premature deaths relative to 2015 would be cut by half in 2030. Implementation of stricter and aspirational policy scenarios could reduce the 2015 mortality burden by substantially more (by a total of 62% and 77%, respectively). Requiring use of marine fuels with 0.1% sulfur content out to an extended emissions control area boundary of 100 nautical miles (NM) would provide the most benefit of the shipping emissions controls.

INTRODUCTION AND BACKGROUND

Air pollution has posed a major challenge in China. Although there has been recent progress, many sources continue to contribute to air pollution in quantities that vary geographically. Some are more important than others; several previous studies have identified substantial contributions from the industrial, power generation, transportation, agricultural biomass burning, and residential sectors (Ding et al. 2019; GBD MAPS Working Group 2016). Although China's first Action Plan for Air Pollution Prevention and Control, which was initiated in 2013 to improve air quality, led to reductions of 25% or more in the levels of $PM_{2.5}$ in 2017, the annual average concentrations of $PM_{2.5}$ in China were still estimated at about 53 μg/m^3, well above the World Health Organization's guidelines for healthy air (Health Effects Institute 2019). The potential implications for public health are substantial. In 2015, air pollution from all sources contributed to an estimated 1.1 million deaths in China (Cohen et al. 2017).

Although such national studies have typically not included the shipping sector in their analyses, a number of other studies have examined the global impacts of shipping and, more recently, their specific implications for China. Globally, air pollution from ship emissions has been estimated to contribute around 18,300 to 147,900 premature deaths primarily from the contributions to $PM_{2.5}$ of large ships traveling on international routes (Corbett et al. 2007; Partanen et al. 2013; Winebrake et al. 2009). Liu and colleagues (2016) estimated that shipping contributed 5,560 to 25,500 premature deaths in 2013 in East Asia of which about 18,000 were in mainland China. A recent global analysis estimated that 137,000 cardiovascular and lung cancer deaths globally related *to ship emissions* — 80% of them in Asia — could be avoided by stricter controls, specifically by decreasing the sulfur content of marine fuel from approximately 2.7% (mass/mass) to less than 0.5% by 2020 (Sofiev et al. 2018).

The overall goal of this project was to conduct a comprehensive assessment of the current and potential future air quality and health impacts of shipping and related activities at finer spatial scales in the city of Shanghai and the broader Yangtze River Delta region than have been conducted to date (Figure ES-1). We sought to estimate the impacts of shipping prior to the implementation of Chinese DECAs, using 2015 as a baseline year, as well as the future impacts (2030) of implementing both the latest DECA and more ambitious policies related to ships and green ports initiatives.

SCIENTIFIC APPROACH

The flow chart in Figure ES-2 provides an overview of the steps taken and the related data inputs necessary to assess the impact of ships and shipping-related sources on air pollutant emissions, ambient air quality levels, population exposures, and health burden in this study. The main steps were to:

- Develop emissions inventories for shipping and shipping-related sources in the Yangtze River Delta and Shanghai for the baseline year 2015 and projected for the year 2030 under alternative control scenarios. Emissions from non-shipping sources were obtained from existing national and regional emissions inventories.

- Simulate the impact of total and shipping-specific emissions on ambient pollutant and population-weighted $PM_{2.5}$ concentrations in the Yangtze River Delta and Shanghai using the Weather Research and Forecasting (WRF version 3.3) and Community Multiscale Air Quality (CMAQ version 4.6) modeling system (WRF-CMAQ). Simulations were conducted for 2015 and for 2030 under three alternative emissions control policies, described below.

- Estimate the health burden, defined in terms of excess numbers of deaths and hospital admissions in a given year, using the Environmental Benefits Mapping and Analysis Program-Community Edition (BenMAP-CE version 1.4), an open-source software developed by the U.S. Environmental Protection Agency (U.S. EPA 2015). We worked with Chinese scientists to identify the most appropriate studies with which to characterize the risks associated with exposures to $PM_{2.5}$ for China and to obtain the appropriate mortality and hospital admissions rates for Shanghai and the Yangtze River Delta.

EVALUATION OF ALTERNATIVE CONTROL POLICIES

We examined potential air quality and health benefits of controlling ship emissions for the Yangtze River Delta in 2030 under three alternative policy scenarios (Table ES-1). The "current" policy scenario was intended to examine the benefits of full implementation of China's second domestic emissions control policies (DECA 2.0), first proposed in July 2018. The 0.5% sulfur fuel requirement for cruising ships under this scenario is the same as the International Maritime Organization (IMO) sulfur fuel content limit set to be implemented globally in 2020. However, to estimate the benefits of the China policy alone, we assumed that the
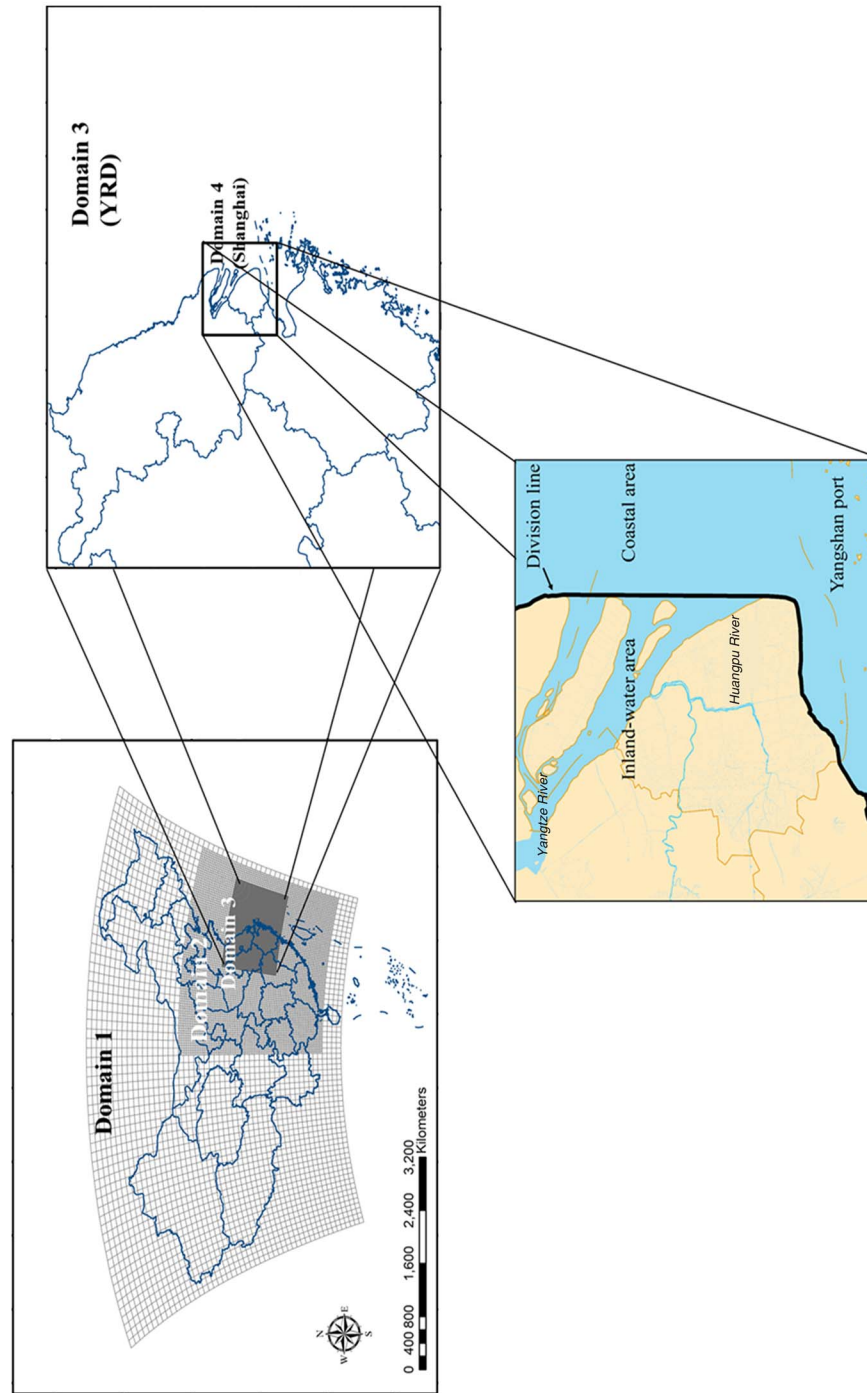
Figure ES-1. Map of nested study areas and delineation of inland-water area in Shanghai. Spatial resolutions for main analyses were 9 km in the Yangtze River Delta (YRD) (Domain 3) and 1 km in Shanghai (Domain 4). The inland-water area was defined by the black line shown above at the mouth of the Yangtze River; inland-water ships are defined as river ships, coastal ships, and ocean-going vessels that enter this area. (Adapted from Feng et al. 2019 [supplement]; distributed under Creative Commons Attribution 4.0 License.)

BASELINE (2015) **FUTURE (2030)**
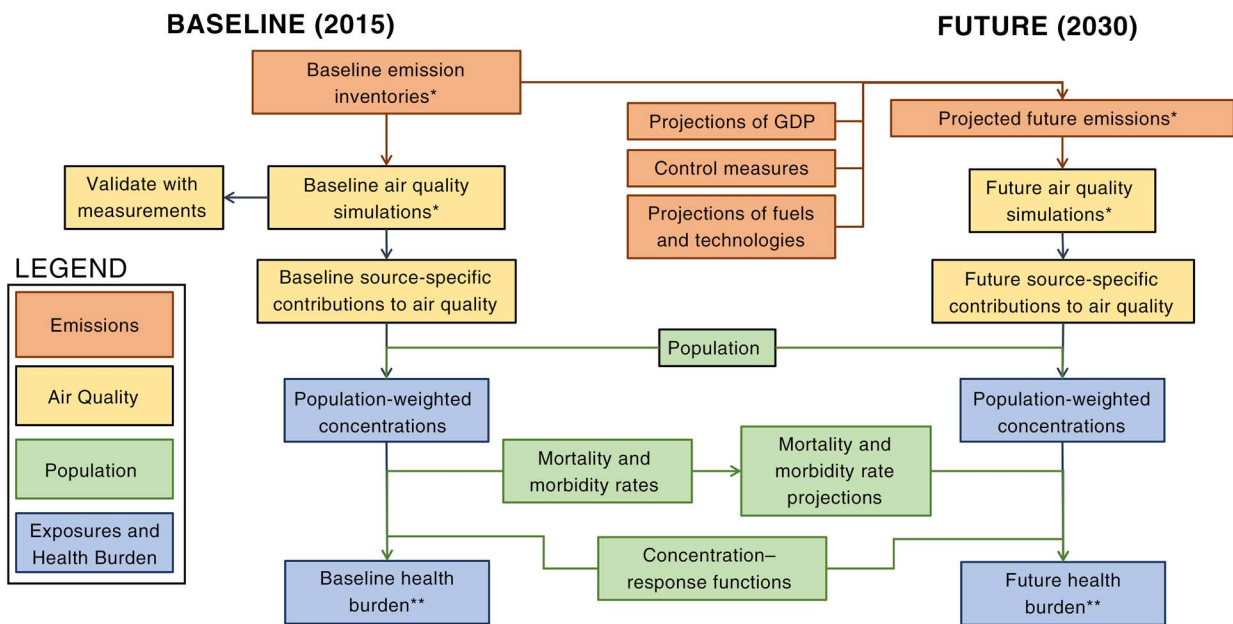
* with and without shipping sources
** includes mortality, morbidity, and disability-adjusted life-years

Figure ES-2. Process flowchart for estimating the impacts of emissions on air quality and health.

Table ES-1. Future Policy Scenarios

Scenario	Control Area	Sulfur Controls	NO$_x$ Controls
Base year (2015)	12 NM	All vessels change over to 0.5% sulfur fuel prior to entering the DECA	No controls on ships built before 2000 Tier I for ships constructed on or after Jan 1, 2000 Tier II for ships constructed on or after Jan 1, 2011
Current policy scenario, year 2030	12 NM	0.1% sulfur fuel at berth 0.5% sulfur fuel while cruising	China II for Chinese inland vessels Tier II for foreign ships
Stricter policy scenario, year 2030	12 NM	0.1% sulfur fuel	Tier III engines for all ships
Aspirational scenario, year 2030	100 NM	0.1% sulfur fuel	Tier III engines for all ships

NM = nautical miles

sulfur fuel content used by vessels beyond 12 NM of shore would remain the same as it was in 2015. The second, "stricter" policy scenario assumed lower fuel sulfur content and tighter NO$_x$ controls than the current policy, but still extended to vessels only 12 NM from shore. The third, "aspirational" policy scenario extended these stricter policies to vessels 100 NM from shore; this policy scenario was more aspirational because implementation would require agreement of the IMO. Although not included in our future policy analyses, emissions from cargo transport and from port machinery were expected to decrease in the future because of upcoming low-sulfur fuel and electrification requirements.

MAIN FINDINGS

BASELINE (2015)

Our assessment of the relative contributions of total ship emissions and their impacts on average PM$_{2.5}$ concentrations in the Yangtze River Delta region at varying distances from shore emphasizes the importance of shipping activities close to shore and to population centers**.** We found that between about 48% and 75% of pollutant emissions from ships are released within 12 NM of shore, depending on the pollutant; over 90% are released within 96 NM. Ship emissions within 12 NM accounted for between 53% and 83% of estimated human exposure to PM$_{2.5}$ in the core cities, represented in this analysis as *population-weighted PM$_{2.5}$ concentrations.*

Annual population-weighted PM$_{2.5}$ concentrations from shipping sources in individual core cities of the Yangtze River Delta region ranged from 0.5 µg/m³ to 2.5 µg/m³ (average 0.93 µg/m³) (Figure ES-3), accounting for 1% to 6% of population-weighted PM$_{2.5}$ concentrations from all pollution sources. The four cities in the Yangtze River Delta with the largest contributions of population-weighted PM$_{2.5}$ from shipping sources were all coastal cities. Of these, Shanghai had the highest average ship-related population-weighted PM$_{2.5}$ concentration (2.5 µg/m³).

The detailed analysis of ship and related emissions within the Shanghai port area (Domain 4) found that inland-water ships contributed the most to average annual population-weighted PM$_{2.5}$ concentrations (0.48 µg/m³), followed by coastal ships (0.18 µg/m³), and trucks and port machinery (0.15 µg/m³), but varied spatially (Figure ES-4).

Inland-water ship contributions to population-weighted PM$_{2.5}$ concentrations were highest in Shanghai due to the combination of dense population and close proximity to the Huangpu and Yangtze rivers.

Our study finds that emissions from shipping contribute meaningfully to the burden of disease from long-term exposures to PM$_{2.5}$ (particulate matter ≤ 2.5 µm in aerodynamic diameter) in the Yangtze River Delta and in Shanghai. We estimated that in 2015 there were about 3,600 premature deaths from stroke, chronic obstructive pulmonary disease, ischemic heart disease, and lung cancer attributable to long-term exposures to air pollution from ship emissions in the Yangtze River Delta region (Figure ES-5). When considering the impact of shipping emissions from across the entire Yangtze River Delta modeling domain, long-term exposures to PM$_{2.5}$ from ships contributed to about 1,100 premature deaths in Shanghai. As the figure indicates, the results are broadly consistent with, and in proportion to, the results presented for other regions and ports, despite differences in underlying data and methods.

Short-term, daily exposures to shipping-related PM$_{2.5}$ also contribute to the health burden. In the Yangtze River Delta, these exposures contributed to an estimated 1,000 additional deaths and to over 270,000 additional hospital admissions from all causes. Within the Shanghai port domain, we estimated that about 73 additional deaths and 16,000 hospital admissions were attributable to short-term exposures to PM$_{2.5}$ from all shipping sources. The largest impacts were from ships traveling on inland waterways, with additional contributions from coastal ships, container-cargo trucks, and in-port machinery.
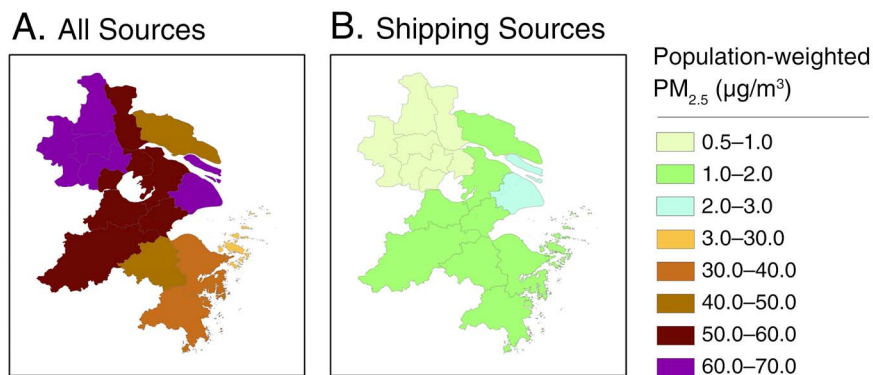
Figure ES-3. Annual average population-weighted PM$_{2.5}$ concentrations (µg/m³) in core cities in the Yangtze River Delta from (A) all air pollution sources and (B) ships. (From Feng et al. 2019; distributed under Creative Commons Attribution 4.0 License.)

A. Inland Shipping

Province

PM$_{2.5}$ contribution
- ≤ 0.080
- 0.080–0.220
- 0.220–0.430
- 0.430–0.730
- 0.730–1.140
- 1.140–2.200

B. Coastal Shipping

Province

PM$_{2.5}$ contribution
- ≤ 0.080
- 0.080–0.160
- 0.160–0.250
- 0.250–0.370
- 0.370–0.620
- 0.620–1.050

C. Diesel Cargo Trucks and Port Machinery

Province
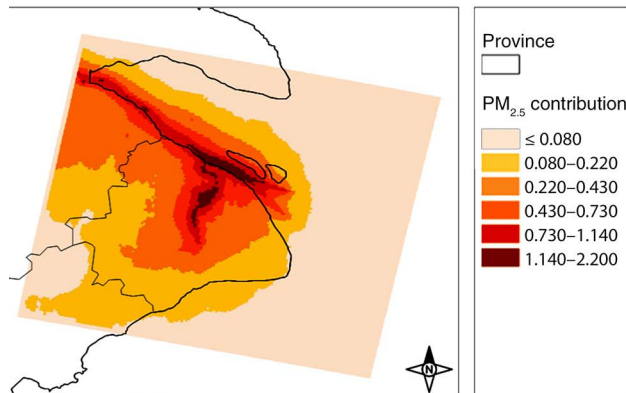
PM$_{2.5}$ contribution
- ≤ 0.040
- 0.040–0.120
- 0.120–0.230
- 0.230–0.420
- 0.420–0.770
- 0.770–1.550
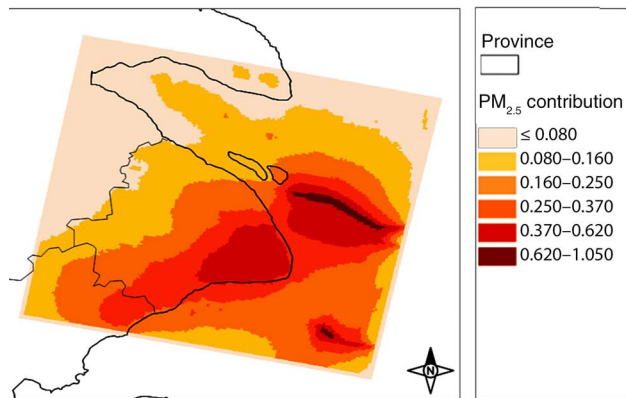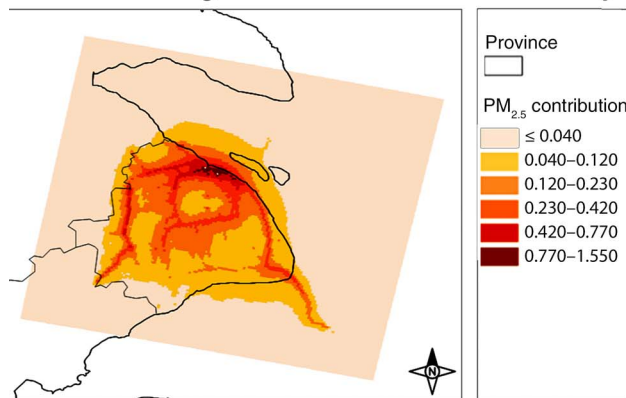
Figure ES-4. Contribution of (A) inland shipping, (B) coastal shipping, and (C) diesel cargo trucks and port machinery to annual average population-weighted PM$_{2.5}$ in Shanghai in the baseline year 2015.

ANALYSIS OF FUTURE POLICY SCENARIOS

Our analysis projected that existing Chinese air quality policies for all sources are likely to reduce population exposures to PM$_{2.5}$ levels substantially in the Yangtze River Delta — from 48 µg/m^3 in 2015 to about 32 µg/m^3 by 2030. Only a small fraction of that change was attributable to reductions in shipping emissions. The projected contributions from shipping to population-weighted annual average PM$_{2.5}$ was 0.36 µg/m^3 in the current scenario, 0.26 µg/m^3 in the stricter scenario, and 0.16 µg/m^3 in the aspirational scenario (accounting for 1.1%, 0.8%, and 0.5%, respectively, of PM$_{2.5}$ from all sources).

Despite these small changes in exposure, we estimated that each of these policies could contribute to important reductions in the numbers of premature deaths attributable to shipping and related emissions in 2030 (Figure ES-6), reflecting the large numbers of people potentially exposed. The current policies were projected to reduce the health burden from stroke, chronic obstructive pulmonary disease, ischemic heart disease, and lung cancer by about half (~1,800) relative to the numbers of estimated deaths attributable to PM$_{2.5}$ in 2015. The stricter and aspirational policies were projected to reduce mortality burden further to 1,400 and 830 deaths, respectively. Ships close to shore contributed more to PM$_{2.5}$ concentrations than those farther from shore, so most of the marginal benefit to air quality and health was obtained by stricter regulations close to shore. However, the aspirational scenario of 0.1% sulfur fuel within a 100 NM DECA would be even more effective in reducing PM$_{2.5}$ pollution and associated health impacts than maintaining the 12 NM DECA area.

CONCLUSIONS AND RECOMMENDATIONS

This study provides a comprehensive and detailed spatial analysis of the impacts of shipping and related activities on air quality and health of the populations of Shanghai and the Yangtze River Delta in a pre-DECA baseline year (2015) and under three future scenarios designed to inform decisions about the efficacy of alternative emissions control policies by 2030. It corroborates previous work and provides additional scientific evidence relevant to controlling future shipping emissions and to improving air quality in China.

Both the baseline and future analyses showed the importance of controlling emissions from shipping and related activities close to population centers. The baseline analysis indicated that 61% of SO$_2$ emissions and 48% of PM$_{2.5}$ emissions from ships in the Yangtze River Delta occur within 12 NM, the current demarcation for the DECA in

Region/ City	Mortality Attributable to Air Pollution from Ships	Mortality Attributable to Ambient $PM_{2.5}$
Global	18,300–147,900	2,723,000
East Asia	5,560–25,500	830,000
China	9,400–26,600	796,200
Pearl River Delta	1,300	47,500
Hong Kong	1,200	4,780
Yangtze River Delta	3,600	120,000
Shanghai	1,100	12,000

East Asia Population: 2.25 billion

China Population: 1.36 billion

Yangtze River Delta Population: 246 million

Shanghai Population: 21.7 million

Pearl River Delta Population: 60 million

Hong Kong Population: 7.2 million

Figure ES-5. Estimated mortality attributable to exposure to air pollution from ships and all sources, including the results for this study. Pollutant is $PM_{2.5}$ and year is 2013 unless otherwise specified for regions outside this study. See figures in the full report for data sources.
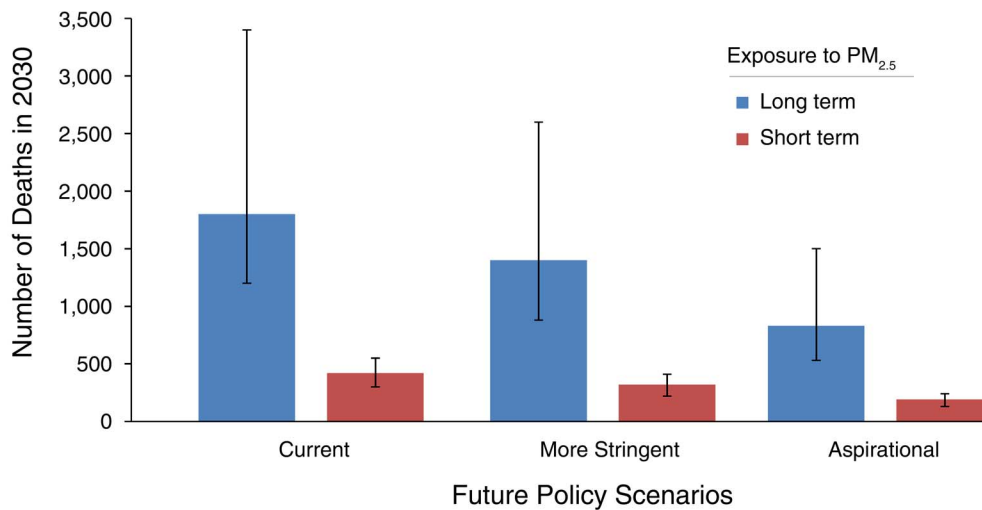
Figure ES-6. Numbers of premature deaths attributable to long- and short-term exposures to shipping-related $PM_{2.5}$ in the Yangtze River Delta in 2030 under alternative future policy scenarios for control of ship emissions.

China. However, over 90% of emissions of these pollutants from ships traveling within 200 NM of shore are released within 96 NM. Due to long distance transport and transformation of primary emissions to $PM_{2.5}$, the influence of ship emissions on air quality and health extends far inland from the coastal cities.

Our analysis of the baseline year 2015 scenario suggested substantial air quality and health benefits of full implementation of the current DECA requirements within 12 NM of shore. The greatest benefits are expected from the more aspirational scenario which, similar to what might be required under an IMO agreement, would require the stricter fuel sulfur requirements out to 100 NM. Further detailed evaluation of the relative contributions to air quality and health burden of inland ships — that is, ships travelling into the inland waterways of Shanghai — reinforces the importance of controlling emissions that occur in close proximity to high-density population centers like Shanghai.

Our analysis of the contributions of cargo-transport trucks and in-port activities (including ships at berth) to air quality was limited and may underestimate the impacts both for the city of Shanghai and for the Yangtze River Delta. More data are needed to more completely identify and characterize the contributions of these sources.

As our analysis assumed 100% compliance with existing and proposed regulations, the air quality and health benefits are likely to be overstated. Consequently, compliance monitoring and enforcement are a critical component of any ongoing and future policies.

Confidence in the benefits of implementing and enforcing strong regulations will come from demonstrable improvements in air quality. See for example the studies that have evaluated the effectiveness of shipping emissions regulations by measuring $PM_{2.5}$ concentrations at nearby air quality monitoring stations (e.g., Mason et al. 2019; Zhang et al. 2019). As the estimated contributions of ships to $PM_{2.5}$ exposures are small in both absolute and relative terms compared with other major sources of $PM_{2.5}$, it would be advisable to ensure ongoing monitoring of air pollution components that are more reliable indicators of ship emissions (e.g., vanadium and nickel) in order to detect and evaluate the impact of any regulations. We recommend that such studies be done in Shanghai and the Yangtze River Delta to evaluate the effectiveness of the regulations at reducing air pollution over time.

REFERENCES

Cohen AJ, Brauer M, Burnett R, Anderson HR, Frostad J, Estep K, et al. 2017. Estimates and 25-year trends of the global burden of disease attributable to ambient air pollution: An analysis of data from the Global Burden of Diseases Study 2015. Lancet 389:1907–1918; doi:10.1016/S0140-6736(17)30505-6.

Corbett JJ, Winebrake JJ, Green EH, Kasibhatla P, Eyring V, Lauer A. 2007. Mortality from ship emissions: A global assessment. Environ Sci Technol 41:8512–8518.

Ding D, Xing J, Wang S, Liu K, Hao J. 2019. Estimated contributions of emissions controls, meteorological factors, population growth, and changes in baseline mortality to reductions in ambient $PM_{2.5}$ and $PM_{2.5}$-related mortality in China, 2013–2017. Environ Health Perspect 127(6); doi:10.1289/EHP4157.

GBD MAPS Working Group. 2016. Burden of Disease Attributable to Coal-Burning and Other Major Sources of Air Pollution in China. Special Report 20. Boston, MA:Health Effects Institute.

Health Effects Institute. 2019. State of Global Air 2019. Boston, MA:Health Effects Institute.

Liu H, Fu M, Jin X, Shang Y, Shindell D, Faluvegi G, et al. 2016. Health and climate impacts of ocean-going vessels in East Asia. Nature Climate Change 6:1037–1041; doi:10.1038/nclimate3083.

Mason TG, Chan KP, Schooling CM, Sun S, Yang A, Yang Y, et al. 2019. Air quality changes after Hong Kong shipping emission policy: An accountability study. Chemosphere 226:616–624; doi:10.1016/j.chemosphere. 2019.03.173.

Partanen AI, Laakso A, Schmidt A, Kokkola H, Kuokkanen T, Pietikainen JP, et al. 2013. Climate and air quality trade-offs in altering ship fuel sulfur content. Atmos Chem Phys 13:12059–12071; doi:10.5194/acp-13-12059-2013.

Sofiev M, Winebrake JJ, Johansson L, Carr EW, Prank M, Soares J, et al. 2018. Cleaner fuels for ships provide public health benefits with climate tradeoffs. Nat Commun 9:406; doi:10.1038/s41467-017-02774-9.

U.S. EPA (U.S. Environmental Protection Agency). 2015. Environmental Benefits Mapping and Analysis Program: Community Edition (BenMAP-CE) user manual and appendices. Available: *www.epa.gov/benmap* [accessed August 30, 2018].

Winebrake JJ, Corbett JJ, Green EH, Lauer A, Eyring V. 2009. Mitigating the health impacts of pollution from oceangoing shipping: An assessment of low-sulfur fuel mandates. Environ Sci Technol 43:4776–4782.

Zhang X, Zhang Y, Liu Y, Zhao J, Zhou Y, Wang X, et al. 2019. Changes in SO_2 level and $PM_{2.5}$ components in Shanghai driven by implementing the Ship Emission Control Policy. Environ Sci Technol 53:11580–11587; doi:10.1021/acs.est.9b03315.

ABBREVIATIONS AND OTHER TERMS

DECA	Domestic Emissions Control Area (China)
GBD MAPS	Global Burden of Disease from Major Air Pollution Sources (initiative)
IMO	International Maritime Organization
NM	nautical miles
$PM_{2.5}$	particulate matter ≤ 2.5 μm in aerodynamic diameter
U.S. EPA	U.S. Environmental Protection Agency
WRF-CMAQ	Weather Research and Forecasting– Community Multiscale Air Quality modeling system
YRD	Yangtze River Delta

Impacts of Shipping on Air Pollutant Emissions, Air Quality, and Health in the Yangtze River Delta and Shanghai, China

Yan Zhang[1], Junlan Feng[1], Cong Liu[1], Junri Zhao[1], Weichun Ma[1], Cheng Huang[2], Jingyu An[2], Yin Shen[3], Qingyan Fu[3], Shuxiao Wang[4], Dian Ding[4], Wangqi Ge[5], Freda Fung[6], Kethural Manokaran[7], Allison P. Patton[7], Katherine D. Walker[7], and Haidong Kan[1]

[1]Fudan University, Shanghai, China; [2]Shanghai Academy of Environmental Science, China; [3]Shanghai Environmental Monitoring Center, China; [4]Tsinghua University, Beijing, China; [5]Shanghai Urban-Rural Construction and Transportation Development Research Institute, China; [6]Natural Resources Defense Council, Hong Kong, China; [7]Health Effects Institute, Boston, Massachusetts, United States of America

1.0 INTRODUCTION

1.1 PROJECT RATIONALE

Shipping — the international, national, and local transport of goods via ships as well as the related port and transportation infrastructure that supports it — has important implications for the environment and human health. Potential adverse effects from ships and the supporting infrastructure include human mortality and morbidity from the degradation of air quality near ports and climate impacts from emitted greenhouse gases (Li et al. 2018a; Liu et al. 2016). Globally, air pollution related to shipping has been estimated to contribute to 18,300 to 147,900 premature deaths from lung cancer and cardiopulmonary disease each year, primarily from the contributions of particulate matter ≤ 2.5 µm in aerodynamic diameter ($PM_{2.5}$*) from large ships traveling on international routes (Corbett et al. 2007; Partanen et al. 2013; Winebrake et al. 2009). As of 2017, 7 out of 10 of the largest container ports by shipping volume (20-foot equivalent units) in the world were in

China, and the shipping volumes at these ports had upward trajectories (United Nations Conference on Trade and Development [UNCTAD] 2018). In the Yangtze River Delta (YRD), Shanghai contains a cluster of several of the largest international ports in China. The Shanghai port cluster is a major transfer hub between coastal transport and transport of goods into mainland China via inland-water ships traveling on major rivers (e.g., the Huangpu and Yangtze Rivers) and trucks to locations within cities and where waterways do not reach. In addition to the large coastal ports, China also has substantial inland shipping with many smaller and less studied river ports. To address the impacts of emissions from these ships near Shanghai and other population centers, China has recently implemented emissions control areas near major ports. To inform future policies in China related to shipping and ports, information is needed on the impacts of shipping-related emissions on air quality and health in local cities and larger regions under different levels of emissions reductions.

This report describes the objectives, methods, and results of a health impact assessment of air pollutant emissions from ships and port-related activities for Shanghai and the YRD region.

1.2 SPECIFIC AIMS

The overall goal of this project was to conduct assessments of the potential air quality and health impacts of shipping as well as related activities to inform future shipping-related emissions control policies in the city of Shanghai and the broader Yangtze River Delta region in

---

The final contents of this document have not been reviewed by private party institutions, including those that support the Health Effects Institute; therefore, it may not reflect the views or policies of these parties, and no endorsement by them should be inferred.

Correspondence concerning this Special Report may be addressed to Dr. Yan Zhang, Department of Environmental and Engineering Sciences, Fudan University, Shanghai 200438, China; e-mail: *yan_zhang@fudan.edu.cn;* or Allison Patton, Health Effects Institute, 75 Federal Street, Suite 1400, Boston, MA 02110, U.S.A.; e-mail: *apatton@healtheffects.org.*

* A list of abbreviations and other terms appears at the end of this volume.

China. We sought to estimate both the impacts of shipping prior to the implementation of Chinese domestic emissions control areas (DECAs), using 2015 as a baseline year, and the future impacts of likely and aspirational policies related to ships and "green ports" initiatives by the year 2030.

The specific aims of this work were to:

1. Develop daily pre-DECA baseline (i.e., 2015) spatially distributed emissions inventories of sulfur dioxide (SO_2), $PM_{2.5}$, nitrogen oxides (NO_x), and volatile organic compounds (VOCs) in the YRD region (9-km resolution) and the city of Shanghai (1-km resolution) from sources related to shipping (i.e., ocean and coastal vessels, inland-water vessels, and shipping-related emissions from port machinery and cargo trucks).

2. Estimate the impacts of shipping and related sources on annual and seasonal ambient concentrations of SO_2, $PM_{2.5}$, nitrogen dioxide (NO_2), and ozone (O_3) in the YRD region and in the city of Shanghai.

3. Estimate the baseline impact of shipping sources on population-weighted exposures and the burden of disease attributable to $PM_{2.5}$ in the YRD region and in the city of Shanghai.

4. Evaluate the impacts of three alternative future policy scenarios on projected shipping activity and related emissions and on ambient air quality, population exposures, and burden of disease for the YRD region in 2030.

2.0 BACKGROUND

Air pollution is a major risk factor for increased risk of disease and mortality (GBD 2017 Risk Factor Collaborators 2018). Air pollution causes adverse health impacts primarily through inflammatory pathways. The causes of death attributed to ambient $PM_{2.5}$ include ischemic heart disease, cerebrovascular disease (stroke), chronic obstructive pulmonary disease (COPD), and infections of the lower respiratory tract (Cohen et al. 2017). These findings have been increasingly supported by epidemiological research in China (see Text Box).

2.1 AIR POLLUTION AND HEALTH IN CHINA

Air pollution is a well-acknowledged issue in China. Government regulatory initiatives over the past several years, including the ongoing 3-year Action Plan for Air Pollution Prevention and Control (2018–2020), have helped

Growing Evidence on the Effects of $PM_{2.5}$ on Health in China

Exposure to air pollution has long been linked to mortality and shortening of life expectancy. In the short-term, exposures over a few hours to a few days can contribute to ear, nose, and throat irritation. Short-term exposure may also aggravate existing lower-respiratory-tract conditions and chronic conditions such as asthma, allergies, and bronchitis (U.S. Environmental Protection Agency 2009). Among all air pollutants, fine particulate matter ($PM_{2.5}$) is arousing greater public health concern because of its independent contribution to these health effects. $PM_{2.5}$ is small enough to penetrate into the pulmonary alveolar region of the lungs causing systemic inflammation and oxidative stress that contribute to important effects on health. A substantial body of scientific evidence shows that long-term exposure to air pollution increases the risk of dying early from heart disease, chronic respiratory diseases, lung infections, lung cancer, diabetes, stroke, and lower respiratory infections (U.S. EPA 2009; World Health Organization [WHO] 2016). Air pollution has also been associated with other conditions and diseases including disorders of the central nervous system and adverse pregnancy and developmental outcomes.

There is a growing body of evidence on the health effects of air pollution from studies conducted in China where

evidence has been limited in the past. The health effects of short-term (e.g., daily) exposures to $PM_{2.5}$ in China have been documented using both individual city time-series studies and multicenter meta-analyses. The results of these studies all point to an increased mortality risk associated with short-term exposures to $PM_{2.5}$ although the study locations, time periods and analytic approaches may differ. More recently, Professors Haidong Kan and Maigeng Zhou led a national-scale time-series study (Chen et al. 2017b) in 272 Chinese cities that provides a comprehensive assessment of the health effects of short-term exposures to $PM_{2.5}$ among other key air pollutants. Additionally, the China CDC has recently conducted a large prospective study with a nationally representative cohort of nearly 190,000 Chinese men and found a significant increase in all-natural-cause and cause-specific mortality associated with long-term $PM_{2.5}$ exposure (Yin et al. 2017). Reported risks of premature mortality in this cohort were greater than those observed in studies in the United States and Europe and have provided new information on the relative risks of the high $PM_{2.5}$ exposures experienced in China. The results of this study have had an important influence on recent efforts to characterize the global concentration response relationships between $PM_{2.5}$ and mortality (Burnett et al. 2018).

lead to declines of as much as 25% in annual average $PM_{2.5}$ exposures from a high of 71 μg/m³ in 2011 to 53 μg/m³ in 2017 (Health Effects Institute 2019). Nevertheless, these levels continue to exceed both the China national standard of 35 μg/m³ and the World Health Organization guideline of 10 μg/m³, with important consequences for the burden of disease. In 2015, ambient $PM_{2.5}$ in China contributed to about 1.1 million premature deaths and the loss of 22 million disability-adjusted life-years (Cohen et al. 2017).

A recent comparative study of the major sources of air pollution in China and their impacts on air quality and health reported that burning coal (to fuel industries, power generation, and household heating) contributed about 40% of ambient population-weighted $PM_{2.5}$ concentrations and to an estimated 366,000 deaths in 2013 (GBD MAPS Working Group 2016). The most important sectors contributing to ambient $PM_{2.5}$-attributed mortality in

China in that study were industry (both coal and non-coal burning industries), which contributed to 250,000 deaths or 27% of the mortality, and household solid fuel (coal, wood, charcoal, and other biomass) combustion for cooking, which contributed to 177,000 deaths or 19% of the mortality attributable to $PM_{2.5}$ in 2013. Although the transportation sector was included in the GBD MAPS study, the emissions inventories did not include data on shipping and ports.

Several studies of the potential impacts of shipping on health have now been conducted at global, regional, and city scales. Although the range of results reflect variability and uncertainties in the data and methods, they are broadly consistent across geographical scales (Figure 2-1). Studies of the health impacts of air pollution from ships have estimated that 5,560 to 25,500 annual premature deaths are attributable to shipping in East Asia, with the
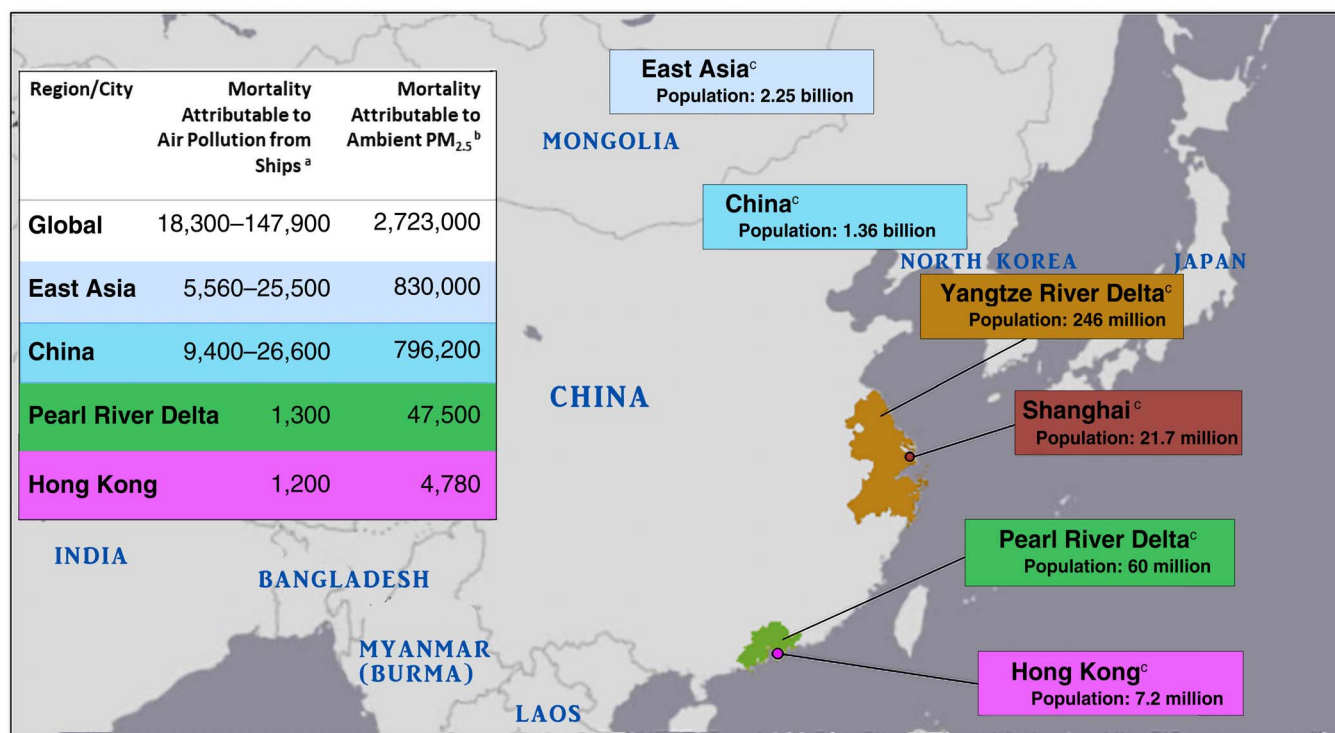
Figure 2-1. Mean estimated mortality attributable to exposure to air pollution from ships and all sources.

[a] **Sources of mortality attributable to air pollution from ships:** *Global:* $PM_{2.5}$ in 2012 (Corbett et al. 2007; Winebrake et al. 2009) and $PM_{2.5}$ and O_3 in 2010 (Partanen et al. 2013); *East Asia*: $PM_{2.5}$ in 2005 (Corbett et al. 2007) and 2008 (Liu et al. 2016); *China*: $PM_{2.5}$ and O_3 in 2008 (Liu et al. 2016); *Pearl River Delta*: combination of SO_2, NO_2, PM_{10}, and O_3 in 2008 (Lai et al. 2013); *Hong Kong*: combination of SO_2, NO_2, PM_{10}, and O_3 in 2008 (Lai et al. 2013). The reported values contain the full range of uncertainty reported across the studies in each category.

[b] **Sources of mortality attributable to ambient $PM_{2.5}$ in 2013:** *Global, East Asia,* and *China* (Health Effects Institute 2019); *Pearl River Delta* (Wu et al. 2019); and *Hong Kong* and *Shanghai* (GBD MAPS Working Group 2016). **Sources of mortality attributable to ambient $PM_{2.5}$ in 2015:** *Yangtze River Delta* (Maji et al. 2018).

[c] **Sources of population data for 2013:** *East Asia* (World Bank 2019); *China, Pearl River Delta,* and *Hong Kong* (National Bureau of Statistics of China 2014). **For 2015:** *Yangtze River Delta* and *Shanghai* (Bright et al. 2016).

13

largest impacts in mainland China (Corbett et al. 2007; Liu et al. 2016; Partanen et al. 2013; Winebrake et al. 2009). Corbett and colleagues (2007) predicted that the impact of increasing shipping activity between 2001/2002 and 2012 would lead to about 18,000 additional deaths globally, of which 2,000 would be in East Asia. Estimates of premature mortality related to ship emissions in Hong Kong were on the order of several hundred to one thousand deaths per year (Lai et al. 2013; Liu et al. 2016).

Several studies have looked at emissions and air quality impacts, but few have looked at health impacts of shipping within individual countries or cities in Asia. To determine whether shipping and port-related emissions substantially affect the health of people in close proximity to the sources, more detailed evaluation of these sources in the most-affected port cities and regions is needed. Although the YRD in general, and Shanghai in particular, are home to many of the largest ports in China, the potential health burdens from shipping-related air pollution in these areas had not previously been evaluated in depth. Therefore, we decided to develop high-resolution emissions inventories and to evaluate the effects of shipping-related emissions in Shanghai and in the broader YRD region.

2.2 SHIPPING-RELATED SOURCES OF AIR POLLUTION

The main sources of shipping-related air pollution emissions are: ships operating on the open ocean, near a coast, or on inland waterways; port equipment, including all land-based machinery operating inside the port boundaries; and land-based transport associated with ports (e.g., container-cargo trucks). Emissions from ships depend on the type of ship (e.g., container, tanker, passenger, fishing, or tugboats) and the conditions in which the ship is operated (Li et al. 2016; Sun et al. 2013). Although the larger coastal and ocean-going vessels usually use higher-sulfur fuel and are tracked using the Automatic Identification System (AIS), inland-water ships typically use a variety of different fuels, and their emissions are often underestimated in emissions inventories because AIS is not required for small ships that do not travel on the ocean (Li et al. 2016; Zhang et al. 2019b). Also, although increasing numbers of inland-water ships in China have installed land-based AIS, the systems are not always turned on or the signals are not accurate. In a study of impacts of shipping on air pollutant concentrations in Europe, ships in the North Sea contributed up to 25% of NO_2 concentrations near shore and up to 6% of NO_2 concentrations 100 km inland; contributions to $PM_{2.5}$ were similar (Aulinger et al. 2016). Another study reported that $PM_{2.5}$ concentrations in European coastal regions increased by about 20% (0.5 to 2 $\mu g/m^3$) due to emissions from ships (Partanen et al. 2013).

Measurable increases in air pollutant concentrations and exposures in people living near waterways with ship activity have also been documented around the world (Corbett and Fischbeck 2000; Fu et al. 2013; Keuken et al. 2014; van der Zee et al. 2012). Finally, impacts of emissions from port machinery (i.e., cranes and other equipment to handle, store, and transfer shipping containers) and land-based transport of goods on air quality in addition to the health of populations living along "goods corridors" have also been documented, particularly near the Ports of Los Angeles and Long Beach in the United States (e.g., Ault et al. 2009; Ault et al. 2010; Giuliano and O'Brien 2007; Houston et al. 2014; Kim et al. 2012; Kozawa et al. 2009).

Although health impacts of shipping-related emissions have not previously been reported for Shanghai, air quality impacts of ship activities have been measured in several studies. One study measuring air quality in Shanghai Port in three seasons (winter, spring, and summer) found that ship traffic contributed 0.63 $\mu g/m^3$ to 3.58 $\mu g/m^3$ (or 4.2 to 12.8%) of the total $PM_{2.5}$ in Shanghai Port (Zhao et al. 2013). Compared with a non-port site, NO_2 and SO_2 levels were higher while O_3 levels were lower. At the port measurement location, vanadium (V) concentrations were highly correlated with ship traffic. In addition, particulate matter (PM) (especially $PM_{2.5}$) was enriched in V and nickel (Ni) relative to crustal material. By comparing the V/Ni ratio measured in port air measurements (V/Ni = 3.4), Zhao and colleagues concluded that in summer, international heavy fuel oils (V/Ni = 3.6) contributed more to the $PM_{2.5}$ concentrations than did domestic fuel oil (V/Ni = 1.9). Liu and colleagues (2017) showed that the influence of ship plumes on shore concentrations of air pollutants in Shanghai is highly dependent on weather and season. The authors estimated that ships could contribute 2 to 7 $\mu g/m^3$ (or 5.9% to 30%) of the total ambient $PM_{2.5}$ concentrations within tens of kilometers of coastal and riverside Shanghai during times when the wind directly transported ship plumes to shore. Another study estimated that ship emissions contribute 36.4% of SO_2 concentrations, 49.5% of V particles, and 5.9% of ambient $PM_{2.5}$ in the Shanghai port region (Wang et al. 2019).

3.0 GLOBAL AND CHINESE REGULATION OF SHIPPING-RELATED EMISSIONS

To reduce the impact of shipping on human health and the environment, various regulations have been proposed and implemented at global, regional, and national or local levels of government to limit these emissions. Regulations related to shipping-related emissions include internationally negotiated regulations promulgated by the International

Figure 3-1. Timeline for national and international regulations of emissions affecting Chinese exposures to air pollution from shipping-related sources.

Acronyms: DECA = Domestic Emission Control Area (extends to 12 NM off the coastlines in YRD and PRD and within the Bohai Sea); IMO = International Maritime Organization; MEP = Ministry of Environmental Protection; MOT = Ministry of Transport; PRD = Pearl River Delta; TPRI = Transportation Planning Research Institute; YRD = Yangtze River Delta.

Early-action ports (11): Shanghai, Ningbo-Zhoushan, Suzhou, and Nantong in the YRD; Shenzhen, Guangszhou, and Zhuhai in the PRD; Tianjin, Qinhuangdao, Tangshan, and Huanghua in the Bohai Sea.

MEP Marine engine standards apply to all new engines used on inland, coastal, river-sea, channel and fishing vessels with net power rating >37 kW. Phase 2 marine engine emissions standards are similar to EU stage IIIA standard and slightly weaker than US Tier 3 standard.

Maritime Organization (IMO), national and international emissions control areas where emissions of air pollutants are limited, and international or national fuel or control technology standards (Figure 3-1). Much of the impact on air quality and health from ship emissions is linked to PM and its precursors, in particular emissions of sulfur and nitrogen, which contribute to the ambient PM in the form of sulfates and nitrates. Therefore, many regulations seek to limit sulfur in fuel to reduce secondary formation of PM from sulfates and to improve the efficiency of catalytic converters and other control technologies that reduce NO_x emissions.

3.1 SHIPPING EMISSIONS REGULATIONS BY THE INTERNATIONAL MARITIME ORGANIZATION

Air pollution and greenhouse gas emissions from ocean-going vessels are regulated by the IMO under Annex VI of the International Convention for the Prevention of Pollution from Ships (MARPOL) (IMO 2019). MARPOL is able to regulate the sulfur or nitrogen content in fuel and emissions from ships. Since 2012, the global fuel sulfur limit has been 3.5% by mass. The limit is set to decrease to 0.5% sulfur in fuel by 2020 (Figure 3-1). Similar decreases in the allowable amount of sulfur in fuel have been made in China and elsewhere (Figure 3-2).

The IMO also designates Emission Control Areas (ECAs) in amendments to MARPOL to benefit the atmospheric environment and human health in port and coastal communities. These benefits are obtained by specifying fuel or emission limits for sulfur oxides (SO_x), nitrogen oxides (NO_x), or PM for all ships within the ECAs. Current ECAs exist for the Baltic Sea (SO_x), North Sea (SO_x), North America (SO_x, NO_x, and PM), and United States Caribbean Sea (SO_x, NO_x, and PM) (IMO 2017). As of January 1, 2015, a limit of 0.1% sulfur by mass was implemented in sulfur ECAs (European Maritime Safety Agency 2010; IMO 2017). As of January 1, 2016, the allowable NO_x emissions in nitrogen ECAs ranged from 2.0 to 3.4 grams per kilowatt hour (g/kWh) depending on the engine's rated speed (IMO 2018). Although the IMO designates the ECA, each nation protected by an ECA separately produces regulations to institute the ECA and ensure compliance (see European Parliament 2012; IMO Marine Environment Protection Committee 2009).

In general, each nation (and not the IMO) has jurisdiction over environmental protection within its exclusive economic zone of up to 200 nautical miles (NM) from shore and including inland waters (United Nations 1982). For example, European member states limit the sulfur content in fuels used by ships at berth (0.1% by mass) or regularly traveling between European Union (EU) ports (1.5% by mass) and encourage electrification of all ships and machinery within the ports through European Directive 2012/23/EU (European Parliament 2012). The United States and Canada each regulate emissions of inland-water emissions from ships traveling in the Great Lakes Region (Harkins 2007).

3.2 CURRENT AND FUTURE CONTROLS ON SHIPPING AND RELATED ACTIVITIES IN CHINA

Over time, China has implemented a series of increasingly strict regulations of shipping-related emissions (see Figure 3-1).

Although China does not have an ECA designated by the IMO, in December 2015 the Chinese Ministry of Transport designated three DECAs in the YRD, Pearl River Delta (PRD), and Bohai Sea, where the emissions from ships are highest (Figure 3-3) (Chinese Ministry of Transport 2015). These DECAs limited fuel sulfur content to 0.5% by mass, first for ships at berth by 2017 and then expanding to domestic vessels within 12 NM from shore by 2019.

In December 2018, the Chinese government announced new regulations for its DECAs (DECA 2.0). From January 1, 2019, the new regulation requires domestic vessels within 12 NM of shore to use marine fuels with a maximum sulfur content of 0.5% by mass (China Classification Society 2018). By this date, the regulations also impose a stricter fuel sulfur limit (0.10% by mass) on inland and "river-sea" ships entering designated "inland
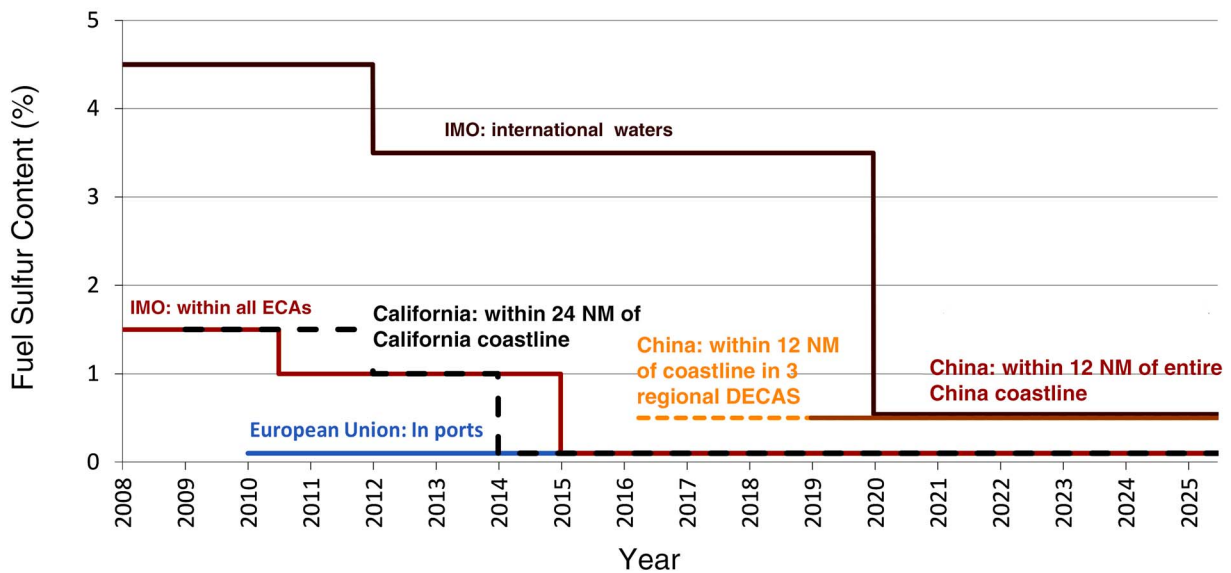
Figure 3-2. Existing fuel sulfur standards or commitments for vessels.
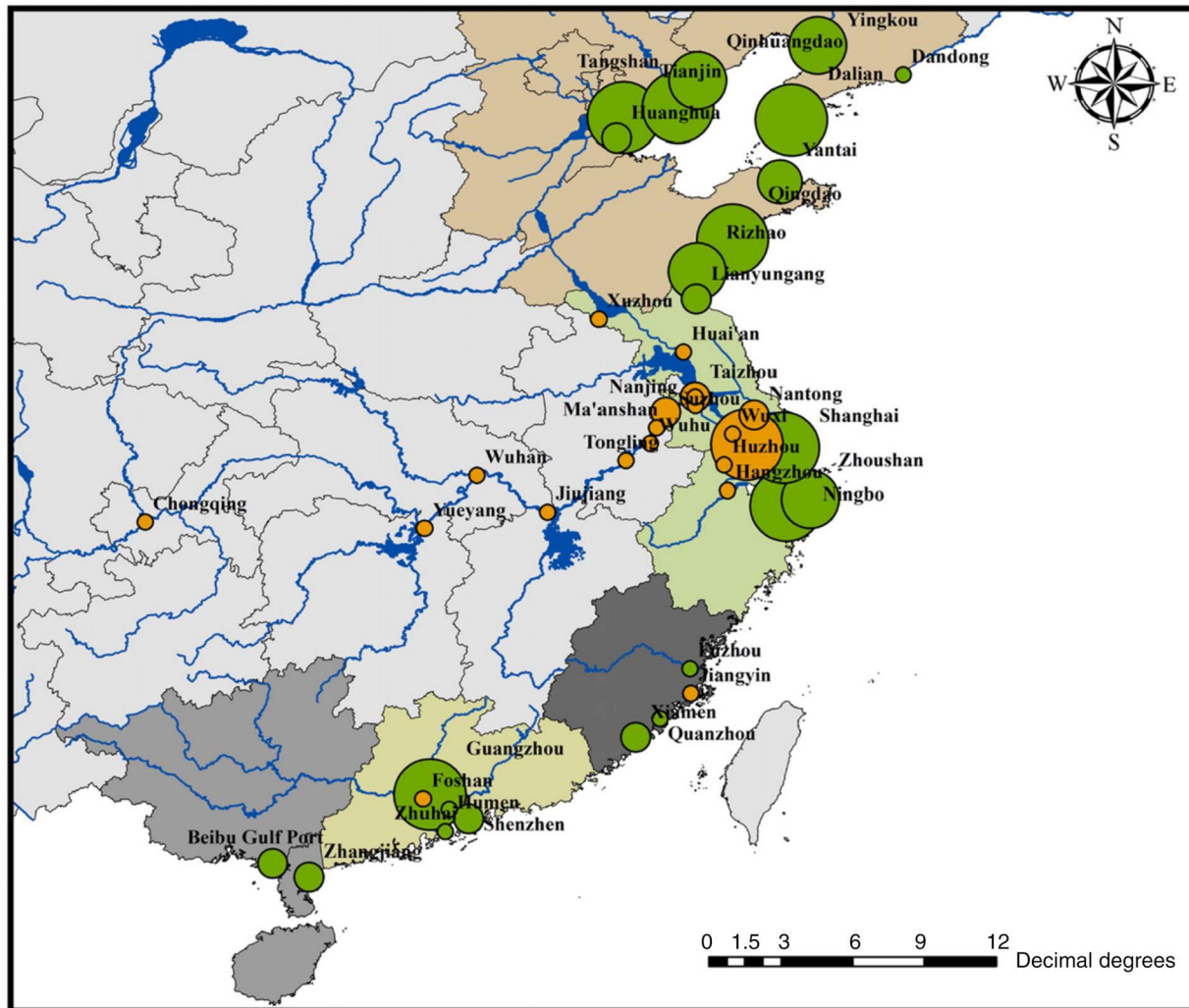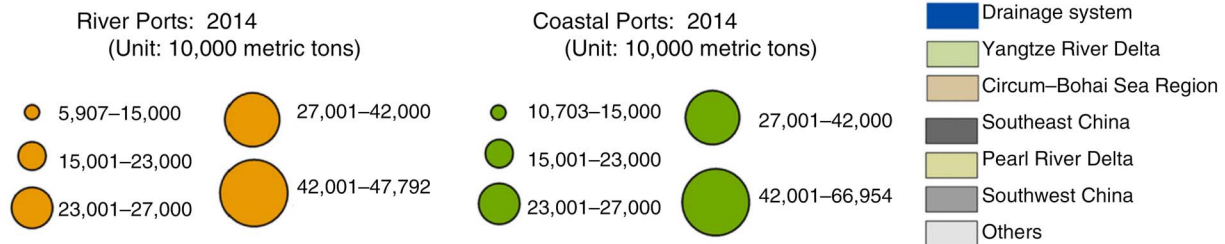
Figure 3-3. Geographical positions and cargo throughputs of major coastal and inland ports in China. (Reprinted from Zhang et al. 2017 with permission from Elsevier.)

emission control areas." These include the navigable waters of the Yangtze River (from Shuifu in Yunnan Province to Liuhe Estuary in Jiangsu Province) and the Xijiang River (from Nanning in Guangxi Province to Zhaoqing in Guangdong Province). Beginning on January 1, 2020, ocean-going vessels entering the inland ECAs must use marine fuels with a fuel sulfur limit of 0.10% by mass. The regulations also govern emissions of NO_x and VOCs and require the use of shore power when at berth for more than 3 hours.

Controls on emissions from river and fishing vessels are stricter than emissions from coastal and ocean-going vessels. These ships must use general diesel fuel as opposed to

the higher sulfur (0.5% by mass) marine fuel used by coastal and ocean-going vessels. By January 1, 2018, general diesel fuel must meet the same China V standard of 0.001% sulfur by mass (or 10 ppm) sulfur as diesel approved for trucks (DieselNet 2018b). However, compliance with these stricter controls is not well-documented and these controls also do not apply to the larger coastal and ocean vessels that sometimes enter the rivers to travel to inland ports.

Regulation of other ports-related sources of air pollution falls under different programs and government agencies. Emissions from trucks involved in the transport of shipping cargo in China are regulated under the national 13th Five Year Plan, Clean Air Action Plan (State Council of the People's Republic of China 2013), and the National 3-year Blue Sky Defense Plan. Cities like Shanghai also develop plans to promote cleaner air quality and transportation alternatives that affect cargo-related transport. For example, see the Shanghai City Plan for 2035, the Shanghai Transport Commission report, and the Shanghai 3-Year Green Port Action Plan (2015–2017) (China Carbon Emissions Trading Network 2015). Some proposed actions under these plans include electrifying all in-port machinery by 2030 and replacing diesel fuel with compressed natural gas for trucks and forklifts (China Carbon Emissions Trading Network 2015). It is challenging to ensure complete compliance by all cargo trucks as Shanghai only has jurisdiction over trucks registered in Shanghai.

3.3 POTENTIAL HEALTH BENEFITS OF SHIPPING EMISSIONS POLICIES IN YANGTZE RIVER DELTA AND SHANGHAI

Health benefits of shipping regulations have been estimated on various scales from global to national to regional. Several studies have suggested that decreasing the global or coastal sulfur content of marine fuel from the current global average of about 2.7% to 0.5% or 0.1% by mass could avoid 33,500 to 137,000 premature deaths on average attributable to ship emissions each year (Partanen et al. 2013; Sofiev et al. 2018; Winebrake et al. 2009); these numbers are similar in magnitude to the number of deaths in the YRD attributable to all sources of air pollution (Wang et al. 2015). Sofiev and colleagues (2018) estimated that of the global adult mortality reductions (137,000), 80% would be in Asia in 2020; in addition, they estimated that there would be 7.6 million avoided cases of childhood asthma morbidity, of which 54% would be in Asia (Sofiev et al. 2018). The authors expected that China would be heavily affected given the concentration of the shipping industry around highly populated cities.

Although Shanghai and other cities in the YRD have major ports and are therefore potentially impacted by shipping-related emissions, little work has been done to evaluate the potential health benefits for these cities of implementing and going beyond the current regulations. This study was undertaken to improve the scientific understanding of these potential benefits.

4.0 METHODS

4.1 STUDY AREA

This study was conducted for the YRD, with a particular focus on the city of Shanghai and the nearby waters regulated by the Shanghai municipal organizations. All analyses were done in a series of nested domains (Figure 4-1): China (Domain 1; 81 km × 81 km), East China (Domain 2; 27 km × 27 km), YRD (Domain 3; 9 km × 9 km), and Shanghai (Domain 4; 1 km × 1 km). The geographical scope for the YRD study area extended from 116.5°E to 127°E and 27°N to 35°N and included an offshore distance of approximately 200 NM. The Shanghai study area included from 120.5°E to 122.3°E and from 30.5°N to 32°N, up to an offshore distance of less than 12 NM, where the water is within the jurisdiction of Shanghai Maritime Safety Administration.

4.2 SHIPPING AND SHIPPING-RELATED SOURCES EVALUATED

Although there are many categories of ships and related sources, this analysis focused on those that have generally been found to be the most important sources in other settings and for which we had access to data. For the YRD and its cities, we assessed the emissions and air quality and health impacts of all ships captured in the AIS dataset within the YRD modeling domain (Domain 3). AIS is a safety technology that is not installed on all ships; consequently, the AIS dataset contains more complete information on large ships traveling on the ocean than on smaller ships or those that travel on inland waters.

Within Shanghai, we sought to understand the impact of emissions released nearer the population centers from the following shipping, or related, sources:

- Coastal and international ships, including both coastal vessels defined as domestic or international ships that travel between Chinese ports in north–south lanes along the coast and ocean-going vessels defined as ships that travel on the open ocean, typically internationally.
- Inland-water ships, which for the purposes of this study are defined as any ships that entered a geographically defined boundary shown in Figure 4-1. These could include ocean-going vessels or coastal vessels as well as river ships or fishing vessels that
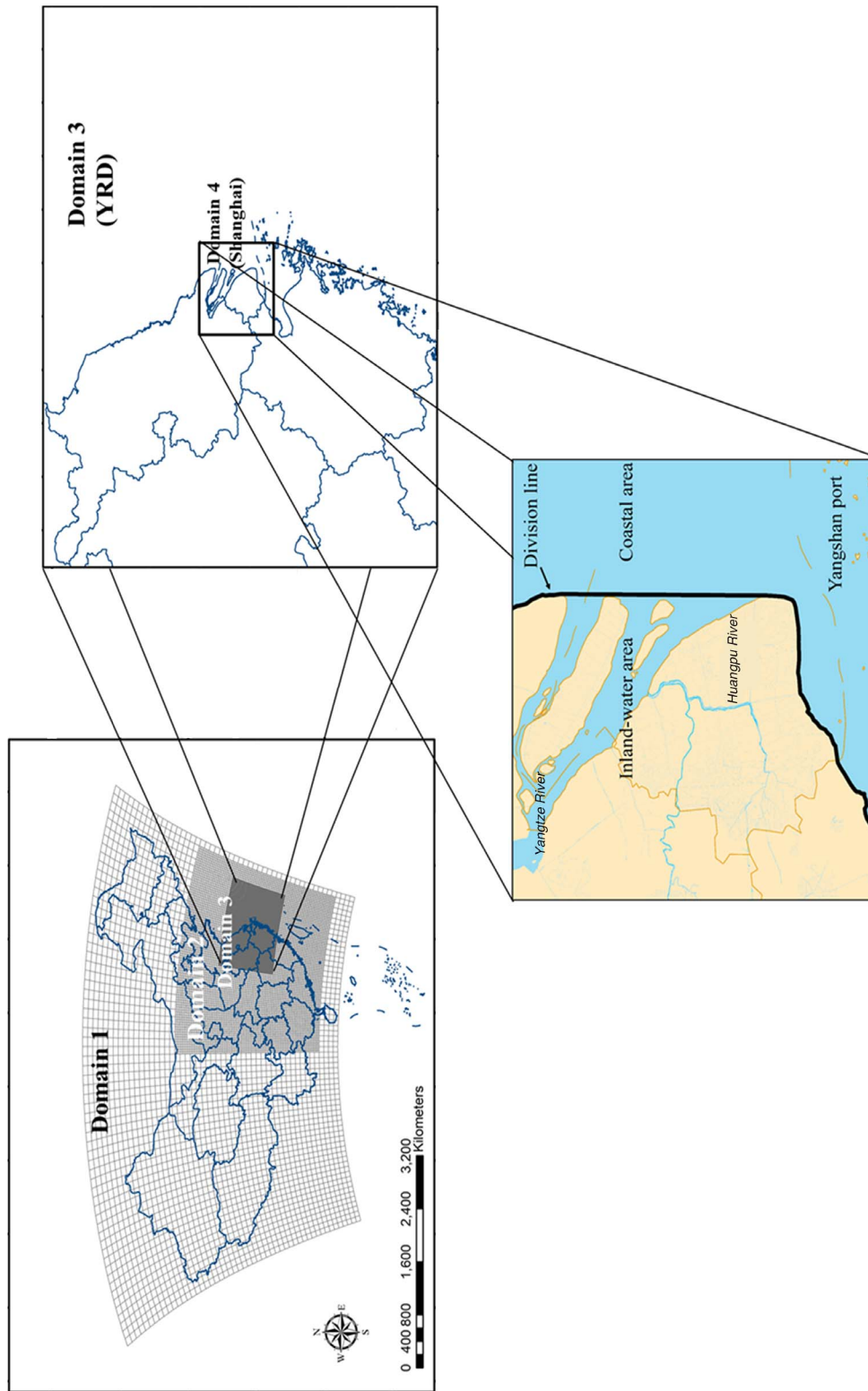
Figure 4-1. Map of nested study areas and delineation of inland-water area in Shanghai. Spatial resolutions for main analyses were 9 km in the YRD (Domain 3) and 1 km in Shanghai (Domain 4). The inland-water area was defined as the inside water area of the Yangtze River mouth (black line); inland-water ships are defined as river ships, coastal ships, and ocean-going vessels that enter this area. (Adapted from Feng et al. 2019 [supplement]; distributed under Creative Commons Attribution 4.0 License.)

regularly travel the inland waterways. To characterize inland-water ships in Shanghai more completely, the AIS data were supplemented with local visa data at river ports.

- Diesel container-cargo transport trucks, defined as trucks that carry cargo to and from the ports located within Shanghai.

- In-port machinery, defined as cranes and other equipment to handle, store, and transfer shipping containers.

More detail on the development of emissions for each of these sources is found in subsequent sections. We recognize that the definition of inland ships in this report differs from those in other studies that may focus on specific classes of vessels that travel inland waterways or that are governed by specific policies. Our goal in defining inland-water ships geographically was to understand the relative impact of emissions from vessels traveling in closer proximity to more densely populated areas through Shanghai compared with the impact of ships that remain at greater distances. The results need to be interpreted with that caveat in mind.

4.3 OVERVIEW OF METHODOLOGICAL APPROACH

The flow chart in Figure 4-2 provides an overview of the steps taken to assess the impact of ships and shipping-related sources on air pollutant emissions (orange boxes),

ambient air quality levels (yellow boxes), population exposures (green boxes), and health burden (blue boxes) in this study:

1. Development of emissions inventories for shipping and shipping-related sources in the YRD and Shanghai for the baseline year 2015 and for these sources for the future year 2030 under alternative control scenarios. Emissions from non–shipping-related sources were obtained from existing national and regional emissions inventories.

2. Simulation of the impact of all emissions sources on ambient SO_2 and $PM_{2.5}$ concentrations in the YRD and Shanghai using the Weather Research and Forecasting (WRF, version 3.3) and Community Multiscale Air Quality (CMAQ, version 4.6) modeling system (WRF-CMAQ).

3. Simulation of the effect on air quality of removing ships and other shipping-related sources of air pollutant emissions for 2015 and for 2030 under various policy scenarios.

4. Estimation of exposures to $PM_{2.5}$ as population-weighted concentrations, combining gridded air quality and population data.

5. Estimation of health burden, defined in terms of increased hospital admissions and mortality, was estimated using the Environmental Benefits Mapping

* with and without shipping sources
** includes mortality, morbidity, and disability-adjusted life-years

Figure 4-2. Process flowchart.

and Analysis Program-Community Edition (BenMAP-CE, version 1.4), an open-source software developed by the U.S. Environmental Protection Agency (U.S. EPA) (2015).

Each of these steps will be described in further detail in subsequent sections.

4.3.1 Baseline Year (2015) Analyses

We defined 2015 as the baseline year because it preceded the implementation of the first Chinese DECAs. The baseline impact of all emissions sources in the region a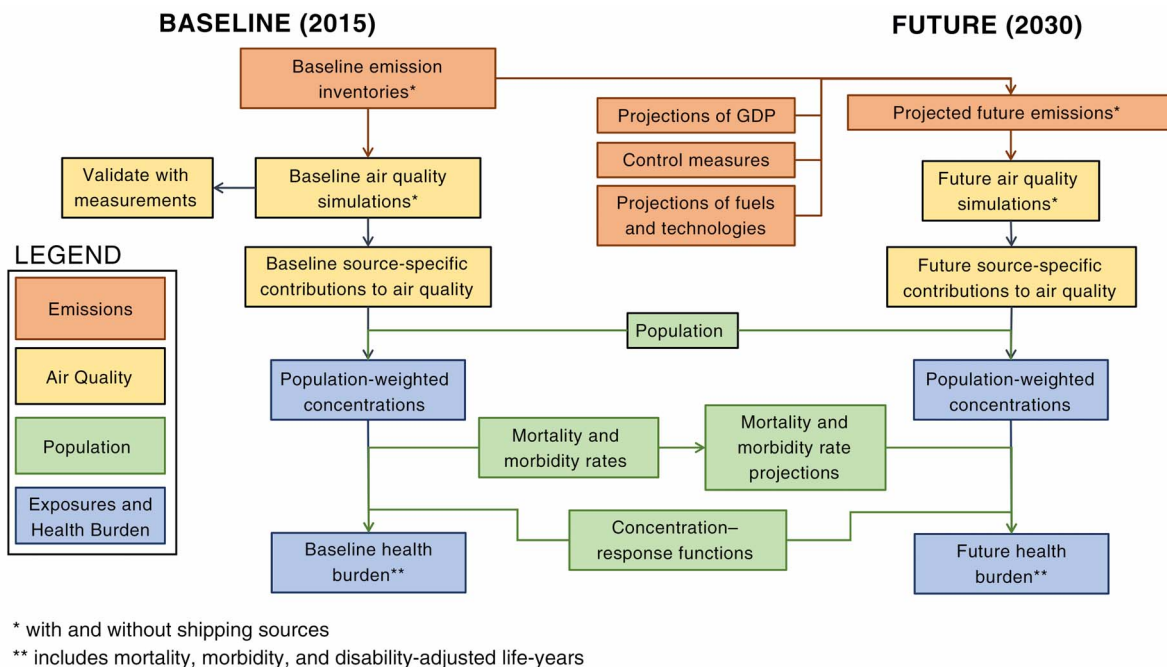re first estimated from inventories of all sources, both land-based non-shipping and shipping-related sources. The contributions of individual shipping-related sources are assessed by excluding the emissions of an individual source from the complete inventory and re-running the air quality simulations; the difference between the impacts on air quality between the baseline analysis and the source-excluded analysis yield the impact of the individual source.

4.3.2 Future Policy Scenarios (2030)

To assess the impact of potential future policy alternatives, three scenarios designed to control SO_2 and NO_x emissions were evaluated: the current policy scenario, a stricter policy scenario, and an aspirational scenario (Table 4-1). The current policy scenario reflects the Chinese Ministry of Transportation's proposal for upgrading the China DECA policy published in July 2018. This scenario assumes that all ships switch to 0.5% sulfur fuel when operating inside the DECA and use fuel with a limit of 0.1% sulfur while at berth. The assumed fuel use is slightly stricter than the final amended DECA policy that requires 0.5% sulfur fuel when operating inside the DECA but has no additional fuel sulfur requirement for ships at berth.

The stricter and aspirational scenarios include policy options that either have been or might be proposed in the future under domestic or international ECAs; these policy options would expand the geographical size of the ECAs, mandate the use of fuel with lower sulfur content, and

Table 4-1. Future Scenario Design for Regional Inventories in the YRD under the DECA and ECA Policies

Scenario / Distance from Shore	Sulfur Controls	NO$_x$ Controls[a]
Base Year (2015)		
12 NM	No DECA controls; 2.7% fuel	No controls on ships built before 2000
		Tier I for ships constructed on or after Jan. 1, 2000
		Tier II for ships constructed on or after Jan. 1, 2011
1: Current Policy Scenario[b]		
12 NM	0.1% sulfur fuel at berth	China II for Chinese inland vessels (Engine power > 500 kW)
	0.5% sulfur fuel while cruising	Tier II for all foreign ships
2: Stricter Policy Scenario[c,d]		
12 NM	0.1% sulfur fuel	Tier III engines for all ships built on or after January 1, 2021
3: Aspirational Scenario[c,e]		
100 NM	0.1% sulfur fuel	Tier III engines for all ships built on or after January 1, 2021

[a] Tiers I, II, and III refer to the IMO emissions limits, whereas China II refers to the domestic emissions limits for general diesel fuel (DieselNet 2018a, b; 2019).

[b] The current policy scenario is consistent with the Ministry of Transportation (Chinese) proposal for upgrading China DECA policy published in July 2018, so the at-berth requirement of 0.1% sulfur fuel is slightly stricter than the current policy requirement.

[c] Tier III requirements would only apply to new ships after an international ECA was enacted.

[d] The stricter policy scenario is consistent with the Shanghai government's 3-year Clean Air Action Plan for 2018-2022, released in July 2018.

[e] The aspirational scenario is consistent with an IMO ECA with a boundary 100 NM from the coastline. A 200 NM ECA boundary was not considered because it might cut into the area of disputed waters with Japan.

require new ships in ECAs to meet stricter NO_x emissions standards. The stricter policy scenario is consistent with the Shanghai government's 3-year Clean Air Action Plan for 2018–2022. The aspirational scenario is consistent with an IMO ECA with a boundary 100 NM from the coastline and assumes the 0.1% sulfur fuel standard in ECAs that was implemented by the IMO in the beginning of 2015 (Figure 3-2).

We recognize that the IMO plans to implement a global limit of 0.5% fuel sulfur content for all ships in international waters in 2020; this policy is not reflected in these scenarios because we wished to compare the impact of fuel changes within the ECAs alone with the base year. For NO_x, Tier III requirements would apply to new vessels that are built if an IMO ECA in China were to be enacted for both the stricter and aspirational scenarios (IMO 2016). We assume that the IMO ECA will be enacted in China by 2021, the same year by which the NO_x ECAs in North Sea and Baltic Sea will take effect. This assumption may be over-optimistic, because the final amended China DECA policy has delayed the decision whether to apply for an IMO ECA to at least 2025.

Changes in future liquefied natural gas (LNG) controls or use were not considered because the related policy is very uncertain. LNG ships emit near-zero sulfur emissions, and up to 88–90% less NO_x emissions than Tier I ships; but some LNG ships using diesel-cycle engines cannot meet Tier III NO_x emissions requirements without after-treatment devices. Although China has issued policies promoting the use of LNG for inland vessels, it has not issued any policies on the preferred deployment schedule for LNG ships at the national or regional level. Consequently, rather than make assumptions about what those future LNG policies might be, we thought that the future policy analyses would be more realistic and informative if they were constructed assuming that ships entering a DECA or ECA met a specific set of fuel sulfur and NO_x emissions requirements. Details of the future policy scenarios are summarized in Table 4-1.

4.4 DEVELOPMENT OF EMISSIONS INVENTORIES

4.4.1 Baseline Ship-Related Emissions Inventories

4.4.1.1 Coastal and Ocean-Going Ships Coastal and ocean-going ship emissions inventories were constructed using bottom-up methods based on ship traffic activity primarily using the AIS-based model (Fan et al. 2016; Ng et al. 2013; Nunes et al. 2017). The ship speeds and operation times within the YRD and Shanghai geographical domains were obtained from AIS data at a 1-minute temporal resolution and 1 km × 1 km spatial resolution provided by the

Maritime Safety department (L Huo, personal communication, June 2016). The installed power of the main engine, auxiliary engine, and auxiliary boiler plus the maximum speed of ships were obtained from Lloyd's register (IHS Fairplay 2015) and the China Classification Society database (China Classification Society 2016). The emissions from the main engine, E_m were calculated as

$$E_m = P_m \times LF_m \times LLAM \times T_m \qquad (1)$$
$$\times EF_m \times FCF_m \times CF_m$$

where P_m is the installed power of the main engine (kW), $LLAM$ is the low load adjustment multiplier for the main engine (unitless), T_m is operation time of the main engine (h), EF_m is the main engine emissions factor (g/kWh), FCF_m is the main engine fuel correction factor (unitless), and CF_m is the main engine control factor (unitless). The main engine load factor, LF_m, was calculated as:

$$LF_m = (ActSpeed / MaxSpeed)^3 \qquad (2)$$

where $ActSpeed$ is the actual speed when ship is cruising and $MaxSpeed$ is the maximum design speed for the ship.

Auxiliary engine emissions in grams, E_a, were calculated as

$$E_a = P_a \times LF_a \times T_a \times EF_a \times CF_a \qquad (3)$$

where P_a is the installed power of the auxiliary engine (kW), LF_a is the auxiliary engine load factor, T_a is operation time of the auxiliary engine (h), EF_a is the auxiliary engine emission factor (g/kWh), and CF_a is the auxiliary engine control factor.

Auxiliary boiler emissions in grams, E_b, were calculated as:

$$E_b = P_b \times LF_b \times T_b \times EF_b \times CF_b \qquad (4)$$

where P_b is the installed power of the auxiliary boiler (kW), LF_b is the auxiliary boiler load factor, T_b is the operation time of the auxiliary boiler (h), EF_b is the auxiliary boiler emission factor (g/kWh), and CF_b is the auxiliary boiler control factor (unitless).

The total emissions of the ship in grams, E, were:

$$E = E_m + E_a + E_b. \qquad (5)$$

For ships available in Lloyd's register (IHS Fairplay 2015), the following data were derived from the Lloyd's database: ship name, ship type, date of construction, flag name, revolutions per minute (RPM) of the main engine, speed, maximum design power of the main engine, maximum design power of the auxiliary engines and gross tonnage.

For some domestic ships unavailable in Lloyd's database, the main engine power was assumed to be 7,000 kW by default, based on the East China Sea-going ships in Lloyd's register (with main engine power mainly ranging from 11,000 kW to 14,000 kW) (IHS Fairplay 2015) and domestic ships from the China Classification Society (2016) (with main engine power mainly ranging from 4,000 kW to 6,000 kW). These ships usually contribute less than 1% of the total cargo volume.

Emission factors, low load adjustment multipliers, and control factors for use in Equations 1–3 were based on international and Chinese data. We assumed that the sulfur content of the fuel burned by the main engines was 2.7% for international coastal ships, and 1.5% for domestic coastal ships. The sulfur content of residual oil was about 2.7%, and the sulfur content of marine distillate was 0.5% based on multiyear data from the China Marine Bunker Fuel Oil Company, as described by Fan and colleagues (2016) and consistent with the assumption used in the Third IMO Greenhouse Gas study (IMO Marine Environment Protection Committee 2014). The emission factors for SO_2, NO_x, CO, non–methane volatile organic compounds (NMVOCs), PM ≤10 μm in aerodynamic diameter (PM_{10}), and $PM_{2.5}$ come primarily from the data published in studies by Cooper and Gostafsson (2004), ICF International (2009), and Goldsworthy and Goldsworthy (2015). Emission factors for organic carbon (OC) and elemental carbon (EC) were obtained from the scientific literature (Agrawal et al. 2008a,b; Moldanová et al. 2013; Petzold et al. 2011). Appendix A, Table A-1 (available on the HEI website) summarizes emission factors used for all of the pollutants in the present study.

Emission factors were adjusted for loads below 20% using tables from studies conducted in other studies (ICF International 2009; Starcrest Consulting Group 2009). Because adjustment multipliers were not available for OC and EC, these pollutants were assigned the same low load adjustment multiplier (*LLAM*) as PM_{10} in the present study. Appendix A, Table A-2 lists values for *LLAM* for main engine emission factors.

Control factors were applied to account for control technologies installed on older ships. For all marine engines over 130 kW with engines built on or after January 1, 2000, NO_x limits in MARPOL Annex VI were applied (DieselNet 2018a). We used a control factor of 0.9024 for main engines and a factor of 0.906 for auxiliary engines to adjust the NO_x emissions. For vessels built after 2010, and thus complying with IMO Tier II, we used a main engine control factor of 0.875 and an auxiliary engine control factor of 0.8767 to adjust main engine emissions from ships with emissions controls. All control factors were obtained from ICF International (2009).

4.4.1.2 Inland-Water Ships Emissions from inland-water ships, as defined in this study, were estimated following the methods used for coastal and ocean-going vessels with AIS devices. This inventory was supplemented with 2015 vessel call data provided by the Shanghai Maritime Safety Administration (MSA) and Shanghai Municipal MSA (Y Shen, personal communication, June 2016) for inland-water ships without AIS devices. The Shanghai Environmental Monitoring Center (EMC) used the vessel call data to estimate emissions of PM_{10}, $PM_{2.5}$, SO_2, NO_x, carbon monoxide (CO), and VOCs from these ships at 3-km spatial resolution. The inland-water ship emissions based on the vessel call data were estimated as:

$$E = MCR \times ACT \times EF \times LF \times FCF \times QCF \qquad (6)$$

where E is the emissions in grams, MCR is the maximum continuous rating of the main engine, ACT is the operation time in Shanghai Port, EF is the emission factor for the main engine, LF is the load factor, FCF is the fuel correction factor, and QCF is the quantity correction factor. The load factor was calculated using the propeller law:

$$LF = \left(V_{actual} \ / \ V_{max} \right)^3 \qquad (6a)$$

where V_{actual} is the actual ship speed and V_{max} is the maximum (i.e., design) ship speed. Although actual load factors may deviate from those predicted by the propeller law when vessel speeds are very different from the design speed (Nunes et al. 2017), Equation 6a was applied to all ships to simplify the calculations. The quantity correction factor was calculated as:

$$QCF = \left(Q_{transit} \ + \ Q_{visa} \right) / Q_{visa} \qquad (6b)$$

where $Q_{transit}$ is the number of transit vessels and Q_{visa} is the number of vessels with visa call data.

Emission factors (Appendix A, Table A-3) and fuel correction factors (Appendix A, Table A-4) reported by the Port of Los Angeles were used in the emissions estimation for vessels with visa call data (Agrawal et al. 2011). The fuel correction factor of 0.005% sulfur was used in the emissions estimation for the fuel regulation of river vessels.

4.4.1.3 Emissions from Container-Cargo Trucks and Port Terminal Equipment Emissions from container-cargo trucks within Shanghai (Domain 4) were estimated using the International Vehicle Emission model (Wang et al. 2008). The vehicular activity data were provided by the Shanghai Traffic Department (Wangqi Ge, personal communication, November 2017). The identification of

container-cargo trucks was based on registration information from the Management Department of Vehicles in Shanghai and the online list of diesel particulate matter (DPM) filter systems setup for cargo trucks. Only trucks that carry container cargo or have DPM filter systems were assumed to be associated with the ports and therefore included in the emissions inventory. The fuel oils consumed by the container trucks were diesel oils with the National Standard-3 diesel oils, and we assumed the vehicles themselves were compliant with China V standards. The emission factors for container-cargo trucks were based on the combination of national guidelines and monitoring data from the Shanghai Academy of Environmental Sciences. The emissions from port terminal equipment including the trucks in port were calculated based on fuel consumption for each part of the port. Emissions from container-cargo trucks and port terminal equipment were gridded at 1-km resolution.

4.4.2 Future Ship Emissions Inventory for 2030

Future emissions from ships in 2030 were estimated by scaling the 2015 baseline ship traffic activity based on projections of future ship traffic activity constrained by projected global gross domestic product (GDP) and emission factors adjusted in accordance with the alternative policy scenarios for SO_x and NO_x in Appendix F, Table F-1 (available on the HEI website). The overall equation used to predict future emissions in 2030 was:

Future emissions in 2030 $\qquad$ (7)

$\quad$ = Future total ship traffic activities

$\quad \times$ Constraint factor related to GDP in 2030

$\quad \times$ Adjustment factors related to 2030 policies.

Future total ship traffic activity was predicted based on past total ship traffic activity using the AIS-based model (Equation 5) with *EF*, *FCF*, and *CF* set to 1 by:

Total ship traffic activity $\qquad$ (8)

$\quad = \left(P_m \times LF_m \times LLAM \times T_m \right)$

$\quad + \left(P_a \times LF_a \times T_a \right).$

The total ship activity is a dynamic combination of cargo volume and travel time that accounts for total shipping demand but does not differentiate between ships of different types or sizes. The calculation assumes that port capacity in 2030 will not be a limiting factor because the

majority of ships pass by the port instead of entering it. The total ship traffic activity was first calculated for historical 2013–2017 AIS data. The model was validated by predicting the ship activities in 2017 and comparing the predictions with the actual traffic activities on each grid cell. Then, we scaled total ship activity from 2015 to predict the total ship activity in 2030.

A constraint factor on ship traffic activity is necessary when scaling from 2015 to 2030 because there is a high level of uncertainty in the estimated amount of ship traffic activity in 2030 based on the historical AIS data for 2013–2017. The annual growth of the global real GDP was chosen as the constraint factor because international trade is the most important underlying demand for shipping. The relationship of freight volume with real GDP in China was provided by the research group from the Vehicle Emission Control Center at the Ministry of Environmental Protection (Emission Prediction of Marine for 2030 in China, Vehicle Emission Control Center (VECC) Ministry of Environmental Protection, personal communication, 2018). The total volume of freight transported by ships in 2030 was calculated as:

Total volume of freight by ships $\qquad$ (9a)

$\quad$ = elasticity $\times$ GDP variation

$\quad \times$ waterway freight rate

and

$$GDP_{2030} = \left(1 + GDP_{growth\ rate\ 1} \right)^5 \qquad (9b)$$

$$\times \left(1 + GDP_{growth\ rate\ 2} \right)^5$$

$$\times \left(1 + GDP_{growth\ rate\ 3} \right)^5$$

where the total freight volume transmitted by ships is the domestic total cargo volume in tons, the GDP variation is percent change in value of GDP from 2015 to 2030, and the waterway freight rate is the proportion of waterway freight in the total freight volume in percentage. The elasticity is the ratio of volume of freight to GDP variation, which is usually characterized as the relationship between volume of freight and GDP. GDP_{2030} is the expected GDP in 2030 in China. The GDP growth rates ($GDP_{growth\ rate1}$, $GDP_{growth\ rate\ 2}$, $GDP_{growth\ rate\ 3}$) are rates of increase of GDP in 2016–2020, 2020–2025, and 2025–2030 in China.

The VECC forecasts that GDP will grow by a factor of 1.43 (GDP variation) between 2015 and 2030 and total freight volume transported by ships will increase by 70% (Emission

Prediction of Marine for 2030 in China, VECC, personal communication, 2018). This study introduced a maximum incremental increase of 70% in the total ship freight volume in 2030 to constrain the forecast of ship activity growth from 2015 to 2030.

Adjustment factors for the prediction of future emissions were related to the current policy, stricter policy, and aspirational scenarios for 2030. Adjustment factors were used to calculate adjusted gridded seaborne trade in 2030 $\left(C_{grd,2030}^{adjusted}\right)$ in individual grid cells and at hourly time points by:

$$C_{grd,2030}^{adjusted} = C_{grd,2015}^{actual} \tag{10}$$

$$+ \left(C_{grd,2017}^{predict} \times \frac{C_{total,2017}^{actual}}{C_{total,2017}^{predict}} - C_{grd,2015}^{actual} \right)$$

$$\times \frac{ROC_{2015-2030}}{1 + ROC_{2015-2017}}$$

where C is the amount of ship traffic activity in units of kWh. Superscripts refer to actual historical ship traffic activities (actual), raw unconstrained predictions of ship traffic activities (predicted), and constrained predictions of ship traffic activities (adjusted). Subscripts refer to gridded (grd) and total (total) ship traffic activities in the years 2030, 2015, and 2017. $ROC_{2015-2030}$ is the rate of change of ship activities from 2015 to 2030 and had an assumed value of 70% to constrain the forecast of ship activity growth. $ROC_{2015-2017}$ was calculated by:

$$ROC_{2015-2017} = \frac{\left(C_{total,2017}^{actual} - C_{total,2015}^{actual} \right)}{C_{total,2015}^{actual}} \tag{11}$$

We estimated SO_2 and NO_x emissions in 2030 in different ways. For sulfur emissions, we adjusted emission factors according to the allowable sulfur content of ship fuels under each emissions control policy. NO_x emission reductions depend on the gradual adoption of new engine technologies (e.g., exhaust gas recirculation, selective catalyst reduction, and liquefied natural gas as stricter NO_x engine standards are enacted and older, higher emitting ships are retired; consequently, we assumed a 25-year lifetime for ships and marine engines for the engine renewal (i.e., 100% turnover) period. Installed NO_x emission reduction technologies for each engine were assumed based on the emissions and control technology requirements in place at the time when the engines were sold.

4.4.3 Non-Shipping Emissions Inventories

To establish the overall baseline impact of all sources on air quality in the YRD and in Shanghai it was necessary to characterize emissions from all other major sources. Major categories of non-shipping air pollutant sources included power plants, industry, mobile sources, area sources, VOC-related sources, and biogenic sources. National (Domain 2) and YRD (Domain 3) emissions inventories were used for non-shipping or land-based emissions. For the national scale domain (Domain 2), we obtained a 2015 national emissions database at 27 km × 27 km resolution that included 5 pollutants (PM_{10}, $PM_{2.5}$, SO_2, NO_x, and VOCs) and 14 pollution source types from investigators at Tsinghua University (S. Wang, personal communication, December 2017). Because the national emissions inventory database available at that time lacked data on CO and ammonia (NH_3) emissions, which are compulsory inputs for CMAQ, supplemental data on these pollutants were obtained at 0.5° × 0.5° resolution from the International Institute for Applied Systems Analysis (IIASA) database (Stohl et al. 2015). The ratio of CO to VOCs was 7.7 in the IIASA inventory and 7.5 in the final combined inventory (Feng et al. 2019). Thus, the CO/VOC shares in these two inventories were very close, and the use of the final combined inventory is acceptable. The Shanghai Academy of Environmental Sciences provided the more detailed YRD land-based emissions inventory at a 4 km × 4 km resolution; it included eight source types and seven pollutants (PM_{10}, $PM_{2.5}$, SO_2, NO_x, CO, VOCs, and NH_3). Pollution sources and pollutants in the non-shipping emissions inventories are listed in Table 4-2.

For evaluation of 2030 policy scenarios in the YRD, emissions inventory projections for non-shipping sources were obtained from Tsinghua University. These inventories assume full implementation of the Chinese government's strictest plans for air pollutant emissions reductions (Cai et al. 2018).

4.5 MODELING AIR QUALITY

An air quality model was used to simulate ambient $PM_{2.5}$ concentrations in the YRD region and Shanghai, with a spatial resolution of 9 × 9 km and 1 × 1 km, respectively (Feng et al. 2019). The air quality model used in this study was the CMAQ model (version 4.6) with meteorological inputs from the WRF model (version 3.3). Model setup and predictions for the 2015 baseline year and for 2030 scenarios differed only in the emissions inventories used as inputs to the models. All other conditions were assumed to be the same.

Table 4-2. Pollution Source Types and Pollutants in National-Scale and YRD-Scale Non-shipping Emissions Inventories

Modeling Domain / Land-Based Pollution Source Types	Pollutants
National-scale emissions inventories: Domain 1 (East Asia) and Domain 2 (China)	
Power plant, steel, cement	SO_2, NO_x, $PM_{2.5}$, PM_{10}, CO, NH_3
Industrial point source	SO_2, $PM_{2.5}$, PM_{10}
Industrial combustion, industrial process, domestic fuel combustion, domestic biomass combustion, on-road traffic, non-road traffic, open combustion	SO_2, NO_x, $PM_{2.5}$, PM_{10}, VOCs, CO, NH_3
Residential solvent, industrial solvent	VOCs
Agriculture, residential and commercial, waste	CO, NH_3
YRD-scale emissions inventories: Domain 3 (YRD), and Domain 4 (Shanghai)	
Power plant, industrial boiler, industrial process, domestic source	SO_2, NO_x, $PM_{2.5}$, PM_{10}, CO, NH_3, VOCs
On-road traffic	NO_x, $PM_{2.5}$, PM_{10}, CO, NH_3, VOCs
Non-road traffic	SO_2, NO_x, $PM_{2.5}$, PM_{10}, CO, VOCs
Dust	$PM_{2.5}$, PM_{10}
Agriculture	NH_3

4.5.1 WRF-CMAQ Model Setup

The initial and boundary conditions for meteorology were generated from the Chinese National Centers for Environmental Prediction Final Analysis with resolution at 1° × 1° at 6-hour time intervals. Vertically, 27 sigma layers were set for the WRF simulation, and the results were then converted to the 24 layers required by CMAQ using the Meteorology-Chemistry Interface Processor. CMAQ was configured to use the Carbon Bond mechanism for gas-phase chemistry and the AERO4 aerosol module (Liu et al. 2017).

Simulations were run for either the full year where resources allowed or for representative months informed by seasonal meteorological patterns. For the base year of 2015, simulations were performed over the full year of January 2015 to December 2015 for the YRD region and for the representative months of January, April, June, and October in 2015 for Shanghai. July is typically used as a representative month for summer in China, but at the time of the study, only June data were available so those were used instead. For the future scenarios, simulations were conducted only for the YRD region for the representative months of January, April, July and October. These representative months were selected from each season to capture the range of wind fields experienced throughout the year. Prevailing winds are from the northeast and southeast in spring (March, April, and May) and during the summer monsoon (June, July, and August), from the

northeast in autumn (September, October, and November), and from the northwest during the winter monsoon season (December, January, and February) (Appendix A, Figure A-1). Especially in summer, under the influence of the summer monsoon, the wind from the ocean to the land is stronger than in the other seasons. Where representative months were used, the average $PM_{2.5}$ concentrations from those months were treated as annual average concentrations. The appropriateness of this assumption was evaluated by comparing annual average $PM_{2.5}$ concentrations in the YRD in 2015 with the average of the $PM_{2.5}$ concentrations in the four representative months (Appendix E, Section 1, available on the HEI website). In addition, the effects of seasonality were evaluated by comparing results for the four seasons in 2015.

Performance of the CMAQ model simulations in January and June 2015 was evaluated spatially by comparing them with monthly-average observations at monitoring stations across the YRD region (Appendix E, Section 2). Also, daily-average observations from 53 monitoring stations in 16 core YRD cities were compared with daily-average simulated ambient SO_2 and $PM_{2.5}$ concentrations. Normalized mean bias, normalized mean error, root mean-square error, and Pearson's correlation coefficient were used to qualify the degree of deviation between the observed data and modeling results (Eder and Yu 2006).

4.5.2 Estimation of Fractional Contributions from Individual Sources to Ambient PM$_{2.5}$ Concentrations in 2015

For the YRD region (Domain 3), simulations were conducted for all ships included in the AIS database. Impacts of ships operating within different boundaries from shore (12 NM, 12–24 NM, 24–48 NM, 48–96 NM, and 96–200 NM) were also modeled and have been published (Feng et al. 2019). For the city of Shanghai (Domain 4), simulations were conducted for: all ship-related activity within approximately 12 NM of shore, coastal and ocean-going vessels, inland-water ships, and the combination of container-cargo transport and port terminal equipment (combined because of their smaller emissions relative to ships and other non-port sources). The detailed assumptions for each of the simulations can be found in Appendix A, Table A-5. Given their smaller emissions relative to shipping and other non-port sources, emissions from container-cargo trucks and terminal equipment were combined and gridded at a resolution of 1 km × 1 km.

4.6 ESTIMATION OF POPULATION EXPOSURE TO PM$_{2.5}$

Population-weighted PM$_{2.5}$ concentrations are a better approximation of potential human exposure than ambient concentrations because they give proportionately greater weight to concentrations in areas where most people live. We estimated population-weighted PM$_{2.5}$ concentrations for the YRD and its 16 core cities and for Shanghai and its 16 administrative districts. The population-weighted PM$_{2.5}$ concentration of the given grid cell i is calculated based on the following equation (Brauer et al. 2012; U.S. EPA 2015):

Population-weighted PM$_{2.5}$ concentration $\qquad$ (12)

$$= \sum_{i=1}^{n} \left(PM_i \times \frac{P_i}{\sum_{i=1}^{n} P_i} \right)$$

where, PM_i is defined as the PM$_{2.5}$ concentration in the ith grid cell, P_i is the population in the ith grid cell, and n is the number of grid cells in the selected geographical area (e.g., city or region).

4.7 ESTIMATION OF SOURCE CONTRIBUTIONS TO HEALTH BURDEN

Environmental Benefits Mapping and Analysis Program-Community Edition software (BenMAP-CE, version 1.4) was used to estimate human health impacts resulting from changes in PM$_{2.5}$ population-weighted concentrations

attributable to individual sources for both the 2015 baseline year and for 2030 under alternative control policies. Developed originally by the U.S. EPA, this model has been widely used in the United States and in international research for quantifying health risks. BenMAP-CE has been incorporated into the Air Benefit and Cost and Attainment Assessment System (ABaCAS, *www.abacas-dss.com*), which is widely used to support policies affecting air quality in China.

4.7.1 Analysis Process

BenMAP-CE relates a change in air quality to an estimated change in the incidence of mortality or morbidity from specific health endpoints in most cases via the following function:

$$\Delta Y = Y_0 \left(1 - e^{-\beta \, \Delta PM_{2.5}} \right) \times Pop \qquad (13)$$

where ΔY is the number of cases attributable to a change in air quality, Y_0 is the baseline incidence rate of the health outcome in the population of interest, the coefficient β is the percentage change in the risk of an adverse health effect due to a unit change in air pollution derived from the epidemiological literature, $\Delta PM_{2.5}$ is the change in PM$_{2.5}$ attributed to a source or particular policy, and *Pop* is the exposed population. For this study, we are focused primarily on mortality outcomes, except for hospital admissions. Where there are multiple concentration–response functions for the same health endpoint (in this study, for example, cause-specific integrated exposure response [IER] functions for different age groups: ≤ 44, 45–64, ≥65), they were combined using a sum-dependent fixed-effects pooling procedure within BenMAP-CE with each estimate weighted in proportion to the inverse of its variance. BenMAP-CE utilizes a Monte Carlo approach to characterize uncertainty in the estimated change in the incidence of the health outcomes of interest. The uncertainty is reported as 95% confidence intervals.

The changes in air quality incorporated into BenMAP for this study were the average gridded changes in PM$_{2.5}$ simulated by CMAQ to estimate the contribution of individual shipping sources relative to the baseline both in 2015 and in 2030 under different policy scenarios.

4.7.2 Data Sources

4.7.2.1 Health Outcomes of Interest and Concentration–Response Functions A workshop with nearly 20 Chinese and international experts in the field of environmental epidemiology and air pollution was convened in December 2017 to evaluate the most relevant Chinese and

international studies for identifying the health effects associated with air pollution exposure and for characterizing the most appropriate concentration–response functions for this analysis (see Additional Materials, available on the HEI website, for the workshop agenda and attendees). The attendees agreed on several broad criteria for inclusion in the discussion. For cohort studies of long-term exposures, preference was given to nationally representative studies, ideally in China, with large sample sizes and at least 5 years of follow-up. For studies of short-term (e.g., daily) exposures, preference was given to multicity time-series studies with large populations (>1 million population) and with at least 1 year of exposure data. Preference was given to studies using measurements of $PM_{2.5}$ directly but conversion factors were considered in some cases where other PM size fractions were measured (e.g., 0.30 for total suspended particulate to $PM_{2.5}$, 0.7 for PM_{10} to $PM_{2.5}$) (Harrison et al. 2003; Yin and Harrison 2008).

Another important consideration was which health outcomes to include in the impact assessment. The workshop attendees agreed that it was appropriate to assess total non-accidental mortality as well as all the health outcomes included in the Global Burden of Disease project as of 2015 (Cohen et al. 2017). For long-term exposures, these included: total non-accidental mortality, and mortality from cerebrovascular disease (stroke), COPD, ischemic heart disease (IHD), and lung cancer as identified and classified by International Classification of Diseases codes, 10th version. For short-term (i.e., daily) exposures, the workshop attendees recommended evaluation of total

nonaccidental mortality, mortality from cardiovascular diseases and respiratory diseases, and morbidity as indicated by total hospital admissions.

Table 4-3 summarizes the studies used to characterize the concentration–response functions for the effects of long- and short-term exposure in this analysis. Although China has recently started to publish the findings from major cohort studies of long-term exposures to $PM_{2.5}$ in Chinese populations, few were available at the time of the workshop. The recommendation was to rely on the 2015 IER functions developed for the Global Burden of Disease project for the mortality outcomes listed above (Cohen et al. 2017). Although the GBD also includes mortality from respiratory infections, they were not included in this study due to lack of available Chinese mortality rate data for the analysis. The following age-specific IER functions were used for the specific causes of death: 25–44 years, 45–64 years, 65–99 years for stroke and IHD; and 30–99 years for COPD and lung cancer.

As concentration–response functions are an important source of uncertainty in health impact analysis, additional sensitivity analyses were conducted using the Global Exposure Mortality Model (GEMM) functions that were published subsequent to the workshop (Burnett et al. 2018). The IERs were developed at a time when epidemiological evidence from regions like China with high levels of $PM_{2.5}$ were unavailable, so the authors combined evidence from studies of other PM exposures — environmental tobacco smoke, household air pollution, and active smoking — along with studies of outdoor air pollution to

Table 4-3. Concentration–Response Functions Used to Characterize Relationships Between $PM_{2.5}$ and Health

PM$_{2.5}$ Exposure: Outcome	Specific Outcomes	Sources of Concentration–Response Functions	
		Main Analyses	Sensitivity Analyses
Long-term: mortality	All natural cause (GEMM only) Cerebrovascular disease (stroke) IHD Lung cancer COPD	Integrated exposure response functions from the Global Burden of Disease project (Cohen et al. 2017)	GEMM functions (Burnett et al. 2018)
Short-term: mortality	Total non-accidental causes Cardiovascular Respiratory	Chinese 272 cities study (Chen et al. 2017b)	None
Short-term: morbidity	Total hospital admissions	Chinese 200 cities study (Tian et al. 2019)	None

Abbreviations: COPD = chronic obstructive pulmonary disease; GEMM = Global Exposure Mortality Model; IHD = ischemic heart disease.

characterize risks across the global range of air pollution exposures. With the publication of more air pollution studies with a wider range of exposures, the GEMM functions were developed by pooling results from 15 cohort studies of ambient air pollution (Burnett et al. 2018), including a cohort of men from China (Yin et al. 2017). The GEMM analysis also includes a response function for all-natural-cause (nonaccidental) mortality to address the criticism that the IERs are limited to specific causes and may underestimate the full effects of air pollution that are reflected in many studies of all-natural-cause mortality. Therefore, we conducted sensitivity analyses using the new GEMM functions as one indication of the uncertainty in the mortality results based on the IERs.

For assessment of the effect of short-term exposures, concentration–response functions from the time-series study of 272 Chinese cities were used to estimate daily mortality from total, cardiovascular, and respiratory endpoints (Chen et al. 2017b). The study of total hospital admissions in 200 Chinese cities was used to quantify the morbidity health burden (Tian et al. 2019). In the absence of daily mortality rate data for China we applied a scalar (1/365) to the annual average mortality rates to convert them to daily rates in BenMAP (N. Fann, personal communication, June 2018). The daily average $PM_{2.5}$ concentrations were assumed to be the same as annual average $PM_{2.5}$ concentrations.

Values for all of the health impact functions used in this study are provided in Appendix A, Table A-6.

4.7.2.2 Baseline Mortality and Morbidity Rates Baseline annual mortality and morbidity rates in the YRD and Shanghai are summarized in Appendix A, Table A-7 for each of the health endpoints included in our study. The cause-specific baseline mortality and morbidity rates were provided by China Center for Disease Control (CDC) across multiple age groups (China CDC, personal communication, July 2018). The total mortality rates were estimated to be 7.61 per 1,000 people and 6.01 per 1,000 people for YRD and Shanghai, respectively, in 2015, derived from the age and cause-specific mortality data provided by the China CDC (see Table A-7 for details). Analysis of morbidity related to $PM_{2.5}$ was limited to total hospital admissions (from all causes) for Shanghai, Zhejiang, and Jiangsu provinces because cause-specific hospitalization data were not available and may therefore overstate the number of hospitalizations attributable to $PM_{2.5}$ (National Bureau of Statistics of China 2019). In 2005–2007, 30% of hospital admissions in Shanghai were for cardiovascular or respiratory diseases, which have been more strongly associated with air pollution exposures (Chen et al. 2010).The baseline morbidity rates in 2015 were 17.87 admissions/1,000 people for YRD, and 22.11 admissions/1,000 people for Shanghai, comparable to rates observed in Hong Kong.

4.7.2.3 Exposed Population The population density of the YRD region in the year 2015 was obtained from Landscan at 1-km resolution (Bright et al. 2016). Population data were used at the 1-km resolution in Shanghai and were aggregated to 9-km grid cells for analyses in the YRD region (Figure 4-3). Figure 4-3 shows the geographical area and population density for the YRD and Shanghai, the location of 16 core cities* of the YRD region, and 16 administrative districts** within Shanghai. The coastal cities in the YRD are Nantong, Shanghai, Jiaxing, Ningbo, Taichou, and Zhoushan. The population density was highest in central Shanghai (35,802/km² in a 9-km grid cell or 68,000/km² in a 1-km grid cell) and was lower in the suburban districts of Shanghai.

For use with the age-specific IER functions, population data were further categorized into the same age groups relevant to the IERs by the proportions of the population in each age group in 2015 according to China CDC data (personal communication, July 2018). As we did not simulate changes in population and baseline mortality rates in the future scenario, the 2015 data were also used for analyses of scenarios in 2030.

5.0 RESULTS

5.1 BASELINE (2015) EMISSIONS

5.1.1 Ships in the YRD Region

Emissions from all ships in the YRD region (modeling Domain 3) included in the AIS dataset were 2.2×10^5 metric tons SO_2 (7.4% of SO_2 emissions from all sources in the YRD), 4.8×10^5 metric tons NO_x (11.7% of NO_x emissions from all sources in the YRD), and 2.7×10^4 metric tons $PM_{2.5}$ (1.3% of $PM_{2.5}$ emissions from all sources in the YRD) in 2015. Comparison of the emissions estimates to those from similar studies suggests that the estimates in this study are reasonable, though some differences exist related to different time periods and spatial coverage among the studies. The estimates of SO_2 and NO_x emissions were close to estimates from 2013 (Fu et al. 2017). However, estimates of SO_2, NO_x, and $PM_{2.5}$ emissions were 22%–45% lower than the estimates of Chen and colleagues for 2014 due to different temporal or spatial scope (Chen et al. 2019) (see also Appendix B, Table B-1; available on the HEI website). The proportion of total China SO_2 emissions from shipping occurring

*The core cities of the YRD are Changzhou, Hangzhou, Huzhou, Jiaxing, Nanjing, Nantong, Ningbo, Shanghai, Shaoxing, Suzhou, Taichou, Taizhou, Wuxi, Zhenjiang, and Zhoushan (see Figure 4-3).

** The administrative districts of Shanghai are Baoshan, Changning, Chongming, Fengxian, Hongkou, Huangpu, Jiading, Jinshan, Jing'an, Minhang, Pudong, Qingpu, Songjiang, and Xuhui (see Figure 4-3).
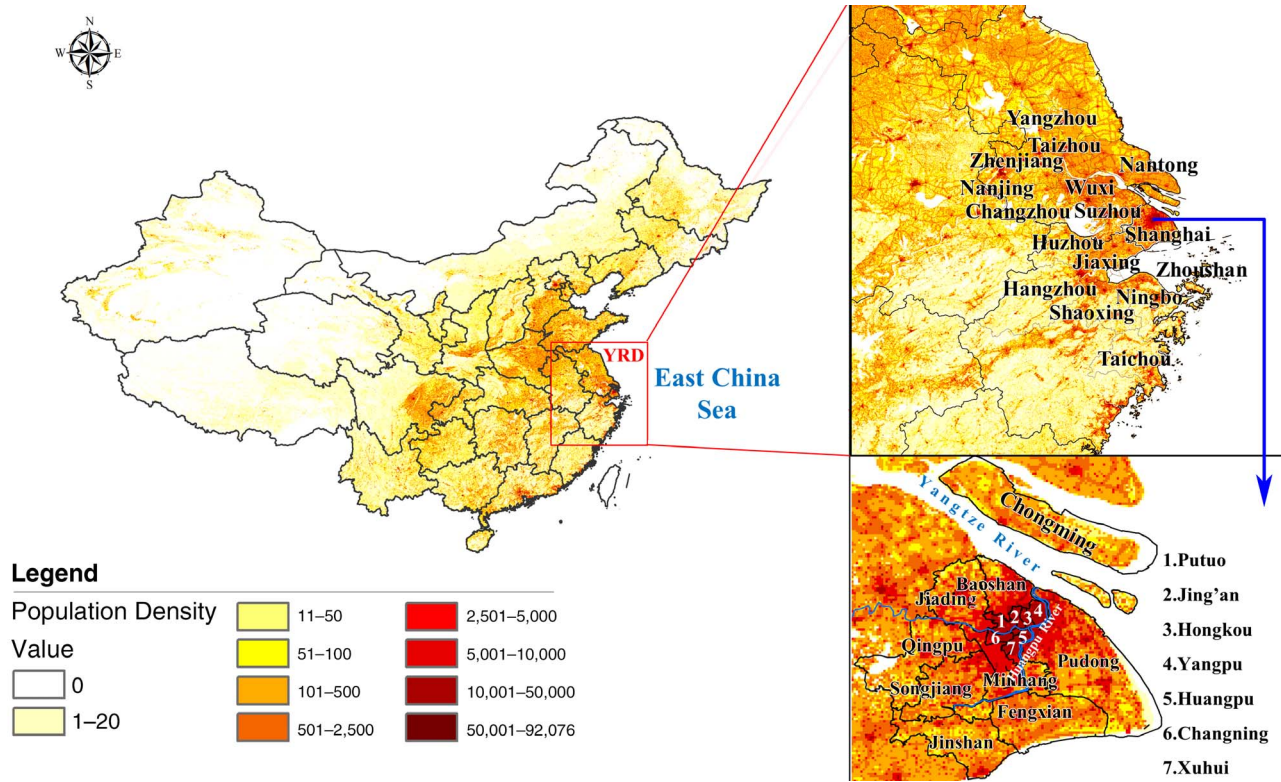
Figure 4-3. Population density (person/km² in 2015 within China (Domain 2, left), the YRD (Domain 3, top right), and Shanghai (Domain 4, bottom right). A total of 16 core cities in the YRD and 16 administrative districts in Shanghai are noted. (Reproduced from Feng et al. 2019; distributed under Creative Commons Attribution 4.0 License.)

Table 5-1. Primary Emissions, Percent of all Emissions from Ships, and Emission Density from Ships at Different Distances up to 200 NM from Shore in the YRD Region in 2015 (Data from Feng et al. 2019.)

Pollutants	Emissions within Distances (NM) from Shore					
	<12	12–24	24–48	48–96	96–200	Total
Ship Emissions (thousands of metric tons/yr)						
SO₂	130	14	25	32	13	214
NOₓ	360	20	35	45	18	478
PM₂.₅	13	2.4	4.5	5.4	1.5	27
VOCs	7.9	0.8	1.3	1.5	0.3	11.8
Emission Density (metric tons/yr/km²)						
SO₂	0.66	0.54	0.49	0.33	0.06	0.41
NOₓ	1.74	0.86	0.77	0.51	0.08	0.89
PM₂.₅	0.08	0.06	0.06	0.04	0.01	0.05
VOCs	0.05	0.02	0.01	0.01	0.001	0.02
Percentage of All Ship Emissions (%)						
SO₂	61	6.5	12	15	6.1	100
NOₓ	75	4.1	7.4	9.6	3.9	100
PM₂.₅	48	9.0	17	20	5.5	100
VOCs	67	7.0	11	13	2.6	100

within the YRD in this study was 31%, consistent with the 33% to 37% range reported in the other studies (Chen et al. 2017, 2019; Liu et al. 2018; Lv et al. 2018).

Spatial analyses of ship emissions in the YRD reinforce the importance of shipping within 12 NM, including inland waterways. Between 48% and 75% of air pollutant emissions occur within 12 NM of shore (Table 5-1), depending on the pollutant, with over 90% of air pollutants accounted for within 96 NM. Geographical patterns of SO_2 emissions from coastal and inland-water ships are illustrated in Figure 5-1. These results are different from those reported by Johansson and colleagues (2017), who found similar $SO_2/PM_{2.5}$ emissions ratios in different water areas near the Chinese coast. We suspect several possible reasons for these differences, including that we accounted for higher proportions of domestic ships using lower-sulfur fuel closer to the coast whereas the study by Johansson and colleagues assumed the same fuel sulfur content for all ships.

When analyzed by months representative of each season, emissions of all pollutants from ships were the greatest in summer (June). The fraction of emissions of different pollutants that occurred during summer months ranged from more than 28% of annual SO_2 to about 32% of annual VOC ship emissions, about 1.09 to 1.54 times higher than other seasons (Appendix B, Figure B-1). Lv and colleagues (2018) reported that the seasonal differences in ship emissions in 2013 in China were similar in magnitude.

The spatial distribution of ship emissions also varied seasonally (see Appendix B, Figure B-2 for SO_2), with larger numbers of ships traveling in the international lanes in spring and summer and more ships traveling between Chinese ports (e.g., between Shanghai port and Ningbo-Zhoushan port) in winter. These patterns were consistent with those of other studies (Fan 2016; Lv et al. 2018). The spatial and seasonal distributions of ship emissions, together with seasonal variations in meteorology, contribute to seasonal differences in air quality across the YRD region.

5.1.2 Individual Ship-Related Sources in Shanghai

In 2015, shipping-related sources in Shanghai (modeling Domain 4) emitted 4.9×10^4 metric tons of primary SO_2, 1.4×10^5 metric tons of NO_x, 6.5×10^3 metric tons of $PM_{2.5}$, and 0.47×10^4 metric tons of VOCs in 2015 (Table 5-2). They accounted for an estimated 17% of SO_2, 29% of NO_x, and 5.9% of $PM_{2.5}$ emissions from all sources in modeling Domain 4. Estimates of emissions from ships in Shanghai from this study can be compared with those from other studies in the same area (Appendix B, Table B-2). On the basis of shipping visa data, Fu and colleagues (2012) estimated that annual emissions in the vicinity of Shanghai port in 2010 were 3.5×10^4 metric tons/year SO_2, 4.7×10^4 metric tons/year NO_x, and 3.7×10^3 metric tons/year $PM_{2.5}$, substantially lower than estimates in this study. However, when they used AIS data from 2013, Fu and colleagues (2017) reported 5×10^4 metric tons of SO_2 and 7×10^4 metric tons of NO_x from shipping in the same area as for the Shanghai city study area (Domain 4), closer to the results in this study. The results of the more recent study by Fu and colleagues may be more similar to those from this
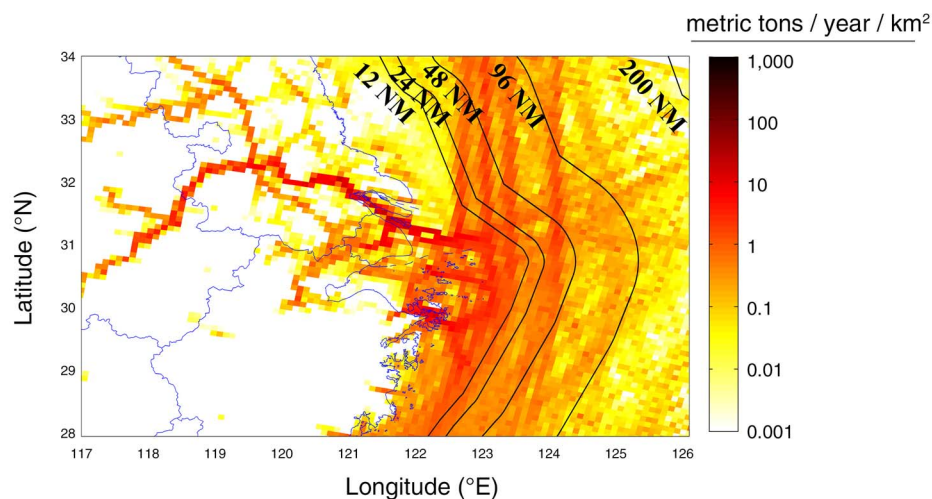

Figure 5-1. Spatial pattern of SO_2 emissions (metric tons/yr/km²) in 2015 from ships in offshore coastal areas and inland rivers in the YRD region.

Table 5-2. Primary Emissions and Percentage of All Pollution Sources for Individual Ship-Related Sources in Shanghai in 2015 (Data from Feng et al. 2019.)

Shipping-Related Source	Percentage Contributions from Pollutants			
	SO_2	NO_x	$PM_{2.5}$	VOCs
Emissions (thousands of metric tons/yr)				
Inland-water ships[a]	33	92	4.0	2.7
Coastal/international ships	16	29	1.8	0.67
Container-cargo trucks	0.00	18	0.64	1.1
Port terminal equipment[b]	0.021	1.8	0.057	0.22
Sum of shipping-related sources	49	141	6.5	4.7
Percent (%) Contribution to Emissions from Shipping-Related Sources in Shanghai				
Inland-water ships[a]	67	66	62	57
Coastal/international ships	33	21	28	14
Container-cargo trucks	0.00	13	9.8	23
Port terminal equipment[b]	0.04	1.3	0.8	4.7
Percent (%) Contribution to Emissions from All Air Pollutant Sources in Shanghai				
Inland-water ships[a]	11.8	18.7	3.6	0.50
Coastal/international ships	5.6	5.8	1.6	0.10
Container-cargo trucks	0.00	3.7	0.60	0.20
Port terminal equipment[b]	0.01	0.36	0.05	0.04
Sum of shipping-related sources	17	29	5.90	0.84

[a] Defined as ships operating in both the outer port and in the inner river region of Shanghai Port, which include Yangtze River, Huangpu River and other river ways in Shanghai (see Figure 4-1).

[b] Includes cranes and forklifts used for internal transport.

study because they more completely assessed emissions from the activity of the larger ships inside and outside of the port areas as captured by AIS or because they also reflected an increase in shipping between 2010 and 2015.

Within Shanghai, inland-water ships were the most important ship-related source of emissions, accounting for 67% of SO_2, 66% of NO_x, 62% of $PM_{2.5}$, and 57% of VOC emissions from all ship-related sources (Table 5-2). They comprised 11.8% of SO_2, 18.7% of NO_x, 3.6% of $PM_{2.5}$, and 0.5% of VOC emissions from all air pollution sources in Shanghai. Contributions of cargo trucks and port terminal equipment to primary emissions were small relative to other shipping-related sources in Shanghai (only 4.1% of NO_x and <1% of SO_2, $PM_{2.5}$, and VOC primary emissions from both sources together); therefore, they were combined into one category for air quality model simulations.

The spatial patterns of annual emissions from ship-related sources in Shanghai are shown in Figure 5-2 for SO_2. SO_2 emissions from coastal and international ships were more prominent on the east–west shipping lanes and in the vicinity of Yangshan port, whereas SO_2 emissions from inland-water ships were concentrated along the Yangtze and Huangpu rivers, which run through the center of Shanghai. SO_2 emissions from cargo trucks and terminal equipment were distributed across the city, with their highest emission density around the Shanghai port cluster (e.g., Yangshan port).

5.2 CONTRIBUTION OF SHIPPING SOURCES TO AMBIENT AIR QUALITY

5.2.1 YRD Region

Ships contributed on average 0.53 μg/m³ of $PM_{2.5}$ over the YRD region (Table 5-3). Within individual grid cells, annual average contributions of ships ranged from 0.4 to 1.3 μg/m³, or 0.5% to 2.5% of all $PM_{2.5}$ (Appendix C, Table C-1, available on the HEI website). Our results are similar to those of Lv and colleagues (2018) and Chen and colleagues (2019), who also reported small contributions of
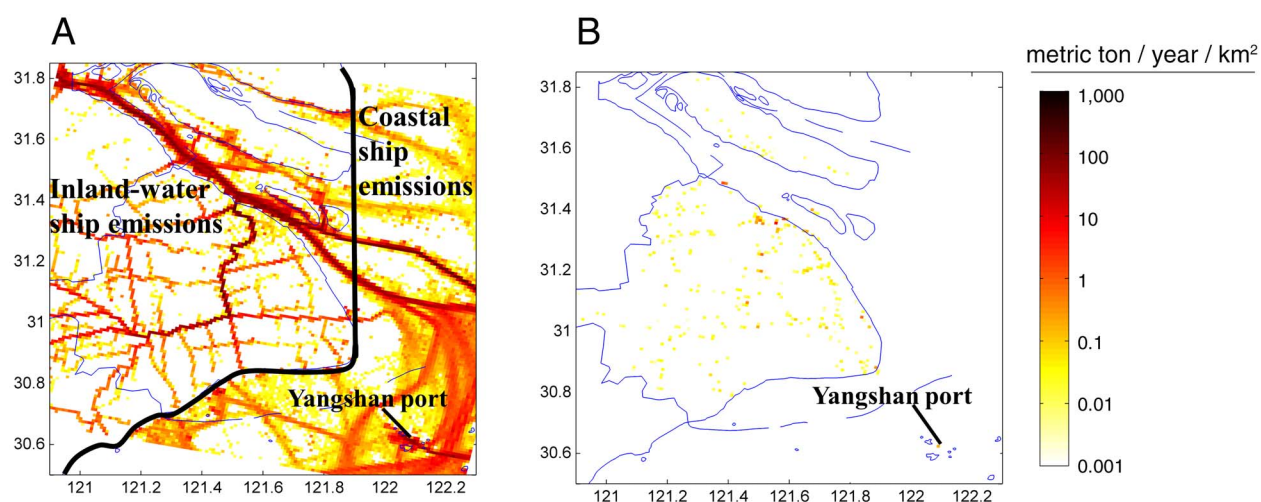
Figure 5-2. Spatial patterns of annual SO$_2$ emissions (metric tons/yr/km^2) at 1-km spatial resolution: (A) from inland-water ships and coastal ships in Shanghai; and **(B)** from container-cargo trucks and port terminal equipment in Shanghai. The black line in (A) refers to the division line between the inland water and coastal water for Shanghai (Domain 4 in this study).

Table 5-3. Summary of Annual Average Ambient PM$_{2.5}$ (µg/m^3) Concentrations in 2015

	YRD[a]	Shanghai[b]		
Scenarios	All Ships	Inland Ships	Coastal Ships	Trucks and Port Machinery
All sources	37.98	49.45	49.45	49.45
No ships	37.45	49.21	49.28	49.37
Ship contribution	0.53	0.24	0.17	0.08

[a] PM$_{2.5}$ estimates from Domain 3 emissions inventory.

[b] PM$_{2.5}$ estimates from Domain 4 emissions inventory. Note that the Shanghai domain did not include emissions from ships outside of the domain, which contributed a large proportion of Shanghai exposure.

ships to the annual average PM$_{2.5}$ over the YRD region. Based on our evaluation of air quality modeling results from all sources of PM$_{2.5}$ and SO$_2$ with monitoring data, these results appear reasonable but are more likely to underestimate the actual contributions than to overestimate them (Appendix E, Section 2).

Shipping-related PM$_{2.5}$ concentrations were higher at greater distances from the sources than would be expected based on primary emissions of PM$_{2.5}$ from ships because of secondary PM$_{2.5}$ formed during long-distance transport. In summer, the prevailing strong monsoon (from sea to the land) also tends to spread ship-emitted PM$_{2.5}$ further inland. Ship-related PM$_{2.5}$ concentrations were in the range of 1.0 to 4.5 µg/m^3 (2% to 17% of PM$_{2.5}$ from all pollution sources) in highly influenced areas near the Yangtze River and Shanghai Port during the summer (also see

Appendix C, Figure C-4). In winter, due to the winter monsoon (prevailing winds flow from land to sea), the impact of shipping on PM$_{2.5}$ concentrations in coastal areas was the lowest, in the range of 0.4 to 2 µg/m^3 (1% to 4% of PM$_{2.5}$ from all pollution sources).

5.2.1.1 Spatial and Seasonal Trends Although the primary focus of the study was on PM$_{2.5}$, for the purposes of completeness we also evaluated the contributions of SO$_2$, NO$_x$, and O$_3$ from shipping-related sources as well as their spatial and temporal trends. As for PM$_{2.5}$, the modeled contributions of shipping to ambient SO$_2$ and NO$_x$ concentrations in 2015 were highest in the vicinity of rivers and ports where primary emissions from shipping were also high (Figure 5-3). The impacts of emissions from ships on SO$_2$ and NO$_x$ concentrations in geographical areas farther

33
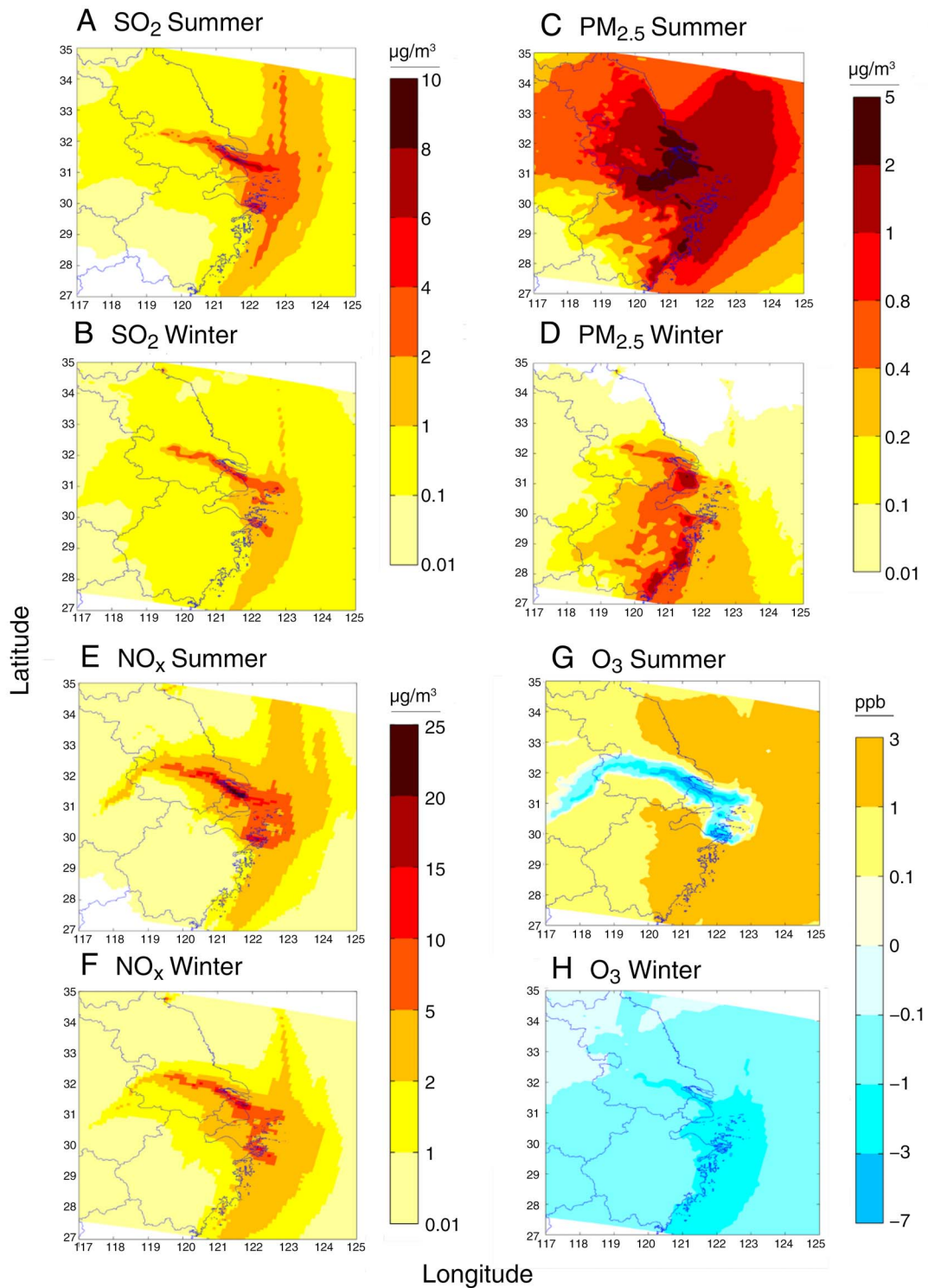
Figure 5-3. Average contribution of ships to ambient SO$_2$ (A and B), PM$_{2.5}$ (C and D), NO$_x$ (E and F), and O$_3$ (G and H) in the YRD in June, July, and August (summer, A, C, E, and G) and December, January, and February (winter, B, D, F, and H) 2015. Results for all four seasons are shown in Appendix C for SO$_2$ (Figure C-1), PM$_{2.5}$ (Figure C-4), NO$_x$ (Figure C-2), and O$_3$ (Figure C-3). Provinces are outlined in purple.

from the high-intensity shipping areas were very small (e.g., contribution of less than 0.1 μg/m³ SO_2). Spatial trends in O_3 were the inverse of the trends in these other pollutants, with levels lowest near the emissions sources, likely because of titration by NO_x.

Variation in meteorological conditions resulted in seasonal differences in the impacts of ship emissions on air pollutant concentrations in the YRD region (Figure 5-3). For example, ships contributed 2–6 μg/m³ SO_2 (20%–50% of all ambient SO_2) near Shanghai Port and Ningbo-Zhoushan Port in summer, but only around 1–2 μg/m³ SO_2 (5% to 20% of all ambient SO_2) in winter (Figure 5-3 and Appendix C Figure C-1). Seasonal trends in contributions of ships to NO_x concentrations in the YRD were similar (Appendix C Figure C-2). Although ships increased O_3 at some locations in the northern and southern YRD areas in summer 2015 (0.1 to 3 ppb), shipping decreased average O_3 concentrations across the YRD region in winter 2015 (range from −3 to −0.1 ppb in individual 9-km grid cells) (see also Appendix C Figure C-3).

The impacts of these spatial and temporal trends can be viewed in more detail by comparison of the impacts of ship emissions on seasonal average concentrations of ship-related air pollutants in 16 government-designated core YRD cities (Appendix C Figures C-5 to C-8). For example, the average contribution of ship-related SO_2 in core YRD cities was higher in summer (0.1 to 2.7 μg/m³) and spring (0.2 to 2.6 μg/m³), followed by autumn (0.2 to 1.8 μg/m³), and lowest in winter (0.1 to 1.2 μg/m³) (Appendix C Figure C-5). Ship contributions to SO_2 were highest in the two biggest ports in the YRD, Zhoushan and Shanghai. In Zhoushan, which is located close to the sea and to Ningbo-Zhoushan port, ship contributions to SO_2 were elevated in all four seasons, ranging from 1.2 μg/m³ in winter to 2.6 μg/m³ in summer. For Shanghai, located close to Shanghai port and the Yangtze River, ship contributions to seasonal average SO_2 were similar, ranging from 1.0 μg/m³ in winter to 2.5 μg/m³ in summer. In most cities, the influence of shipping on ambient SO_2 concentrations was highest in spring or summer. However, several cities south of the Yangtze River were impacted more strongly in autumn (e.g., Jiaxing [0.7 μg/m³], Shaoxing [0.5 μg/m³], and Huzhou [0.4 μg/m³]) than in other seasons, possibly due to the prevailing northeastern wind in autumn that could transport more ship-emitted SO_2.

5.2.1.2 Impacts of Emissions at Different Distances from Shore on Air Quality
January and June were chosen to study the impact on ambient air pollutant concentrations of emissions from ships at different distances offshore because these two months were expected to reflect the

lowest (January) and highest (June) impacts. We focused this part of the analysis on $PM_{2.5}$ given its impact on health and on SO_2 as a marker of primary ship emissions. In both months, the ships closest to shore had the largest impacts on ambient SO_2 and $PM_{2.5}$ concentrations in the YRD (Appendix C Figure C-9). Ships within 12 NM of shore (including inland waters) contributed on average 0.24 μg/m³ to the ambient $PM_{2.5}$ concentrations in January 2015 and 0.56 μg/m³ to ambient $PM_{2.5}$ concentrations in June 2015 (Appendix C Table C-2). Peak contributions from these ships were 1.62 μg/m³ $PM_{2.5}$ in January 2015 and 4.02 μg/m³ $PM_{2.5}$ in June 2015. Relative to all ships within 200 NM of shore in the YRD, they accounted for 30% of ambient SO_2 and $PM_{2.5}$ in January 2015 and 85% of ambient SO_2 and $PM_{2.5}$ in June 2015 (Appendix C Figure C-10). Ships beyond 12 NM had smaller impacts, but could be important (e.g., ships from 24–48 NM from shore contributed a maximum of 0.11 μg/m³ $PM_{2.5}$ in January 2015 and 0.34 μg/m³ $PM_{2.5}$ in June 2015). These results are similar to those of Lv and colleagues (2018) who reported that emissions from ships within 12 NM of shore contributed 30% to 90% of the $PM_{2.5}$ related to ship emissions within 200 NM of shore.

As expected, trends in ship contributions to SO_2 were similar to trends in ship contributions to $PM_{2.5}$; however, emissions of SO_2 from ships beyond 12 NM had a smaller relative impact on ambient SO_2 than emissions had on $PM_{2.5}$ (Appendix C Table C-2 and Figure C-5). We previously published a detailed analysis of the ship emissions at different distances offshore in the YRD region and their associated contributions to SO_2 and $PM_{2.5}$ in January and June 2015 (Feng et al. 2019).

5.2.2 Shanghai

Shipping-related sources contributed annual average $PM_{2.5}$ concentrations in Shanghai of 0.24 μg/m³ from inland-water shipping, 0.17 μg/m³ $PM_{2.5}$ from coastal and international shipping, and 0.08 μg/m³ $PM_{2.5}$ from trucks and port machinery (Table 5-3). Maximum contributions of shipping-related sources to ambient $PM_{2.5}$ at individual 1 km × 1 km grid cells in Shanghai were 2.20 μg/m³ for inland-water ships, 1.05 μg/m³ for coastal ships, and 1.75 μg/m³ for trucks and port machinery. Within individual 1 × 1 km grid cells, annual average contributions of ships ranged from 1.0–2.5 μg/m³ $PM_{2.5}$ (Appendix C Table C-1). These contributions are slightly smaller than those reported by Lv and colleagues (2018), who used larger grid cells for the Shanghai modeling domain.

Contributions to ambient air pollutant concentrations varied in space and time for different shipping-related sources. The impact of coastal ships on $PM_{2.5}$ (Figure 5-4),
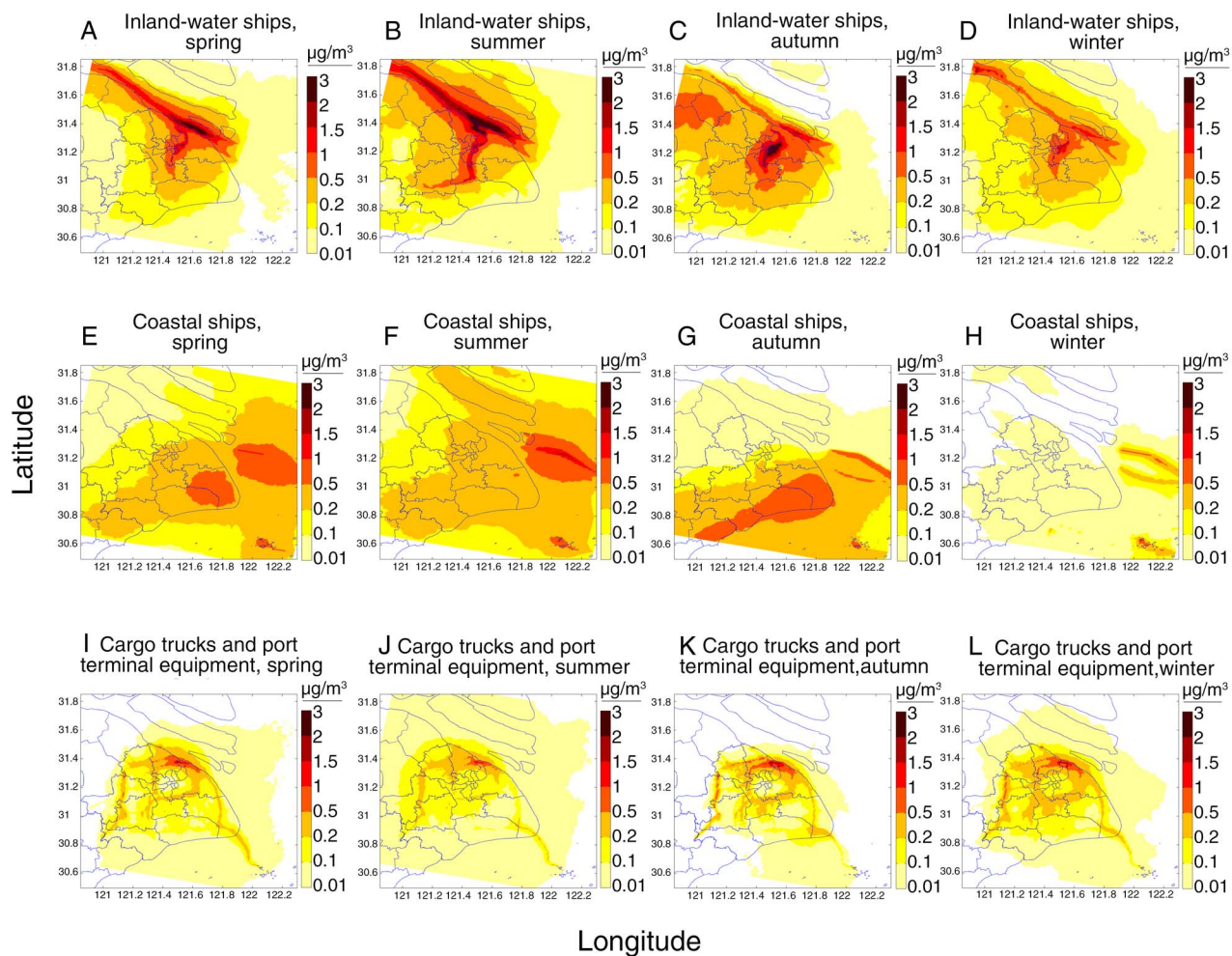
Figure 5-4. Contributions to PM$_{2.5}$ concentrations (µg/m^3) from inland-water ships (A–D), coastal ships (E–H), and container-cargo trucks and port terminal equipment (I–L) in spring (A, E, I), summer (B, F, J), autumn (C, G, K), and winter (D, H, L) in Shanghai in 2015.

SO$_2$ (Appendix C, Figure C-11), NO$_x$ (Appendix C, Figure C-12), and O$_3$ (Appendix C, Figure C-13) concentrations were highest in the east of Shanghai, close to the East China Sea, whereas inland-water ships most strongly impacted concentrations of these pollutants in the vicinity of Yangtze River and Huangpu River. Container-cargo trucks running primarily on China V motor diesel fuel (50 ppm sulfur) emitted almost no SO$_2$ and SO$_2$ emissions from port terminal equipment were much lower than from the other two shipping-related sources. Therefore, container-cargo trucks and port terminal equipment had little

impact on SO$_2$ concentrations, with seasonal average contributions less than 0.01 µg/m^3 and peak contributions less than 0.6 µg/m^3. The impact of container-cargo trucks and port terminal equipment on PM$_{2.5}$ concentrations was higher in the vicinity of Shanghai port and transportation routes (e.g., the inner-, middle-, and outer-ring highways) than in other parts of the city.

The average contribution of inland-water ships to ambient PM$_{2.5}$ concentrations in individual grid cells was higher in June (average: 0.4 µg/m^3, maximum: 3.0 µg/m^3) than in January (average: 0.2 µg/m^3, maximum: 1.8 µg/m^3)

(Figure 5-4). Similarly, the average contribution of coastal ships to ambient PM$_{2.5}$ concentrations was also higher in June (average: 0.3 µg/m^3, maximum: 0.9 µg/m^3) than in January (average: 0.02 µg/m^3, maximum: 0.1 µg/m^3). Due to shifting wind directions, the location of the greatest impact from coastal ships shifted seasonally from eastern Shanghai in summer towards the south of Shanghai in autumn. In winter, the impact was the lowest because the direction of the prevailing winds from the winter monsoon is from land to sea. Unlike for ships, the impact of container-cargo trucks and port terminal equipment on PM$_{2.5}$ concentrations were higher in January (average: 0.15 µg/m^3, maximum: 2.2 µg/m^3) than in June (average: 0.11 µg/m^3, maximum: 1.4 µg/m^3) because the lower wind speed in winter hindered dispersion and the strong summer wind quickly dispersed pollutants emitted within the city.

5.3 POPULATION-WEIGHTED PM$_{2.5}$ CONCENTRATIONS

5.3.1 YRD Region

Over the entire YRD region, shipping contributed 0.93 µg/m^3 of population-weighted PM$_{2.5}$, which accounted for 1.9% of all ambient PM$_{2.5}$ (Table 5-4). Exposures to emissions from ships were highest in the coastal cities and in Shanghai in particular.

Annual population-weighted PM$_{2.5}$ concentrations from shipping sources in individual core cities of the YRD region were on average 0.93 µg/m^3 (range: 0.5 µg/m^3 to 2.5 µg/m^3) (Figure 5-5), accounting for 1% to 6% of population-weighted PM$_{2.5}$ concentrations from all pollution sources. Annual average population-weighted PM$_{2.5}$

Table 5-4. Summary of Population-Weighted Exposures to PM$_{2.5}$ (µg/m^3) in 2015

Scenarios	YRD[a] All Ships	Shanghai[b] Inland Ships	Shanghai[b] Coastal Ships	Shanghai[b] Trucks and Port Machinery
All sources	48.52	62.33	62.33	62.33
No ships	47.59	61.85	62.15	62.18
Ship contribution	0.93	0.48	0.18	0.15
Ship contribution relative to all sources (%)	1.9	0.77	0.29	0.24

[a] PM$_{2.5}$ estimates from Domain 3 emission inventory.

[b] PM$_{2.5}$ estimates from Domain 4 emission inventory. Note that the Shanghai domain did not include emissions from ship emissions from outside of the domain, which contributed a large proportion of Shanghai exposure.

A. All Sources   **B. Shipping Sources**

Population-weighted PM$_{2.5}$ (µg/m^3)

- 0.5–1.0
- 1.0–2.0
- 2.0–3.0
- 3.0–30.0
- 30.0–40.0
- 40.0–50.0
- 50.0–60.0
- 60.0–70.0

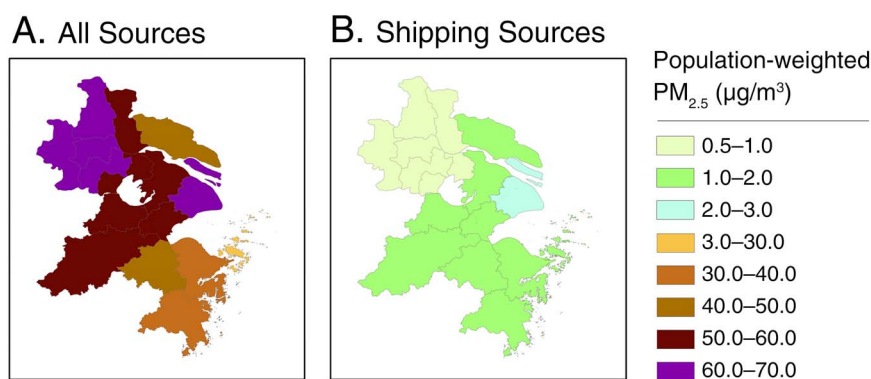**Figure 5-5. Annual population-weighted PM$_{2.5}$ concentrations (µg/m^3) in core YRD cities: (A)** from all air pollution sources and **(B)** from ships.

concentrations from all pollution sources in the core YRD cities ranged from 21.3 μg/m³ to 67.0 μg/m³ (Figure 5-5). Of the 16 core YRD cities, the highest population-weighted annual average $PM_{2.5}$ concentrations contributed by ships were found for Shanghai (2.5 μg/m³), 1.3 times higher than the second-highest city Taichou (1.9 μg/m³). The four cities in the YRD with the largest contributions of population-weighted $PM_{2.5}$ from shipping sources were all coastal cities, which suggests that people living in coastal regions have higher exposures to air pollution from shipping-related sources than people living in farther inland.

Among the 16 core YRD cities, ships within 12 NM of shore (including on inland waters) contributed from about 53% to 83% of the population-weighted $PM_{2.5}$ concentrations from all ships within 200 NM of shore (Appendix C, Figure C-14). The population-weighted $PM_{2.5}$ concentrations resulting from more distant ships were lower than those from ships within 12 NM from shore (including inland-water ships). Ships 12–24 NM from shore accounted for 2.5% to 6.6% of population-weighted $PM_{2.5}$, ships 24–48 NM from shore accounted for 6.8% to 11.5%, and ships 48–96 NM from shore accounted for 6.3% to 31.6%. The contributions of ships 24–48 NM and 48–96 NM from shore were greater than the contributions from ships 12–24 NM from shore because they contained the busier shipping lanes. Therefore, although ships within 12 NM of shore were the dominant contributor to potential population exposure to $PM_{2.5}$, emissions from ships as far as 24–96 NM from shore cannot be ignored.

5.3.2 Shanghai

Population-weighted $PM_{2.5}$ concentrations from ship-related sources in Shanghai were generally larger than the average $PM_{2.5}$ concentrations because the population was denser in the areas with the highest shipping and container-cargo truck activity. The relative contributions were similar for ambient and population-weighted $PM_{2.5}$ concentrations; inland-water ships were also the largest shipping-related contributors to population-weighted $PM_{2.5}$ (Figure 5-6). The annual average contributions of shipping-related sources to population-weighted $PM_{2.5}$ exposures (as estimated from the average of four representative months) were 0.48 μg/m³ for inland-water ships, 0.18 μg/m³ for coastal ships, and 0.15 μg/m³ for trucks and port machinery (Table 5-4). In seasonal analyses, population–weighted $PM_{2.5}$ from shipping-related sources was lower in January than in June, while population-weighted $PM_{2.5}$ from container-cargo trucks and port terminal equipment was slightly higher in January. (Appendix C, Figure C-15).

A. Inland Shipping

B. Coastal Shipping

C. Diesel Cargo Trucks and Port Machinery

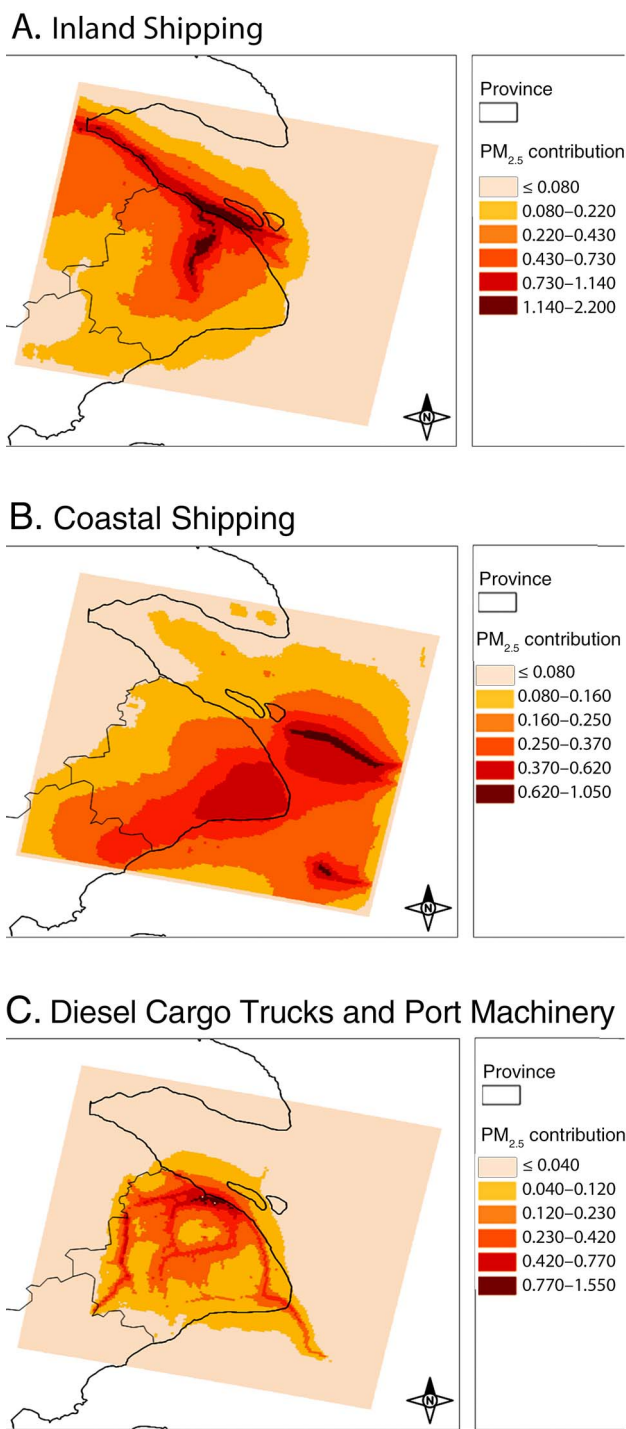**Figure 5-6. Contribution of (A) inland shipping, (B) coastal shipping, and (C) diesel cargo trucks and port machinery to population-weighted $PM_{2.5}$ in Shanghai in the baseline year 2015.**

Population-weighted $PM_{2.5}$ concentrations were not evenly distributed across Shanghai (Appendix C, Figure C-16). Areas in the Shanghai city center had higher population-weighted $PM_{2.5}$ from inland-water ships because of the combination of dense population and location close to Huangpu River. Among city-center administrative districts, Baoshan and Yangpu had the highest population-weighted $PM_{2.5}$ concentrations from inland-water ships (both around 1.31 μg/m³) in June. Similarly, the coastal district (Fengxian) had the highest population-weighted $PM_{2.5}$ from coastal ships (0.17 μg/m³ to 0.40 μg/m³). As for population-weighted $PM_{2.5}$ from container-cargo trucks and port terminal equipment, the administrative region next to Shanghai Port (Baoshan) had the highest population-weighted $PM_{2.5}$ in both January (0.4 μg/m³) and June (0.45 μg/m³) due to its high population and location close to the source.

5.4 BASELINE (2015) HEALTH IMPACTS OF $PM_{2.5}$ FROM SHIPPING-RELATED SOURCES

5.4.1 YRD Region

5.4.1.1 Impacts of Long-Term Exposure Using the IERs from the Global Burden of Disease project, we estimated that ship emissions contributed to a total of about 3,640 premature deaths attributable to long-term exposure to $PM_{2.5}$ in the YRD region in 2015. This reflects the sum of deaths from stroke (750), COPD (1,450), IHD (550), and lung cancer (840) (Table 5-5).

The spatial patterns in these impacts reflect the patterns in population-weighted $PM_{2.5}$ concentrations. Health impacts associated with $PM_{2.5}$ from ships were the largest in coastal cities, with the highest number of deaths in Shanghai (Appendix D, Figure D-11 and Table D-2, available on the HEI website). The highest mortalities associated with $PM_{2.5}$ from ship emissions in a single 9-km grid cell were estimated to be 21 deaths from stroke, 42 from COPD, 17 from IHD, and 30 from lung cancer (Appendix D Figure D-1).

These estimated health impacts of $PM_{2.5}$ from ships in the YRD in 2015 are consistent with previous reports from similar studies of ship emissions. For instance, a global analysis of ship emissions estimated a sum of 20,300 avoided deaths from cardiopulmonary diseases and 2,200 from lung cancer in East Asia in 2012 (Winebrake et al. 2009). Another global assessment of mortality from ship emissions estimated 3,860 deaths from all causes, 3,490 deaths from cardiopulmonary causes, and 370 deaths from lung cancer to be associated with ship-driven PM in East Asia in 2012 (Corbett et al. 2007). Differences among the

Table 5-5. Mortality and Hospital Admissions Associated with Long-Term and Short-Term Exposure to $PM_{2.5}$ from Ship Emissions in the YRD Region in 2015

Endpoint	Mean (95% CI)
Long-Term Exposure: Mortality	
Sum of cause-specific mortality[a]	3,600 (2,400–6,900)
Stroke	750 (230–1,300)
COPD	1,450 (670–220)
IHD	550 (140–960)
Lung cancer	840 (630–1,100)
Short-Term Exposure: Mortality	
All-natural cause	1,100 (750–1,400)
Cardiovascular	73 (49–97)
Respiratory	42 (23–59)
Short-Term Exposure: Hospital Admissions (total)	270,000 (107,000–440,000)

Abbreviations: CI = confidence interval; COPD = chronic obstructive pulmonary disease; IHD = ischemic heart disease; stroke = cerebrovascular disease.

[a] The sum of cause-specific mortality from long-term exposures to $PM_{2.5}$ is the sum of mortality from stroke, COPD, IHD, and lung cancer. In the absence of a reliable concentration–response function for all-natural-cause mortality associated with $PM_{2.5}$, this estimate is provided for comparison with the estimates of mortality from short-term exposure to $PM_{2.5}$.

studies can be attributed to variation in time period, emissions data and methods, as well as assumptions about the exposure–response relationships used to estimate health impacts.

Our analyses of the mortality impacts using the alternative GEMM functions proposed by Burnett and colleagues (2018) found that the estimates were highly sensitive to this choice (Appendix E, Table E-2). The first analysis used the GEMM function that incorporates data from a major Chinese cohort study; it projected over 20,000 excess deaths from all causes attributable to ship-related $PM_{2.5}$ exposures in the YRD region. This estimate is nearly six times larger than the estimate for the four causes of death in the main analysis using the GBD IERs, reflecting a number of factors, among them that the GEMM estimate of total mortality captures a broader set of $PM_{2.5}$ effects on health. Estimates for individual causes of death using the GEMM functions ranged from 1.5 times (COPD) to about 7 times (IHD) the estimates for the main analysis. Additional sensitivity analyses using GEMM functions that exclude the Chinese cohort study led to somewhat smaller health impact estimates, but they were still substantially greater than those in the main analysis with the IERs (Appendix E, Table E-2).

Although the estimates using the GEMM concentration–response functions were much higher than the estimates using the IERs, it is important to note that these functions apply to $PM_{2.5}$ from all sources. So, although the estimates of mortality associated with long-term exposure to $PM_{2.5}$ are larger for the GEMMs, this does not impact the relative ranking of $PM_{2.5}$ sources and the percentage contributions of ships and other shipping-related sources to health impacts.

5.4.1.2 Impacts of Short-Term Exposure We estimated that short-term exposure to $PM_{2.5}$ from ship emissions in the YRD region in 2015 was associated with about 1,100 deaths from all natural causes, 73 deaths from cardiovascular disease, and 42 deaths from respiratory causes (Table 5-5). In addition, we estimated that short-term exposures to shipping-related $PM_{2.5}$ contributed to an additional 270,000 hospital admissions in 2015 from all causes. Most of those deaths and hospital admissions were in highly populated coastal areas (Appendix D, Figures D-3 and D-12). Numbers of hospital admissions generally greatly exceeded numbers of deaths in a given year, so the numbers of hospital admissions attributed to $PM_{2.5}$ were also higher (Tian et al. 2019).

5.4.2 Shanghai

5.4.2.1 Impacts of Long-Term Exposure We estimated that in Shanghai long-term exposure to $PM_{2.5}$ from inland

shipping contributed about 21 deaths from stroke, 57 from COPD, 25 from IHD, and 35 from lung cancer in 2015 (Table 5-6). These impacts were higher than those estimated for mortality associated with long-term exposures to $PM_{2.5}$ from coastal and international shipping as well as from container-cargo trucks and port machinery.

In Shanghai, the health impacts attributed to long-term exposures to shipping-related $PM_{2.5}$ were mainly focused in central Shanghai, which has the highest population density (Appendix D, Figures D-4, D-5, and D-6). For example, the impacts of inland shipping were larger nearer the Huangpu River and the Yangtze River (Appendix D, Figure D-4), whereas the impacts of coastal and international ships were larger along the shore of the Pudong District (Appendix D, Figure D-5). Impacts from container-cargo trucks occurred close to population centers and the ring roads (Appendix D, Figure D-6). As for the YRD sensitivity analysis, the estimated mortality associated with long-term exposures to ship-related $PM_{2.5}$ in Shanghai was also higher when applying the GEMM response functions (Appendix E, Table E-3).

Note that the source-specific analyses in Shanghai only include local shipping-related sources (i.e., those within modeling Domain 4 and reported in Table 5-6) and do not represent the impact of all shipping on Shanghai. The total impact of ships on Shanghai is better represented by extracting results from the YRD results in modeling Domain 3 (i.e., those presented in Table 5-5). When doing so, we estimate that 1,100 deaths associated with long-term exposure to $PM_{2.5}$ from ships within the YRD region (Domain 3) — about one-third of all mortality — would have occurred within the Shanghai modeling domain (Domain 4) (Appendix D, Table D-1), as would be expected given that Shanghai accounts for a large proportion of the region's population.

5.4.2.2 Impacts of Short-Term Exposure In Shanghai, the total numbers of deaths attributable to short-term exposures to $PM_{2.5}$ from shipping-related sources were about 46 deaths for inland-water ships, 17 for coastal ships, and 10 from diesel cargo trucks and port machinery within the city boundaries in 2015 (Table 5-6). The corresponding estimates of numbers of hospital admissions were about 160,000 (95% CI; 6,300, 26,000) for inland shipping; 6,000 (95% CI; 2,400, 9,600) for coastal shipping; and 5,100 (95% CI; 2,000, 8,200) for trucks and port machinery (Table 5-6). Note that these estimates are based on impacts of shipping-related $PM_{2.5}$ within Shanghai (Domain 4) and thus do not reflect emissions from the broader YRD region (Appendix D, Figure D-9).

Table 5-6. Summary of Cause-Specific Mortality and Total Hospital Admissions Associated with Long-Term and Short-Term PM$_{2.5}$ Exposure Due to Ship-Related Emissions in Shanghai in 2015

Ship-Related Source	Long-Term Exposure Mortality Mean (95% CI)					Short-Term Exposure Mortality Mean (95% CI)			Short-term Exposure Hospital Admissions
	Sum of Cause-Specific Mortality[a]	Stroke	COPD	IHD	Lung Cancer	All-Natural Cause	Cardio-vascular	Respiratory	
Inland ships	136 (64–210)	21 (5.5–36)	57 (24–89)	23 (7.0–39)	35 (27–42)	46 (32–59)	2.1 (1.4–2.9)	1.6 (0.9–2.3)	16,000 (6,300–26,000)
Coastal and international ships	56 (26–85)	8.6 (2.4–15)	23 (10–36)	10 (2.7–17)	14 (11–17)	17 (12–22)	0.8 (0.5–1.1)	0.6 (0.3–0.9)	6,000 (2,400–9,600)
Diesel cargo trucks and port machinery	46 (21–70)	6.9 (1.8–12)	19 (8.2–30)	7.8 (2.3–13)	12 (9.1–15)	10 (7.2–13)	0.6 (0.4–0.7)	0.4 (0.2–0.6)	5,100 (2,000–8,200)

Abbreviations: CI = confidence interval; COPD = chronic obstructive pulmonary disease; IHD = ischemic heart disease; stroke = cerebrovascular disease.

[a] The sum of cause-specific mortality is the sum of mortality from stroke, COPD, IHD, and lung cancer associated with long-term exposure to PM$_{2.5}$. In the absence of a reliable integrated exposure response function for all-natural-cause mortality associated with PM$_{2.5}$, this estimate is provided for comparison with mortality from short-term exposure to PM$_{2.5}$.

5.5 FUTURE (2030) EMISSIONS IN THE YRD REGION

5.5.1 Projection of Ship Traffic Activities to 2030

Regional GDP growth was highly influenced by import and export trade and therefore annual ship traffic activities and GDP in the YRD region had similar annual trends in the years 2013–2017 (Pearson's $r = 0.96$; Figure 5-7). Over this period, the regional GDP increased from 10,198.9 billion yuan to 16,517.1 billion yuan and total ship traffic activity in the YRD increased from 5.1×10^{10} kWh to 1.4×10^{11} kWh (National Bureau of Statistics of China 2019). Assuming the economy of China continues to develop as expected, the YRD region GDP is projected to increase to 20,000 billion yuan and the total ship traffic activity in this region is projected to increase to 1.9×10^{11} kWh.
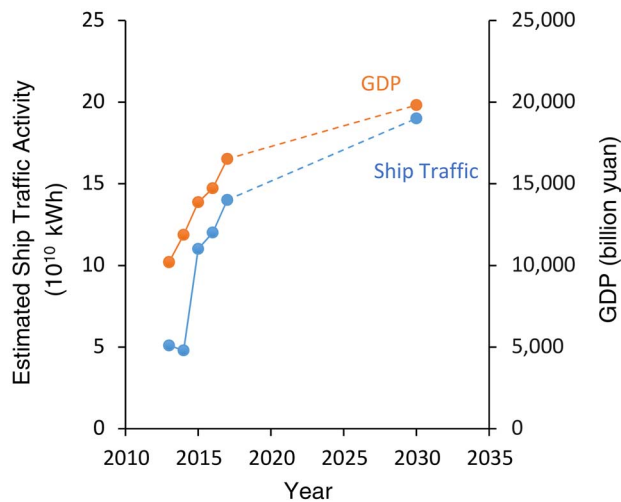

Figure 5-7. Ship traffic activities and GDP trends in YRD region from 2013 to 2017. Actual values are shown for 2013–2017 (solid lines) and projected values are shown for 2030 (dashed lines). See Appendix F, Table F-1 for values in this figure.

Increases in annual ship traffic activities in the YRD region from 2013 to 2017 occurred mainly in the highest-traffic areas on the Yangtze River and in the coastal areas of the East China Sea (Appendix F, Figure F-1). At present, more than 90% of China's import and export trade is completed by maritime transport, and inland rivers are important channels for collecting and distributing cargo. Projections assumed that existing trends will increase so that ship traffic activities in 2030 will also be high at the mouth of the Yangtze River and in the East China Sea.

5.5.2 Ship Emissions Under Three Future Policy Scenarios

Ship traffic activities were combined with emission factor assumptions to obtain a shipping emissions inventory for the YRD region under the current, stricter, and aspirational policies described in Table 4-1. Compared with 2015, SO_2 emissions in 2030 were expected to decrease by 73.1% in the current policy scenario, 77.9% in the stricter policy scenario, and 90.8% in the aspirational policy scenario, respectively (Figure 5-8). $PM_{2.5}$ emissions would be expected to decrease by similar proportions: 72.8% in the current policy scenario, 77.8% in the stricter policy scenario, and 90.3% in the aspirational policy scenario. These proportional relationships between $PM_{2.5}$ emission factors and fuel sulfur content are consistent with the results presented in the Third IMO Greenhouse Gas Study (see Figure 74 of IMO Marine Environment Protection Committee 2014). In the same period in the YRD, NO_x emissions were projected to decrease by 13.4% in the current policy scenario, 37.3% in the stricter policy scenario, and 67.9% in the aspirational policy scenario, less than the decreases in SO_2 and $PM_{2.5}$. NO_x emissions are not expected to decline as rapidly as SO_2 and $PM_{2.5}$ emissions because the NO_x adjustment factor depends on the engine and technology standards in place at the time of manufacture and applies only to new vessels, while the fuel sulfur requirements
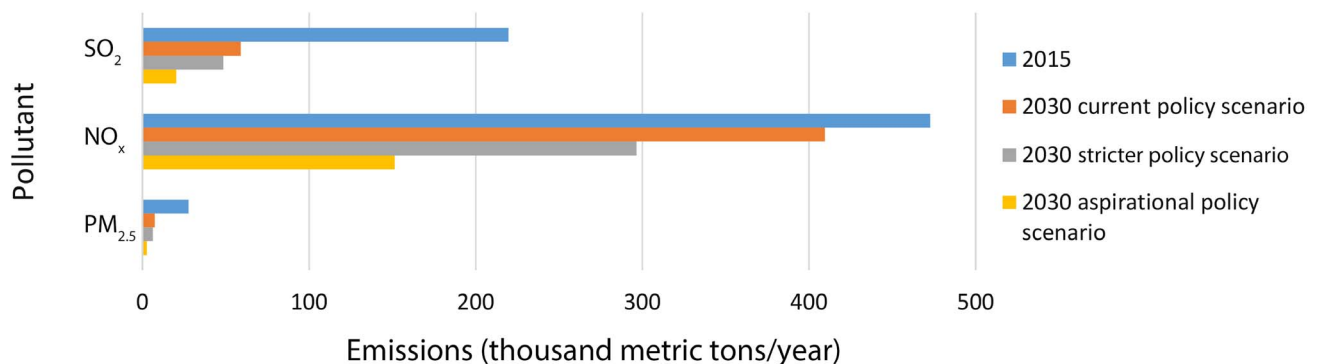

Figure 5-8. Ship emissions estimated in the YRD region in 2015 and projected under three policy scenarios in 2030. See Appendix F, Table F-2 for values in this figure.

apply to all vessels. Due to the long service life of ocean-going ships (25 years on average), the full impact of the NO_x requirement will take decades to realize as new vessels are introduced and old ones are retired.

The effectiveness of policies in reducing emissions of the different pollutants is expected to vary spatially and by pollutant. The current policy scenario covers the same spatial extent of controls as was covered in the baseline 2015 scenarios, so the spatial distribution emissions mainly reflects changes in global fuel sulfur content and improved controls of emissions in inland waters (Figure 5-9). Controls under the stricter policies also will only extend out to 12 NM from shore, but the emissions of SO_2, NO_x, and $PM_{2.5}$ would all decrease near the coast relative to the current policy scenario. The projected emissions reductions for the aspirational policy scenario were larger than those for the current policy scenario and the stricter policy scenario because only the aspirational policies extend the control areas out to 100 NM from shore.

5.5.3 Projected PM$_{2.5}$ Concentrations in 2030

Ambient $PM_{2.5}$ concentrations contributed by all sources in 2030 were estimated to be 26.24 μg/m^3 to 26.38 μg/m^3 for the future policy scenarios (Table 5-7). The ambient concentrations of $PM_{2.5}$ for future scenarios were similar with and without shipping sources because shipping contributed a small fraction of the total concentrations. The projected contributions of ship emissions to annual average ambient $PM_{2.5}$ were 0.25 μg/m^3 (0.95% of all sources) in the current policy scenario, 0.18 μg/m^3 (0.68% of all sources) in the stricter policy scenario, and 0.11 μg/m^3 (0.42% of all sources and almost one-half of the ship impact under the current policy scenario) in the aspirational policy scenario (Table 5-7). The corresponding contributions of ship emissions to annual average ambient SO_2 concentrations were 0.37 μg/m^3 (2.3% of all sources) for the current policy scenario, 0.33 μg/m^3 (2.1% of all sources) for the stricter policy scenario, and 0.23 μg/m^3 (1.8% of all sources) for the aspirational policy scenario.
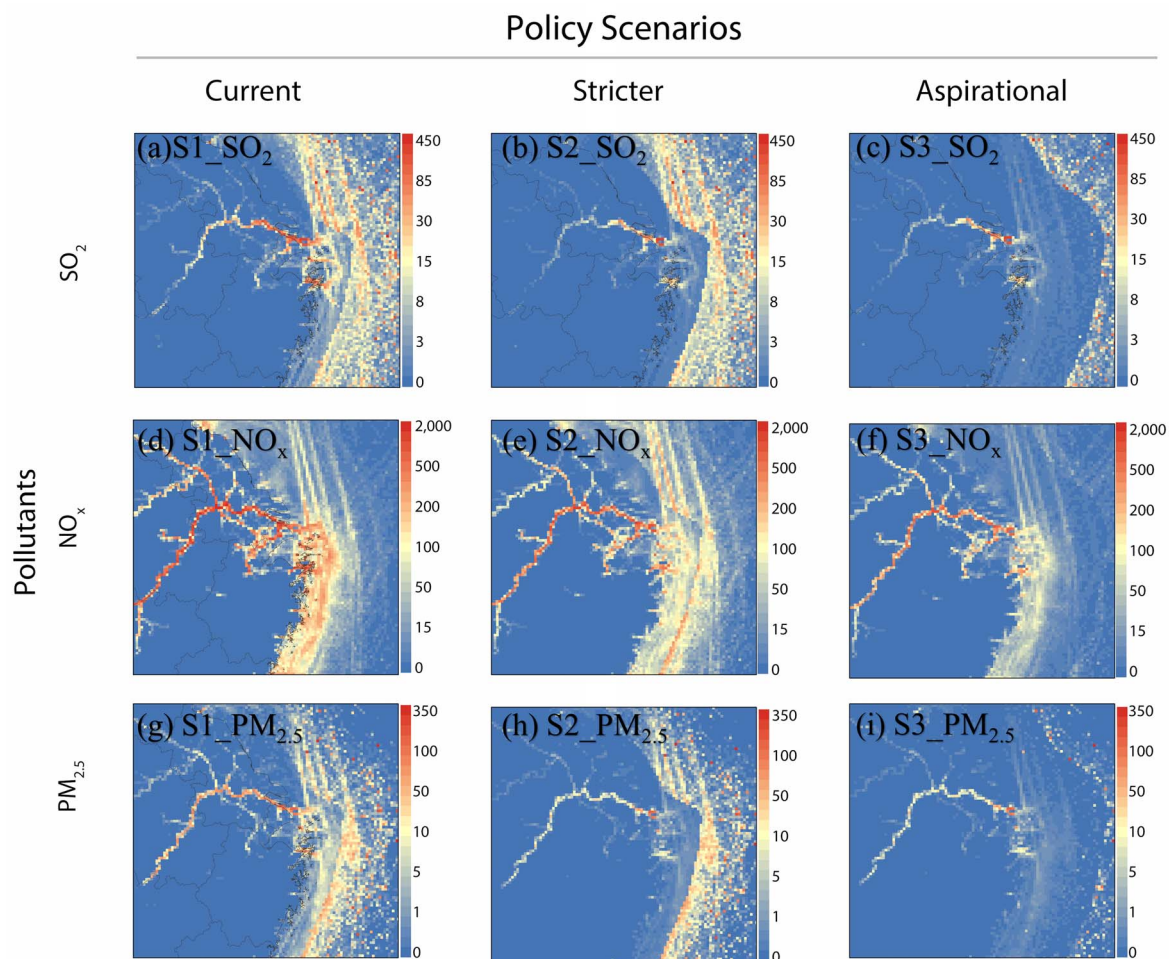

Figure 5-9. Spatial distribution of SO$_2$ (a–c), NO$_x$ (d–f), and PM$_{2.5}$ (g–i) emissions from ships in 2030 under current policy (S1), stricter policy (S2), and aspirational policy (S3) scenarios. The units are metric tons per 9-km^2 grid cell.

All three future scenarios projected lower $PM_{2.5}$, NO_x, and SO_2 concentrations from ship emissions in 2030 than in 2015 (Figure 5-10). Between 2015 and 2030, ambient $PM_{2.5}$ concentrations were projected to decrease by 62% in the current policy scenario, 68% in the stricter policy scenario, and 83% in the aspirational policy scenario. Compared to 2015, the contribution of ships to ambient SO_2 concentrations was projected to decrease by 48% in the current policy scenario, 54% in the stricter policy scenario, and 68% in the aspirational policy scenario, mainly because of reductions in SO_2 emissions. The relative reductions in $PM_{2.5}$ concentrations were much higher than those for SO_2 concentrations and NO_x concentrations in the three scenarios because the emissions of both precursor gases (SO_2 and NO_x) and primary particles decreased significantly.

The contributions of ships to both ambient air pollutant concentrations and reductions in air pollutant contributions from ships were highest in the areas with the greatest ship impacts, with similar relative contributions to those in 2015. The largest reduction in ambient $PM_{2.5}$ concentrations in a single grid cell was more than 3.3 $\mu g/m^3$ $PM_{2.5}$

Table 5-7. Summary of Ambient Concentrations of $PM_{2.5}$ and Population-Weighted Exposure to $PM_{2.5}$ ($\mu g/m^3$) in the YRD Region in 2030 Under Future Policy Scenarios

Category / Scenarios	Policy Scenario		
	Current	Stricter	Aspirational
Ambient PM$_{2.5}$ Concentration			
All sources	26.38	26.31	26.24
No ships	26.13	26.13	26.13
Ship contribution	0.25	0.18	0.11
Ship contribution relative to all sources (%)	0.95	0.68	0.42
Population-Weighted PM$_{2.5}$ Exposure			
All sources	32.33	32.23	32.13
No ships	31.98	31.98	31.98
Ship contribution	0.36	0.26	0.16
Ship contribution relative to all sources (%)	1.10	0.81	0.50
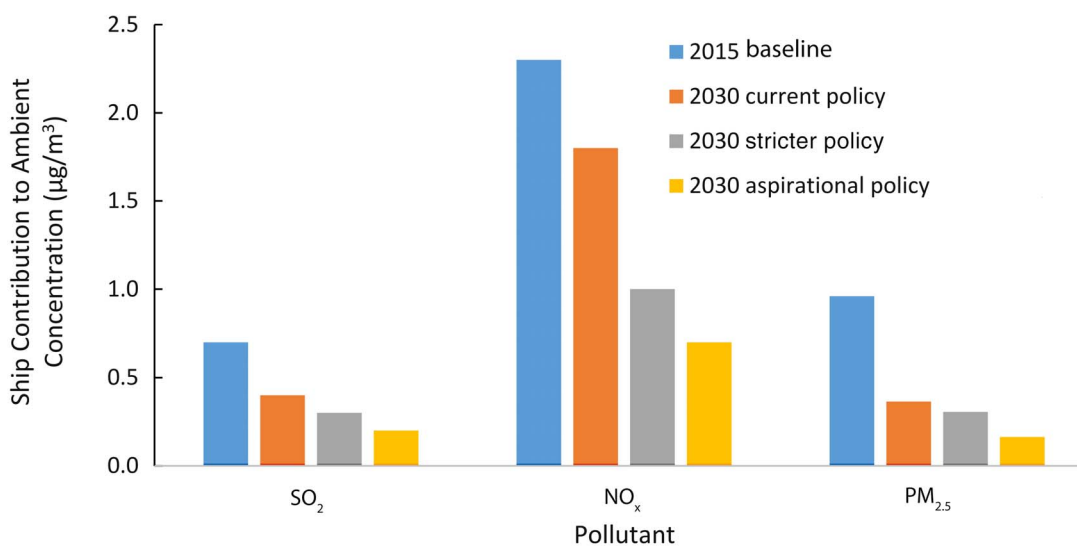
Figure 5-10. Ship contributions to ambient SO_2, NO_x, and $PM_{2.5}$ concentrations in 2015 and in 2030 under current, stricter, and aspirational future policy scenarios.

near Shanghai Port in the aspirational policy scenario (Figure 5-11). The decreases in ambient PM$_{2.5}$ concentrations related to ship emissions were generally consistent with PM$_{2.5}$ source apportionment and its sensitivity to different emission controls on PM$_{2.5}$ reduction in the YRD region (Li et al. 2018b). As for 2015, PM$_{2.5}$ was transported

more regionally than SO$_2$ (Appendix F, Figure F-2) and NO$_x$ (Appendix F, Figure F-3), which closely followed the spatial distribution of ship traffic activity.

The spatial patterns of ship contributions to PM$_{2.5}$ concentrations in 16 core YRD cities in the three 2030 scenarios were similar to that in 2015 (Appendix F, Figure

Figure 5-11. Comparisons of the impact of the three future policy scenarios on reductions in ship emissions contributions to PM$_{2.5}$ concentrations (µg/m³) in the YRD region between 2015 and 2030 (top row), to the annual mean PM$_{2.5}$ concentrations in the YRD region in 2030 (middle row), and as a percentage (%) contributions total emissions in the YRD region in 2030 (bottom row).

F-6). For example, of the 16 core YRD cities, Shanghai had the highest ship contribution to ambient $PM_{2.5}$ concentrations (0.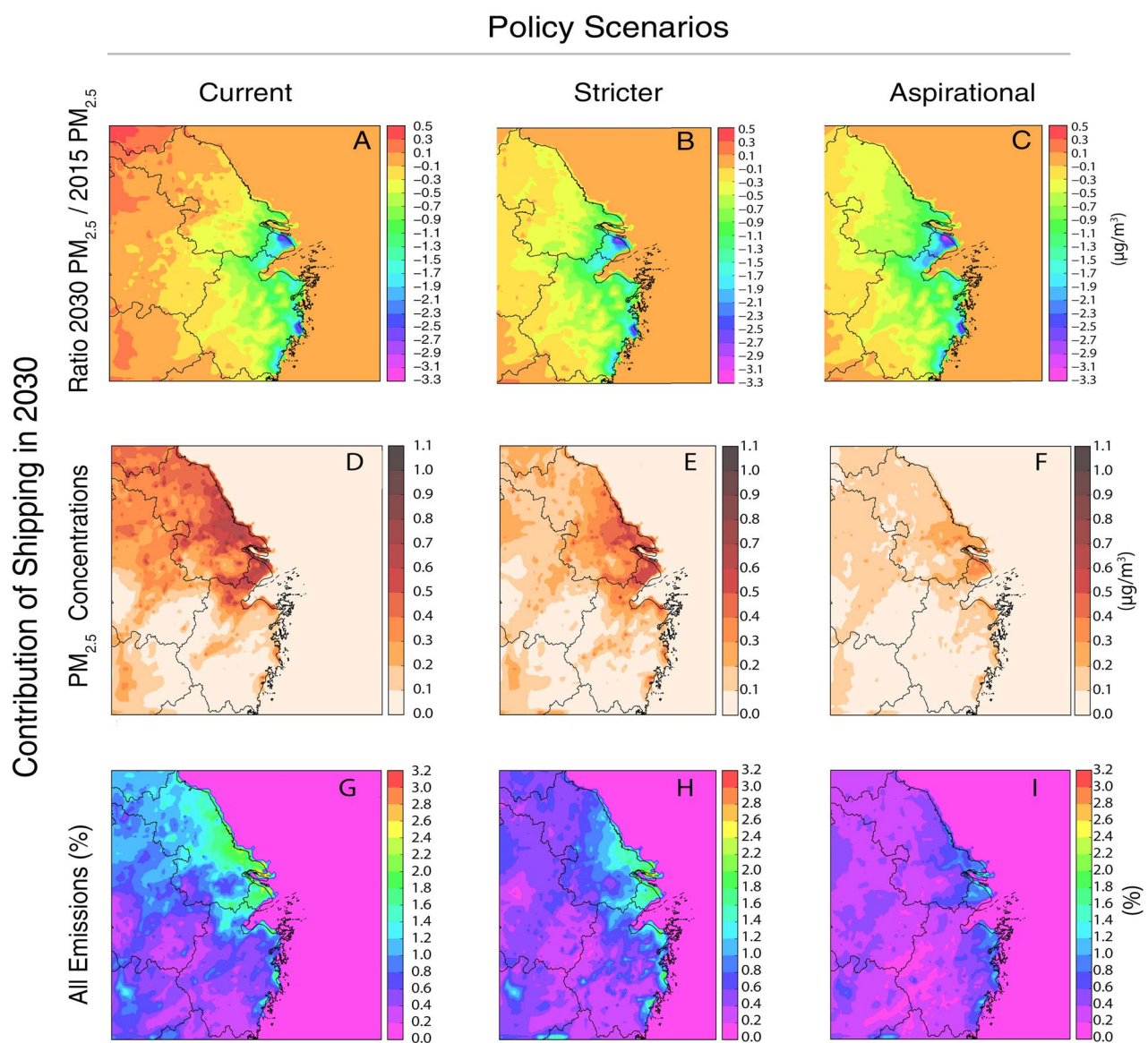31 µg/m³ in the aspirational policy scenario to 0.57 µg/m³ in the current policy scenario) because it is close to the Yangtze River and East China Sea. The greatest impacts were predicted near the Shanghai Port, where ships contributed up to 1.1 µg/m³ (3.2% of the total) ambient $PM_{2.5}$ in the grid cell with the highest ship contribution to $PM_{2.5}$ under the current policy scenario (compared with 3.6 µg/m³ $PM_{2.5}$ [8.0%] in the same area in 2015). The cities with the second-highest ship contributions to $PM_{2.5}$ were not the same for all scenarios because the spatial extent and control policies were different. The lowest contributions of ship emissions to ambient $PM_{2.5}$ concentrations were predicted in Shaoxing for the current policy scenario and the stricter policy scenario and in Hangzhou for the aspirational policy scenario.

Similar to the results for 2015, the core YRD city with the highest contributions of ship emissions to ambient SO_2 and NO_x concentrations in all three 2030 scenarios was Zhoushan (e.g., 0.89 µg/m³ SO_2 in the current policy scenario to 0.48 µg/m³ SO_2 in the aspirational policy scenario) which is located close to shipping lanes. Shanghai had the second-highest shipping contributions to SO_2 and NO_x concentrations (e.g., 0.65 µg/m³ SO_2 in the current policy scenario to 0.42 µg/m³ SO_2 in the aspirational policy scenario) (Appendix F, Figure F-4 and Figure F-5). This finding differs from the 2015 simulations where Shanghai

had higher NO_x and lower SO_2 than Zhoushan. Differences in the projected reductions in pollutant concentrations in different cities could be attributed to uneven spatial distribution of the reduction of air pollutant emissions.

5.5.4 Population-Weighted $PM_{2.5}$ Concentrations in 2030

The projected population-weighted $PM_{2.5}$ contributions from shipping ranged from 0.16 µg/m³ to 0.36 µg/m³ in the YRD region (Table 5-7). These contributions were only 0.5% to 1.1% of the population-weighted exposure levels of $PM_{2.5}$ from all sources under the three future policy scenarios. The fraction of ambient $PM_{2.5}$ contributed by ships is projected to decrease between 2015 and 2030; these projections of the fraction of $PM_{2.5}$ from ships relative to all sources are only one-quarter to one-half of the population-weighted $PM_{2.5}$ concentrations in 2015 (Table 5-4).

5.5.5 Projected (2030) Health Impacts

We projected that in 2030 long-term exposure to $PM_{2.5}$ from ships would contribute around 830 (aspirational policy scenario) to 1,800 (current policy scenario) deaths in the YRD region from the combination of stroke, COPD, IHD, and lung cancer (Table 5-8). These projected impacts on mortality are less than half as large as the impacts in 2015 (Table 5-6) and reflect the combination of cleaner fuels and better control technologies in the future scenarios. Similarly, short-term exposure to $PM_{2.5}$ from ship emissions would contribute to a total of 190 to 430 deaths

Table 5-8. Health Impacts of Long-Term and Short-Term Exposure to $PM_{2.5}$ from Ships in the YRD Region in 2030 Under Alternative Control Scenarios

Type of Exposure and Health Outcome /Health Endpoint	Policy Scenario		
	Current	Stricter	Aspirational
Long-Term Exposure — Mortality: Mean (95% CI)			
Sum of individual causes[a]	1,800 (1,200–3,400)	1,400 (880–2,600)	830 (530–1,500)
Stroke	370 (210–760)	290 (160–580)	170 (98–350)
COPD	750 (480–1,400)	570 (360–1,000)	340 (220–610)
IHD	280 (190–730)	220 (150–560)	130 (90–340)
Lung cancer	410 (280–540)	310 (210–410)	180 (120–250)
Short-Term Exposure — Mortality: Mean (95% CI)			
All-cause	420 (300–550)	320 (220–410)	190 (130–240)
Cardiovascular	29 (19–39)	20 (14–29)	13 (8.5–17)
Respiratory	17 (9.4–24)	12 (7–18)	7.3 (4.1–10.3)

Abbreviations: CI = confidence interval; COPD = chronic obstructive pulmonary disease; IHD = ischemic heart disease; stroke = cerebrovascular disease.

[a] The sum of cause-specific mortality is the sum of mortality from stroke, COPD, IHD, and lung cancer associated with long-term exposure to $PM_{2.5}$. In the absence of a reliable integrated exposure–response function for all-natural-cause mortality associated with $PM_{2.5}$, this estimate is provided for comparison with mortality from short-term exposure to $PM_{2.5}$.

from all causes. The spatial distributions of these health impacts are similar to those of population-weighted concentrations and maps of the impacts of long-term (Figure F-7 to Figure F-9) and short-term (Figure F-10 to Figure F-12) exposures to $PM_{2.5}$ from ships in the YRD region are shown in Appendix F.

6.0 DISCUSSION

Over the last 20 to 30 years, scientists have become increasingly interested in the potential contributions of the global shipping industry to changes in climate, air quality, and health. From early studies of broad global emissions (e.g., Corbett and Fischbeck 1997), there has been steady growth in the number of studies around the world that examine emissions, air quality, and health impacts of shipping at more regional and local scales. A number of these studies are in the region of East Asia and, more particularly, in China, which is home to 10 of the largest ports in the world and where air pollution levels have been among the highest in the world. To date, most of these studies have focused on emissions and impacts on air quality, and to a lesser extent on health. Few have estimated impacts at a finer local scale within cities.

This study aimed to build on previous work, providing a more detailed analysis of the impacts of shipping and related activities on air quality and health in both the broader YRD region and, more specifically within Shanghai, by using both existing and newly developed emissions inventories. The study evaluated these impacts for a baseline year set at 2015, which was prior to the implementation of China's first domestic emissions control areas, and for a future year, 2030, under three alternative scenarios with increasingly strict future emissions control policies.

6.1 HEALTH IMPACTS OF SHIPPING AND RELATED EMISSIONS

6.1.1 Baseline (2015) Health Impacts in the YRD Region

Our study finds that emissions from shipping contribute meaningfully to the burden of disease from exposure to $PM_{2.5}$ in the YRD and in Shanghai. We estimated that in 2015 there were about 3,640 premature deaths from stroke, COPD, IHD, and lung cancer attributable to long-term exposures to air pollution from ship emissions in the YRD region (Table 5-5). Short-term daily exposures were also estimated to contribute to about 1,000 additional deaths but also to over 270,000 additional hospital admissions (Table 5-5). When considering shipping-related emissions

within the YRD modeling domain, the contribution of short-term exposures to $PM_{2.5}$ inside of the Shanghai city domain was about 1,100 premature deaths of which about 240 are attributable to air pollution from ships, cargo transport, and in-port machinery from within the smaller port domain. Approximately 73 additional deaths and 16,000 hospital admissions were attributable to short-term exposures to $PM_{2.5}$ from all shipping sources within the Shanghai port domain. The largest impacts were from international ships traveling on inland waterways, with additional contributions from coastal ships, container-cargo trucks, and in-port machinery.

In providing detailed results for the YRD and Shanghai, this study adds to the global, regional, and more local Chinese evidence on the impacts of shipping on population health from long-term exposures to air pollution (Figure 6-1). As the figure indicates, the results are broadly consistent with and in proportion to the results presented for other regions and ports, despite differences in underlying data and methods. However, direct comparison of the various studies is challenging because they differed in how the emissions inventories were developed in the geographical domains of analysis and in the concentration–response functions used to assess health impacts.

In addition, this study is one of few that have examined the impacts of short-term (e.g., daily) exposures on mortality and hospital admissions attributable to ship-related $PM_{2.5}$ in China, in particular for the YRD and at high resolution in Shanghai. Our study estimated that 1,100 premature deaths from all causes could be attributed to daily exposures to ship emissions across the YRD, with 70 from cardiovascular causes and 40 from respiratory causes specifically. Over 270,000 hospital admissions from all causes were also attributed to $PM_{2.5}$ exposures. Although these estimates of hospital admissions are based on concentration–response functions drawn from a recent study in China, the study lacked data that would allow for differentiation of health outcomes that have been most strongly associated with exposures to $PM_{2.5}$, for example cardiovascular and respiratory effects. Additional research on the effects of short-term exposure to air pollution on cause-specific hospital admissions in China is needed to improve estimates of health impacts.

6.1.2 Relative Importance of Shipping-Related Sources in Shanghai

The analysis within the Shanghai port domain was a first step toward understanding the relative importance of ships compared with other port-related activities, specifically, land-based cargo or goods transport and in-port activities (e.g., cranes, forklifts, and trucks). Although these latter
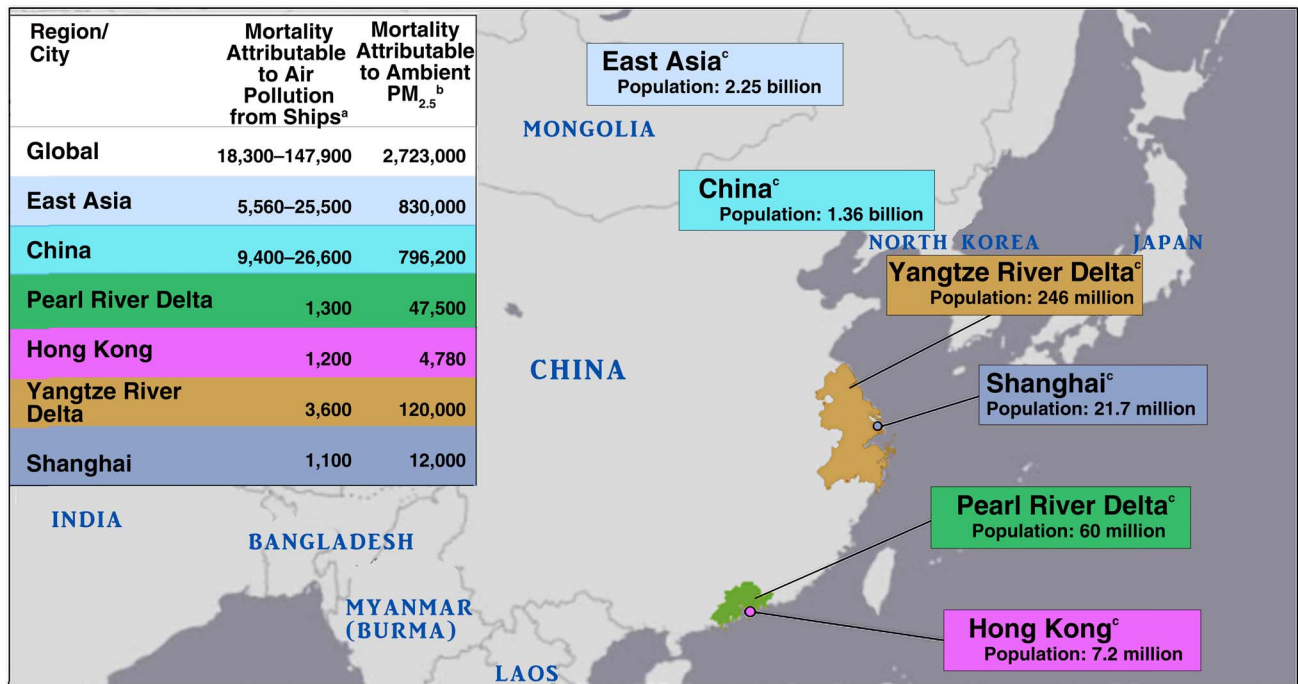
Region/ City	Mortality Attributable to Air Pollution from Ships[a]	Mortality Attributable to Ambient PM$_{2.5}$ [b]
Global	18,300–147,900	2,723,000
East Asia	5,560–25,500	830,000
China	9,400–26,600	796,200
Pearl River Delta	1,300	47,500
Hong Kong	1,200	4,780
Yangtze River Delta	3,600	120,000
Shanghai	1,100	12,000

East Asia[c]
Population: 2.25 billion

China[c]
Population: 1.36 billion

Yangtze River Delta[c]
Population: 246 million

Shanghai[c]
Population: 21.7 million

Pearl River Delta[c]
Population: 60 million

Hong Kong[c]
Population: 7.2 million

Figure 6-1. Mean estimated mortality attributable to exposure to air pollution from ships and all sources, including the results from this study.[a,b,c]

[a] **Sources of mortality attributable to air pollution from ships:** *Global:* PM$_{2.5}$ in 2012 (Corbett et al. 2007; Winebrake et al. 2009), and PM$_{2.5}$ and O$_3$ in 2010 (Partanen et al. 2013); *East Asia*: PM$_{2.5}$ in 2005 (Corbett et al. 2007) and 2008 (Liu et al. 2016); *China*: PM$_{2.5}$ and O$_3$ in 2008 (Liu et al. 2016); *Pearl River Delta*: combination of SO$_2$, NO$_2$, PM$_{10}$, and O$_3$ in 2008 (Lai et al. 2013); *Hong Kong*: combination of SO$_2$, NO$_2$, PM$_{10}$, and O$_3$ in 2008 (Lai et al. 2013); *Yangtze River Delta and Shanghai*: PM$_{2.5}$ in 2015 (current study). The reported values contain the full range of uncertainty reported across the studies in each category.
[b] **Sources of mortality attributable to ambient PM$_{2.5}$ in 2013:** *Global, East Asia,* and *China* (Health Effects Institute 2019); *Pearl River Delta* (Wu et al. 2019); and *Hong Kong* and *Shanghai* (GBD MAPS Working Group 2016). **Sources of mortality attributable to ambient PM$_{2.5}$ in 2015:** *Yangtze River Delta* (Maji et al. 2018).
[c] **Sources of population data in 2013:** *East Asia* (World Bank 2019); *China, Pearl River Delta,* and *Hong Kong* (National Bureau of Statistics of China 2014). **Sources of population data in 2015:** *Yangtze River Delta* and *Shanghai* (Bright et al. 2016).

sources have been the subject of intensive examination in other studies, particularly near the port of Los Angeles in California, United States, they have not been studied carefully in China. In assessing the role of ship emissions, our analysis further distinguished between emissions from ocean-going and coastal vessels that enter inland waterways and operate at different distances from shore. The analysis points to the greater contributions of ships to emissions, air quality, and health relative to cargo transport or in-port machinery (Table 5-6). More specifically, the analysis identifies a larger contribution to health burden when ships enter inland waters, in closer proximity to population centers. We acknowledge that our definition of inland-water ships differs from other regulatory classification schemes or jurisdictional boundaries, so our results need to be interpreted in that context. We defined inland-water ships and their emissions geographically;

that is, to include emissions from any ships traveling to the west of a line at the mouth of the Yangtze and Huangpo rivers (Figure 4-1). Consequently, we were capturing emissions from ships that travel between the rivers and the ocean, so the same ship might be classified as coastal when traveling between ports and inland water when it enters the inner harbor. Large international ships may therefore contribute to the emissions that we classify as inland-water ships. Also, although we did assign emissions to individual ships based on their operating mode (i.e., hoteling at berth, maneuvering in-port, or cruising) we did not separately analyze at-berth versus moving ships, although this may be an important distinction when estimating contributions to emissions (Zhang et al. 2019b). Therefore, it is important to interpret our results as indicating the relative importance of the proximity of the emissions to population centers, rather than strictly to the

class or operating mode of a vessel along with its associated fuel and emissions regulations.

Our estimates of the contributions of container-cargo trucks were lower than those estimated previously for several reasons. First, our emissions inventory of trucks provided by the Shanghai Urban-Rural Construction and Transportation Development Research Institute only included container-cargo trucks that were associated with the Shanghai ports; therefore, our estimates of emissions and impacts from cargo transport by road only include about 28% of cargo transport in Shanghai. Second, the institute assumed zero sulfur in the fuel used by trucks because diesel fuel has minimal sulfur content when compared with marine fuel.

Our findings for Shanghai echo our analysis of the relative contributions of ship emissions to total emissions at varying distances from shore for the YRD. We found that between about 48% and 75% of pollutant emissions from ships occurred within 12 NM of shore, depending on the pollutant, with over 90% within 96 NM. In June 2015, ship emissions within 12 NM contributed about 0.56 μg/m³ to average ambient $PM_{2.5}$ concentrations, representing about 75% of total contribution of ships out to 200 NM (Appendix C, Table C-2, available on the HEI website). The emission results are similar to those of Lv and colleagues (2018) who reported that ship emissions within 12 NM of shore contributed 30% to 90% of the $PM_{2.5}$ from ship emissions within 200 NM. The relative importance of these contributions is further reflected in their impacts on average $PM_{2.5}$ concentrations in the YRD region.

6.1.3 Comparison with Other Sources and ECA Analyses

Compared with other major sources of air pollution in China generally, and in the YRD and Shanghai particularly, the percentage contributions of shipping to population-weighted $PM_{2.5}$ concentrations are relatively small. We estimated about 1.9% on average in the YRD domain and about 1.3% on average in Shanghai from ships, cargo transport, and port machinery (see Table 5-4). Percentages varied for the 16 core cities of the YRD depending on the particular mix of sources in the surrounding areas (Figure 5-6). Although we did not estimate percentage attributable mortality in this study, it tends to closely track the population-weighted exposures from which it is calculated.

These relative contributions of shipping to ambient and population-weighted $PM_{2.5}$ are not surprising given the importance of much larger emissions sources in the region (Figure 5-6). For example, a 2013 study of the major sources of air pollution in China estimated coal burning (industrial, power, and domestic) to be the largest contributor (34%) to annual average $PM_{2.5}$ concentrations in

Shanghai province; all transport (which did not include ship emissions at the time) contributed about 13% of the annual average $PM_{2.5}$ concentrations in Shanghai province (GBD MAPS Working Group 2016, Appendix Table V.1).

The estimated contributions of shipping to ambient $PM_{2.5}$ in the YRD were somewhat lower than those estimated by other studies. The 2009 application for the United States and Canada IMO ECA for SO_2, NO_2, and PM estimated that shipping contributed 5%–15% of national annual average $PM_{2.5}$ concentrations in 2002, which in the United States ranged between 5 and 12 μg/m³, or as little as 0.25 μg/m³ to 1.8 μg/m³ on average. As with this study, their analysis found strong geographical variability in shipping's contributions to $PM_{2.5}$ levels with the highest concentrations in major ports along the coasts. For example, they estimated that shipping contributed to greater than 3 μg/m³ in highly populated areas of Southern California and 1.5 μg/m³ in Louisiana and Florida. Their analyses projected that ship emissions off the U.S. and Canadian coasts, if unaddressed, would contribute up to 12,000 premature deaths, 4,300 cases of chronic bronchitis, 8,900 non-fatal heart attacks, 5,600 hospital admissions and emergency room visits in the year 2020, among other non-fatal impacts, in the United States alone (IMO Marine Environment Protection Committee 2009).

6.1.4 Future (2030) Health Impact of Emissions from Ships

We examined potential air quality and health benefits of controlling ship emissions for the YRD in 2030 under three alternative policy scenarios (Table 4-1). The scenario for current policies under business as usual was intended to examine the benefits of China's second DECA policies (DECA 2.0) as they were first proposed in July 2018 with fuel sulfur content limits of 0.1% sulfur during berthing and 0.5% sulfur while cruising. The 0.5% sulfur fuel requirement for cruising ships under this scenario is the same as the global IMO sulfur fuel content limit set to be implemented in 2020. However, to estimate the benefits of the China policy alone relative to the base year, we assumed that the sulfur fuel content outside of the 12 NM would remain the same as it was in 2015. Therefore, our current policy scenario may overestimate the independent impacts of current Chinese policies. The second policy scenario assumed stricter fuel sulfur content and NO_x controls than the current policy, but still extending only 12 NM from shore. The third policy scenario extended these stricter policies to 100 NM from shore; this policy scenario was more aspirational because implementation would require agreement of the IMO. Although our future policy scenarios only included changes in ship emissions, truck and port-machinery emissions are also expected to

decrease in the future because of upcoming low-sulfur fuel and electrification requirements.

We estimated that each of these policies could contribute to important reductions in the numbers of premature deaths attributable to shipping and related emissions in 2030. Relative to 2015, the current policies were projected to reduce the health burden by about half, for example to about 1,900 deaths from stroke, COPD, IHD, and lung cancer. The stricter and aspirational policies were projected to reduce mortality burden further to 1,400 and 830 deaths, respectively. Ships close to shore contributed more to $PM_{2.5}$ concentrations than those farther from shore, so most of the marginal benefit to air quality and health was obtained by stricter regulations close to shore. However, the aspirational scenario of 0.1% sulfur fuel within a 100 NM DECA would be even more effective in reducing $PM_{2.5}$ pollution and associated health impacts than maintaining the 12 NM DECA area.

The results of these future policy scenarios were intended to reflect the impacts of changing ship emissions control policies assuming constant population and age structure, relationship of ship activity to GDP, and meteorology. Therefore, we kept these parameters the same for each of the baseline and future policy scenario simulations. However, we do recognize that each of these assumptions may cause the simulations to be less representative of actual conditions in 2030 than they might otherwise be. For example, population growth (through both births and migration) and aging can contribute to increases in air pollution–attributable deaths, even as air pollution declines (Cohen et al. 2017). Similarly, the average age of the Chinese population is projected to increase over the next decade, increasing the number of people susceptible to air pollution related disease, so our estimates of the absolute numbers of deaths in the baseline and future years may be underestimated. In addition, the assumption that current trends in the relationships between ship activity and its relationship with regional GDP would remain the same could not be validated and was based on the best available data. Although these assumptions may be overly simplistic, they did allow for each scenario to only reflect the impacts of different policies related to ship emissions, a primary purpose of the study.

6.2 STRENGTHS AND LIMITATIONS

Our overall approach to assess the impacts of ship emissions on air quality and health was to use the best available data and methods at each stage so that the results would be as accurate as possible. At each step, we evaluated the robustness of the findings to key assumptions to characterize important uncertainties that might affect interpretation of the final results.

This analysis was grounded in detailed bottom-up emissions inventories at the local, regional, and national level. The inventories for the shipping and related sources were developed by, and in consultation with, local government agencies to ensure the relevance of baseline and future scenario assumptions for policy. To build these emissions inventories, we used the best available tracking data for large ships (i.e., AIS data). For the analysis of local sources in Shanghai, we supplemented the AIS data with local visa data for ships calling at river ports because smaller ships and those that travel solely on inland waterways are not required to have AIS installed, and even if those ships are equipped with AIS, the system is not always turned on.

However, we likely underestimated the impacts of military ships, which are not included, and fishing vessels, which are incompletely captured in the AIS dataset. For example, based on VECC's data, there are about 150,000 inland-water vessels and 4.6 million fishing vessels in China and few of these vessels have AIS installed or always turned on (Ministry of Ecology and Environment of China 2018). Inclusion of those ships would increase the total emissions, but we were unable to quantify the magnitude of their contributions because of the lack of data. Ultimately, our emissions inventories were broadly consistent with other ship emissions inventories developed for the YRD (Appendix B, Table B-1, available on the HEI website) and Shanghai (Appendix B, Table B-2) using similar methods (Chen et al. 2019; Liu et al. 2017; Lv et al. 2018).

However, our study was not designed to estimate the impact of ships missing from our inventory. It is well known that ships traveling outside of the major international shipping lanes, in particular those that are small enough not to require installation of AIS technology, may be substantially underestimated in shipping emissions inventories (e.g., Coello et al. 2015). Even when included, the emissions from smaller vessels (e.g., other than large cargo or passenger ships) are more uncertain as the emission rates for these vessels are less well studied and their operation modes and locations are less well tracked (Coello et al. 2015; Jafarzadeh et al. 2017; Zhang et al. 2018). There are indications that their contributions to exposure and health may also be important (Coello et al. 2015; McKuin and Campbell 2016).

For non-shipping emissions we relied on high resolution anthropogenic multiple-pollutant (SO_2, NO_x, $PM_{2.5}$, VOC, NH_3) emissions inventories for mainland China developed and refined by investigators at Tsinghua University for the period of 2005–2017 (Cai et al. 2017). These inventories were developed to quantify emissions

reductions associated with the Chinese government's air pollution control regulations during the 11th (2006–2010) and 12th (2011–2015) five-year plans, the Air Pollution Prevention and Control Action Plan (2013–2017), and the ongoing three-year Action Plan (2018–2020). The inventories have been extensively evaluated and compared with other inventories through comparison of their predictive performance in models against observations (Zhao et al. 2018; Zheng et al. 2019). More detailed regional inventories developed by the Shanghai Academy of Environmental Sciences were used for the YRD and Shanghai city domains.

We recognize that our predictions of future emissions in 2030, which used projected changes in ship traffic activities between 2013 and 2016 to extrapolate from 2015, did not include the IMO's policy requiring a maximum of 0.5% sulfur content for all ships starting in 2020. However, we estimate that had we taken the IMO's policy into consideration, future SO_2 and $PM_{2.5}$ emissions from shipping would be further reduced by 6%–18% and 2%–17%, respectively, and the annual average contributions of ship emissions to ambient SO_2 and $PM_{2.5}$ would be further reduced by 5%–8% and 2%–11% in 2030, respectively.

Another source of uncertainty in our emissions inventories is the rate of compliance with regulations. Although our analysis assumed 100% compliance with regulations, this assumption is almost certainly overly optimistic. For example, airborne monitoring campaigns conducted in Europe showed that about 7% of ships in the Danish waters were suspected of using non-compliant fuel in 2018 (Explicit ApS 2019), and the non-compliance rate was ~6% from 2015–2017 in Belgian waters (Van Roy 2018).

Air pollutant concentrations were modeled using the state-of-the-science WRF-CMAQ air quality modeling system. Our predicted ambient $PM_{2.5}$, SO_2, NO_2, and O_3 concentrations compared well with measurements made in the baseline year (Appendix E, Section 3). Although computer resource limitations prevented analysis of full-year data for some of the simulations and scenarios, we showed that the representative months we chose characterized the annual averages well.

Our estimated contributions of shipping to ambient $PM_{2.5}$ concentrations in the YRD region and Shanghai city in 2015 compared well with those of other studies (Figure 6-1). They fell within the range of the findings reported by Liu and colleagues (2017), but were a bit lower than Lv and colleagues (2018) and Chen and colleagues (2019), probably due to the differences in shipping emissions inventory and modeling uncertainties (see Appendix C, Tables C-1 and C-2). The relative contributions of ships to $PM_{2.5}$ concentrations in different seasons were consistent with

previous results (Lv et al. 2018). The fraction of ambient $PM_{2.5}$ concentrations attributable to ships ranged from 1%–6% across seasons, which fell into the range of 1%–15% reported by other studies (Contini et al. 2011; Kim and Hopke 2008; IMO Marine Environment Protection Committee 2009; Minguillón et al. 2008).

Finally, we worked with Chinese epidemiologists and atmospheric scientists from both academia and government to select studies and concentration–response functions that they considered to be most relevant for China. In the absence of sufficient evidence from Chinese cohort studies, the group recommended that the primary analysis rely on the GBD IERs for 2015 to estimate cause-specific mortality from long-term exposures to $PM_{2.5}$ (Cohen et al. 2017). However, the group also recommended that data from a recent Chinese study of air pollution be used as a sensitivity analysis (Yin et al. 2017); we ultimately used the GEMM functions, which include the Chinese study among others for this purpose (Burnett et al. 2018). For analysis of the impact of short-term exposures, we relied solely on Chinese studies for mortality (Chen et al. 2017b) and hospital admissions (Tian et al. 2019). The necessary Chinese mortality and hospitalization rates were obtained from the China CDC and local government sources.

The results of sensitivity analyses reflect ongoing scientific uncertainty about the true quantitative relationship between exposures to $PM_{2.5}$ and the risk of premature mortality, particularly at the higher levels of exposure observed in China and elsewhere. Use of the GEMM functions suggests that the estimates of mortality could be underestimated. These functions have the advantages that (1) unlike the GBD IERs, they are based solely on air pollution and health studies, and (2) they provide an estimate of all-cause mortality, which in many epidemiological studies is greater than the sum of cause-specific mortality. Nonetheless, GEMM functions continue to be debated in the scientific community.

We also note that because our study relied as much as possible on Chinese studies and health data our study does not include some of the cause-specific data on mortality and morbidity related to short-term exposures to air pollution that have been reported in other studies of shipping-related health impacts. For example, the North American ECA application projected impacts on chronic bronchitis, non-fatal heart attacks, days of work lost, and days with restricted activity related to both $PM_{2.5}$ and O_3 exposures. A study of the goods movement related to the Port of Long Beach in southern California estimated potential impacts of goods movement on childhood asthma (Perez et al. 2009). Sofiev and colleagues (2018) more recently included asthma in a global impact study of shipping,

using data from international studies. Both kinds of studies reflect a growing concern about the global contribution of $PM_{2.5}$ and NO_2 to increased emergency department visits and hospital admissions for asthma (Anenberg et al. 2018), a concern that should be considered for future studies in China.

6.3 OVERALL UNCERTAINTY

This discussion has identified a number of sources of uncertainty that may exist in the data, assumptions, and models used to characterize both air quality and health impacts in this study, uncertainties that are only partially reflected in the final results. The confidence intervals in the final health impacts, for example only reflect uncertainties in the concentration–response functions (an assumption of the BenMAP-CE model) and do not reflect uncertainties in the emissions inventories or $PM_{2.5}$ concentrations. We recognize that the contributions of ships and related sources to ambient and population-weighted $PM_{2.5}$ over the entire modeling domains were small, similar to the findings of other studies of this kind, and that they may be small relative to the uncertainties in emissions inventories and CMAQ models. For example, although we used the best available emissions inventories in China for non-shipping sources, we are aware that in evaluations, the normalized mean error in modeled $PM_{2.5}$ using the inventory relative to $PM_{2.5}$ measurements was 49%–64% and the Pearson's correlation coefficient was 0.50–0.68 in various cities in the Beijing–Tianjin–Hebei region (Zheng et al. 2019). In our own comparison of simulations with the measured concentrations of SO_2 and $PM_{2.5}$, we found normalized mean errors of 27.8%–49.15% for $PM_{2.5}$ and 26.5%–61.53% for SO_2 and Pearson's correlation coefficients of 0.47–0.78 for $PM_{2.5}$ and 0.61–8.87 for SO_2 in the 16 core cities of the YRD region (Appendix E and Feng et al. 2019).

Nonetheless, our fine-resolution simulations lead us to conclude that the impacts of shipping-related air pollution are not likely to be evenly distributed across the study domains. Our estimates of the contributions of shipping-related sources to ambient $PM_{2.5}$ were consistently higher closer to ports, shipping lanes, and rivers — often in more highly populated areas — than they were farther away. The simulated highly spatially resolved distributions of shipping-related air pollutant concentrations therefore increase our confidence in the overall results attributing increased exposures and health impacts to air pollution from shipping and its associated activities.

7.0 CONCLUSIONS AND RECOMMENDATIONS

This study provides a comprehensive and detailed spatial analysis of the impacts of shipping and related activities on air quality and the health of the populations of the city of Shanghai and the YRD region in a pre-DECA baseline year (2015) and under three future scenarios designed to inform decisions about the efficacy of alternative emissions control policies by 2030. It both corroborates other studies and provides additional scientific evidence relevant to several policy discussions for controlling future ship emissions and for improving air quality in China.

Both the baseline and future analyses showed the importance of controlling emissions from shipping and related activities close to population centers. The baseline analysis indicated that 60% of ship emissions in the YRD region occur within 12 NM of shore, the current demarcation for the DECA in China, but that 78% of SO_2 emissions from ships traveling within 200 NM are released within 96 NM of shore. Due to long distance transport and transformation of primary emissions to $PM_{2.5}$, the influence of these emissions on air quality and health extends far inland from the coastal cities. Further detailed evaluation of the relative contributions to air quality and health burden of inland ships, ships travelling into the inland waterways of Shanghai, reinforce the importance of controlling emissions that occur in close proximity to high-density population centers like Shanghai.

Consistent with these results, although our analysis of the full implementation of the currently proposed DECA requirements for 2030 did suggest substantial air quality and health benefits of compliance within 12 NM, the more aspirational policy scenario, which assumed more stringent fuel sulfur requirements out to 100 NM, found even greater potential health benefits. Assessment of the feasibility and costs of implementation of the different policy scenarios was beyond the scope of our analysis but such assessments would also be important factors in decisions about the most effective approaches to improving air quality and health in Shanghai and the YRD.

Limitations of our analysis could cause some of our estimates to be either over- or underestimated. Our analysis of the contributions of cargo-transport trucks and in-port activities (including ships at berth) to air quality was limited in a number of ways and may have underestimated the impacts both for the city of Shanghai and for the YRD. More data are needed to more completely identify and characterize these source contributions not only within Shanghai but throughout the YRD. At the same time, we assumed 100% compliance with existing and proposed regulations; given evidence that compliance can be poor,

the air quality and health benefits may be generally overstated. Consequently, regional and local compliance monitoring and enforcement are a critical component of any ongoing and future policies.

Confidence in the benefits of implementing and enforcing strong regulations will come from demonstrable improvements in air quality. See, for example, studies that have evaluated the effectiveness of ship emissions regulations measuring $PM_{2.5}$ concentrations at nearby air quality monitoring stations (e.g., Mason et al. 2019; Zhang et al. 2019a). As the estimated contributions of ships to $PM_{2.5}$ exposures are small in absolute and relative terms compared with other major sources of $PM_{2.5}$, it would be advisable to ensure ongoing monitoring of air pollution components that are more reliable indicators of ship emissions, such as V and Ni, in order to detect and evaluate the impact of any regulations. We recommend that such studies be done in Shanghai and the YRD to evaluate the effectiveness of the regulations at reducing air pollution over time.

REFERENCES

Agrawal A, Aldrete G, Anderson B, Pirveysian Z, Ray J. 2011. Port of Los Angeles air emissions inventory 2010[A]. ADP#050520-525. Los Angeles:Port of Los Angeles.

Agrawal H, Malloy QGJ, Welch WA, Wayne Miller J, Cocker DR. 2008a. In-use gaseous and particulate matter emissions from a modern ocean going container vessel. Atmos Environ 42:5504–5510; doi:10.1016/j.atmosenv.2008.02.053.

Agrawal H, Welch WA, Miller JW, Cockert DR. 2008b. Emission measurements from a crude oil tanker at sea. Environ Sci Technol 42:7098–7103.

Anenberg SC, Henze DK, Tinney V, Kinney PL, Raich W, Fann N. 2018. Estimates of the global burden of ambient $PM_{2.5}$, ozone, and NO_2 on asthma incidence and emergency room visits. Environ Health Perspect 126:107004; doi:10.1289/EHP3766.

Aulinger A, Matthias V, Zeretzke M, Bieser J, Quante M, Backes A. 2016. The impact of shipping emissions on air pollution in the greater North Sea region — Part 1: Current emissions and concentrations. Atmos Chem Phys 16:739–758; doi:10.5194/acp-16-739-2016.

Ault AP, Gaston CI, Wang Y, Dominguez G, Thiemens MH, Prather KA. 2010. Characterization of the single particle mixing state of individual ship plume events measured at the Port of Los Angeles. Environ Sci Technol 44:1954–1961; doi:10.1021/es902985h.

Ault AP, Moore MJ, Furutani H, Prather KA. 2009. Impact of emissions from the Los Angeles port region on San Diego air quality during regional transport events. Environ Sci Technol 43:3500–3506.

Brauer M, Amann M, Burnett RT, Cohen A, Dentener F, Ezzati M, et al. 2012. Exposure assessment for estimation of the global burden of disease attributable to outdoor air pollution. Environ Sci Technol 46:652–660; doi:10.1021/es2025752.

Bright E, Rose A, Urban M. 2016. Landscan 2015 high-resolution global population data set[R]. Oak Ridge, Tennessee, USA:Oak Ridge National Lab (ORNL).

Burnett R, Chen H, Szyszkowicz M, Fann N, Hubbell B, Pope CA, 3rd, et al. 2018. Global estimates of mortality associated with long-term exposure to outdoor fine particulate matter. Proc Natl Acad Sci USA 115:9592–9597; doi:10.1073/pnas.1803222115.

Cai S, Ma Q, Wang S, Zhao B, Brauer M, Cohen A, et al. 2018. Impact of air pollution control policies on future $PM_{2.5}$ concentrations and their source contributions in China. J Environ Manage 227:124–133; doi:10.1016/j.jenvman.2018.08.052.

Cai SY, Wang YJ, Zhao B, Wang SX, Chang X, Hao JM. 2017. The impact of the "Air Pollution Prevention and Control Action Plan" on $PM_{2.5}$ concentrations in Jing-Jin-Ji region during 2012–2020. Sci Tot Environ 580:197–209.

Chen D, Tian X, Lang J, Zhou Y, Li Y, Guo X, et al. 2019. The impact of ship emissions on $PM_{2.5}$ and the deposition of nitrogen and sulfur in Yangtze River Delta, China. Sci Tot Environ 649:1609–1619; doi:10.1016/j.scitotenv.2018.08.313.

Chen D, Wang X, Li Y, Lang J, Zhou Y, Guo X, et al. 2017a. High-spatiotemporal-resolution ship emission inventory of China based on AIS data in 2014. Sci Tot Environ 609:776–787; doi:10.1016/j.scitotenv.2017.07.051.

Chen R, Chu C, Tan J, Cao J, Song W, Xu X, et al. 2010. Ambient air pollution and hospital admission in Shanghai, China. J Hazard Mater 181:234–240; doi:10.1016/j.jhazmat.2010.05.002.

Chen R, Yin P, Meng X, Liu C, Wang L, Xu X, et al. 2017b. Fine particulate air pollution and daily mortality: A nationwide analysis in 272 Chinese cities. Am J Respir Crit Care Med 196:73–81; doi:10.1164/rccm.201609-1862OC.

China Carbon Emissions Trading Network. 2015. Three-Year Action Plan for Shanghai Green Port (2015–2017). Available: *www.tanpaifang.com/zhengcefagui/2015/111648960.html.*

China Classification Society. 2016. International Ship Record. Available: *http://csm.ccs.org.cn/busInformation/internationalShipsList#.*

China Classification Society. 2018. CCS Technical Notice No.57. Available: *www.nepia.com/media/965885/CCS-Technical-Notice-No57-Implementation-Marine-Air-Pollutant-Emissi.pdf* [accessed July 17, 2019].

Chinese Ministry of Transport. 2015. Ship and Port Pollution Prevention Special Action Plan (2015–2020). Available: *www.nepia.com/insights/industry-news/china-emission-control-areas-starupdatestar/.*

Coello J, Williams I, Hudson DA, Kemp S. 2015. An AIS-based approach to calculate atmospheric emissions from the UK fishing fleet. Atmos Environ 114:1–7; doi:10.1016/j.atmosenv.2015.05.011.

Cohen AJ, Brauer M, Burnett R, Anderson HR, Frostad J, Estep K, et al. 2017. Estimates and 25-year trends of the global burden of disease attributable to ambient air pollution: An analysis of data from the Global Burden of Diseases Study 2015. Lancet 389:1907–1918; doi:10.1016/S0140-6736(17)30505-6.

Contini D, Gambaro A, Belosi F, De Pieri S, Cairns WR, Donateo A, et al. 2011. The direct influence of ship traffic on atmospheric $PM_{2.5}$, PM_{10}, and PAH in Venice. J Environ Manage 92:2119–2129; doi:10.1016/j.jenvman.2011.01.016.

Cooper D, Gustafsson T. 2004. Methodology for calculating emissions from ships: 1. Update of emission factors. Swedish Methodology for Environmental Data (SMED). Norrköping, Sweden:Swedish Meteorological and Hydrological Institute.

Corbett JJ, Fischbeck P. 1997. Emissions from ships. Science 278:823–824.

Corbett JJ, Fischbeck PS. 2000. Emissions from waterborne commerce vessels in United States continental and inland waterways. Environ Sci Technol 34:3254–3260; doi:10.1021/es9911768.

Corbett JJ, Winebrake JJ, Green EH, Kasibhatla P, Eyring V, Lauer A. 2007. Mortality from ship emissions: A global assessment. Environ Sci Technol 41:8512–8518.

DieselNet. 2018a. IMO Marine Engine Regulations. Available: *www.dieselnet.com/standards/inter/imo.php* [accessed 3 June 2019].

DieselNet. 2018b. China: Fuels. Available: *www.dieselnet.com/standards/cn/fuel.php.*

DieselNet. 2019. China: Marine Engines. Available: *www.dieselnet.com/standards/cn/marine.php* [accessed June 3, 2019].

Eder BK, Yu S. 2006. A performance evaluation of the 2004 release of models-3 CMAQ. Atmos Environ 40:4811–4824; doi: 10.1016/j.atmosenv.2005.08.045.

European Maritime Safety Agency (EMSA). 2010. The 0.1% sulphur in fuel requirement as from 1 January 2015 in SECAs — An assessment of available impact studies and alternative means of compliance.

European Parliament. 2012. Directive 2012/33/EU of the European parliament and of the council of 21 November 2012 amending Council Directive 1999/32/EC as regards the sulphur content of marine fuels. Official Journal of the

European Union. Luxembourg:Publications Office of the European Union.

Explicit ApS. 2019. Airborne monitoring of sulphur emissions from ships in Danish waters. Environmental Project no. 2001.Copenhagen:Ministry of Environment and Food of Denmark Environmental Protection Agency

Fan Q, Zhang Y, Ma W, Ma H, Feng J, Yu Q, et al. 2016. Spatial and seasonal dynamics of ship emissions over the Yangtze River Delta and East China Sea and their potential environmental influence. Environ Sci Technol 50:1322–1329; doi:10.1021/acs.est.5b03965.

Feng J, Zhang Y, Li S, Mao J, Patton AP, Zhou Y, et al. 2019. The influence of spatiality on shipping emissions, air quality and potential human exposure in the Yangtze River Delta/Shanghai, China. Atmos Chem Phys 19:6167–6183; doi:10.5194/acp-19-6167-2019.

Fu ML, Ding Y, Ge YS, Yu LX, Yin H, Ye WT, et al. 2013. Real-world emissions of inland ships on the Grand Canal, China. Atmos Environ 81:222–229; doi:10.1016/j.atmosenv.2013.08.046.

Fu M, Liu H, Jin X, He K. 2017. National- to port-level inventories of shipping emissions in China. Environ Res Letters 12:114024; doi:10.1088/1748-9326/aa897a.

Fu Q, Shen Y, Zhang J. 2012. On the ship pollutant emission inventory in Shanghai port. J Safety Environ 12:57–64.

GBD 2017 Risk Factor Collaborators. 2018. Global, regional, and national comparative risk assessment of 84 behavioural, environmental and occupational, and metabolic risks or clusters of risks for 195 countries and territories, 1990–2017: A systematic analysis for the Global Burden of Disease Study 2017. Lancet 392:1923–1994; doi:10.1016/S0140-6736(18)32225-6.

GBD MAPS Working Group. 2016. Burden of disease attributable to coal-burning and other major sources of air pollution in China. Special Report 20. Boston, MA:Health Effects.

Giuliano G, O'Brien T. 2007. Reducing port-related truck emissions: The terminal gate appointment system at the ports of Los Angeles and Long Beach. Transport Res D - Transport and Environ 12:460–473; doi:10.1016/j.trd.2007.06.004.

Goldsworthy L, Goldsworthy B. 2015. Modelling of ship engine exhaust emissions in ports and extensive coastal waters based on terrestrial AIS data — An Australian case study. Environ Modelling & Software 63:45–60; doi:10.1016/j.envsoft.2014.09.009.

Harkins RW. 2007. Great Lakes marine air emissions — we're different up here! Marine Tech SNAME News 44:151–174.

Harrison RM, Jones AM, Lawrence RG. 2003. A pragmatic mass closure model for airborne particulate matter at urban background and roadside sites. Atmos Environ 37:4927–4933; doi:10.1016/j.atmosenv.2003.08.025.

Health Effects Institute. 2019. State of Global Air 2019. Boston, MA:Health Effects Institute.

Houston D, Li W, Wu J. 2014. Disparities in exposure to automobile and truck traffic and vehicle emissions near the Los Angeles–Long Beach port complex. Am J Public Health 104:156–164; doi:10.2105/ajph.2012.301120.

ICF International. 2009. Current methodologies in preparing mobile source port-related emission inventories: Final report. Available: *www.epa.gov/cleandiesel/documents/ports-emission-inv-april09.pdf.*

IHS Fairplay. 2015. Lloyd's Register of Ships. Redhill, UK:IHS Maritime.

IMO (International Maritime Organization). 2016. Marine Environment Protection Committee (MEPC), 70th session 24–28 October 2016. Available: *www.imo.org/en/Media-Centre/MeetingSummaries/MEPC/Pages/MEPC-70th-session.aspx.*

IMO (International Maritime Organization). 2017. Sulphur Oxides (SO_x) – Regulation 14. Available: *www.imo.org/en /OurWork/Environment/PollutionPrevention/AirPollution/Pages/Sulphuroxides(SOx)%E2%80%93Regulation 14.aspx* [accessed 23 March 2017].

IMO (International Maritime Organization). 2018. Nitrogen Oxides (NOx) – Regulation 13. Available: *www.imo.org/en/ourwork/environment/pollutionprevention/airpollution/pages/nitrogen-oxides-(nox)-%E2%80%93-regulation-13.aspx [accessed 11/26/2018].*

IMO (International Maritime Organization). 2019. Prevention of Air Pollution from Ships. Available: www.imo.org/en/OurWork/Environment/PollutionPrevention/AirPollution/Pages/Air-Pollution.aspx [accessed 17 My 2019].

IMO Marine Environment Protection Committee. 2009. Interpretations of, and amendments to, MARPOL and related instruments: Designation of an Emission Control

Area for nitrogen oxides, sulphur oxides and particulate matter.

IMO Marine Environment Protection Committee. 2014. Reduction of GHG Emissions from Ships Third IMO GHG Study 2014 — Final Report Note by the Secretariat, 67th session, Agenda item 6, MEPC 67/INF.3. Available: *www .imo.org/en/OurWork/*Environment/PollutionPrevention/ AirPollution/Documents/MEPC%2067-INF.3%20- %20Third%20IMO%20GHG%20Study%202014%20- %20Final%20Report%20(Secretariat).pdf.

Jafarzadeh S, Paltrinieri N, Utne IB, Ellingsen H. 2017. LNG-fuelled fishing vessels: A systems engineering approach. Transport Res D - Transport and Environ 50:202–222; doi:10.1016/j.trd.2016.10.032.

Johansson L, Jalkanen J-P, Kukkonen J. 2017. Global assessment of shipping emissions in 2015 on a high spatial and temporal resolution. Atmospheric Environment 167:403– 415; doi:10.1016/j.atmosenv.2017.08.042.

Keuken MP, Moerman M, Jonkers J, Hulskotte J, van der Gon H, Hoek G, et al. 2014. Impact of inland shipping emissions on elemental carbon concentrations near waterways in The Netherlands. Atmos Environ 95:1–9; doi:10.1016/j.atmosenv.2014.06.008.

Kim E, Hopke PK. 2008. Source characterization of ambient fine particles at multiple sites in the Seattle area. Atmos Environ 42:6047–6056; doi:10.1016/j.atmosenv .2008.03.032.

Kim J, Rahimi M, Newell J. 2012. Life-cycle emissions from port electrification: A case study of cargo handling tractors at the port of Los Angeles. Int J Sustainable Transport 6:321–337; doi:10.1080/15568318.2011.606353.

Kozawa KH, Fruin SA, Winer AM. 2009. Near-road air pollution impacts of goods movement in communities adjacent to the ports of Los Angeles and Long Beach. Atmos Environ 43:2960–2970; doi:10.1016/j.atmosenv .2009.02.042.

Lai HK, Tsang H, Chau J, Lee CH, McGhee SM, Hedley AJ, et al. 2013. Health impact assessment of marine emissions in Pearl River Delta region. Marine Pollution Bulletin 66:158–163; doi:10.1016/j.marpolbul.2012.09.029.

Li C, Yuan Z, Ou J, Fan X, Ye S, Xiao T, et al. 2016. An AIS-based high-resolution ship emission inventory and its uncertainty in Pearl River Delta region, China. Sci Tot Environ 573:1–10; doi:10.1016/j.scitotenv.2016.07.219.

Li M, Zhang D, Li C-T, Mulvaney KM, Selin NE, Karplus VJ. 2018a. Air quality co-benefits of carbon pricing in China. Nature Climate Change 8:398–403; doi:10 .1038/s41558-018-0139-4.

Li N, Lu Y, Liao H, He Q, Li J, Long X. 2018b. WRF-Chem modeling of particulate matter in the Yangtze River Delta region: Source apportionment and its sensitivity to emission changes. PloS One 13:e0208944; doi:10 .1371/journal.pone.0208944.

Liu H, Fu M, Jin X, Shang Y, Shindell D, Faluvegi G, et al. 2016. Health and climate impacts of ocean-going vessels in East Asia. Nature Climate Change 6:1037–1041; doi:10.1038/nclimate3083.

Liu H, Meng ZH, Shang Y, Lv ZF, Jin XX, Fu ML, et al. 2018. Shipping emission forecasts and cost–benefit analysis of China ports and key regions' control. Environ Pollut 236:49–59; doi:10.1016/j.envpol.2018.01.018.

Liu Z, Lu X, Feng J, Fan Q, Zhang Y, Yang X. 2017. Influence of ship emissions on urban air quality: A comprehensive study using highly time-resolved online measurements and numerical simulation in Shanghai. Environ Sci Technol 51:202–211; doi:10.1021/acs.est .6b03834.

Lv Z, Liu H, Ying Q, Fu M, Meng Z, Wang Y, et al. 2018. Impacts of shipping emissions on $PM_{2.5}$ pollution in China. Atmos Chem Phys 18:15811–15824; doi:10.5194/acp-18-15811-2018.

Maji KJ, Dikshit AK, Arora M, Deshpande A. 2018. Estimating premature mortality attributable to $PM_{2.5}$ exposure and benefit of air pollution control policies in China for 2020. Sci Tot Environ 612:683–693; doi:10.1016/j.scitotenv .2017.08.254.

Mason TG, Chan KP, Schooling CM, Sun S, Yang A, Yang Y, et al. 2019. Air quality changes after Hong Kong shipping emission policy: An accountability study. Chemosphere 226:616– 624; *https://doi.org/10.1016/j.chemosphere.2019.03.173.*

McKuin B, Campbell JE. 2016. Emissions and climate forcing from global and Arctic fishing vessels. J Geophysical Research-Atmospheres 121:1844–1858; doi:10.1002 /2015jd023747.

Minguillón MC, Arhami M, Schauer JJ, Sioutas C. 2008. Seasonal and spatial variations of sources of fine and quasi-ultrafine particulate matter in neighborhoods near the Los Angeles–Long Beach harbor. Atmos Environ 42:7317–7328; doi:10.1016/j.atmosenv.2008.07.036.

Ministry of Ecology and Environment of China. 2018. China Vehicle Environmental Management Annual Report [in Chinese].

Moldanová J, Fridell, E, Winnes H, Holminfridell S. 2013. Physical and chemical characterisation of PM emissions from two ships operating in European Emission Control Areas. Atmos Meas Tech 6:3577–3596; doi:10.5194/amt-6-3577-2013.

National Bureau of Statistics of China. 2014. China Statistical Yearbook—2014. Available: *www.stats.gov.cn/tjsj/ndsj/ 2014/indexeh.htm* [accessed 9/6/2019].

National Bureau of Statistics of China. 2019. China Statistical Yearbook. Available: *http://data.stats.gov.cn/.*

Ng SKW, Loh C, Lin CB, Booth V, Chan JWM, Yip ACK, et al. 2013. Policy change driven by an AIS-assisted marine emission inventory in Hong Kong and the Pearl River Delta. Atmos Environ 76:102–112; doi:10.1016/j.atmosenv .2012.07.070.

Nunes RAO, Alvim-Ferraz MCM, Martins FG, Sousa SIV. 2017. The activity-based methodology to assess ship emissions — A review. Environ Pollut 231:87–103; doi:10.1016/j.envpol.2017.07.099.

Partanen AI, Laakso A, Schmidt A, Kokkola H, Kuokkanen T, Pietikainen JP, et al. 2013. Climate and air quality trade-offs in altering ship fuel sulfur content. Atmos Chem Phys 13:12059–12071; doi:10.5194/acp-13-12059-2013.

Perez L, Kunzli N, Avol E, Hricko AM, Lurmann F, Nicholas E, et al. 2009. Global goods movement and the local burden of childhood asthma in southern California. Am J Public Health 99 Suppl 3:S622–628; doi:10.2105 /ajph.2008.154955.

Petzold A, Lauer P, Fritsche U, Hasselbach J, Lichtenstern M, Schlager H, et al. 2011. Operation of marine diesel engines on biogenic fuels: Modification of emissions and resulting climate effects. Environ Sci Technol 45:10394–10400; doi:10.1021/es2021439.

Sofiev M, Winebrake JJ, Johansson L, Carr EW, Prank M, Soares J, et al. 2018. Cleaner fuels for ships provide public health benefits with climate tradeoffs. Nat Commun 9:406; doi:10.1038/s41467-017-02774-9.

Starcrest Consulting Group. 2009. Port of Los Angeles Inventory of Air Emissions 2008, Technical Report Revision. Available: *www.portoflosangeles.org/environment / air-quality/air-emissions-inventory.*

State Council of the People's Republic of China. 2013. The Action Plan for Control and Prevention of Air Pollution. Available: *www.gov.cn/zwgk/2013-09/12/content_2486773 .htm* [accessed 10 Sep 2013].

Stohl A, Aamaas B, Amann M, Baker L, Bellouin N, Berntsen T, et al. 2015. Evaluating the climate and air quality impacts of short-lived pollutants. Atmos Chem Phys 15:10529–10566.

Sun X, Yan XP, Wu B, Song X. 2013. Analysis of the operational energy efficiency for inland river ships. Transport Res D - Transport Environ 22:34–39; doi:10.1016/j.trd .2013.03.002.

Tian Y, Liu H, Liang T, Xiang X, Li M, Juan J, et al. 2019. Fine particulate air pollution and adult hospital admissions in 200 Chinese cities: A time-series analysis. Int J Epidemiol 48:1142–1151; doi:10.1093/ije/dyz106.

UNCTAD (United Nations Conference on Trade and Development). 2018. Review of Maritime Transport 2018. Available: *https://unctad.org/en/PublicationsLibrary /rmt2018_en.pdf* [accessed July 30, 2019].

United Nations. 1982. UN Convention on the Law of the Sea, Article 19 and Article 21, 1(f).

U.S. EPA (U.S. Environmental Protection Agency). 2009. Integrated Science Assessment (ISA) for Particulate Matter. Washington, DC:U.S. Environmental Protection Agency.

U.S. EPA (U.S. Environmental Protection Agency). 2015. Environmental Benefits Mapping and Analysis Program: Community Edition (BenMAP-CE) User Manual and Appendices. Available: *www.epa.gov/benmap* [accessed August 30, 2018].

van der Zee SC, Dijkema MBA, van der Laan J, Hoek G. 2012. The impact of inland ships and recreational boats on measured NO_x and ultrafine particle concentrations along the waterways. Atmos Environ 55:368–376; doi:10 .1016/j.atmosenv.2012.03.055.

Van Roy W. 2018. Airborne MARPOL Annex VI monitoring Belgium Coast Guard aircraft. In: International Workshop on DECA Enforcement, May 3–4, 2018, Shenzhen; Available: *hnrdc.cn/information/information info?id=189&cook=1c.*

Wang H, Chen C, Huang C, Fu L. 2008. On-road vehicle emission inventory and its uncertainty analysis for Shanghai, China. Sci Tot Environ 398:60–67; doi:10 .1016/j.scitotenv.2008.01.038.

Wang J, Wang S, Voorhees AS, Zhao B, Jang C, Jiang J, et al. 2015. Assessment of short-term $PM_{2.5}$-related mortality due to different emission sources in the Yangtze River Delta, China. Atmos Environ 123:440–448; doi:10 .1016/j.atmosenv.2015.05.060.

Wang X, Shen Y, Lin Y, Pan J, Zhang Y, Louie PKK, et al. 2019. Atmospheric pollution from ships and its impact on local air quality at a port site in Shanghai. Atmos Chem Phys 19:6315–6330; doi:10.5194/acp-19-6315-2019.

WHO (World Health Organization). 2016. Ambient air pollution: A global assessment of exposure and burden of disease. Geneva, Switzerland:World Health Organization.

Winebrake JJ, Corbett JJ, Green EH, Lauer A, Eyring V. 2009. Mitigating the health impacts of pollution from oceangoing shipping: An assessment of low-sulfur fuel mandates. Environ Sci Technol 43:4776–4782.

World Bank. 2019. Population, total — East Asia & Pacific, China. Available: *https://data.worldbank.org/indicator/SP.POP.TOTL?end=2018&locations=Z4-CN&name_desc=false&start=1960&view=chart* [accessed 9/6/2019].

Yin J, Harrison RM. 2008. Pragmatic mass closure study for $PM_{1.0}$, $PM_{2.5}$, and PM_{10} at roadside, urban background and rural sites. Atmos Environ 42:980–988; doi:10.1016/j.atmosenv.2007.10.005.

Yin P, Brauer M, Cohen A, Burnett RT, Liu J, Liu Y, et al. 2017. Long-term fine particulate matter exposure and non-accidental and cause-specific mortality in a large national cohort of Chinese men. Environ Health Perspect 125:117002; doi:10.1289/ehp1673.

Zhang F, Chen Y, Chen Q, Feng Y, Shang Y, Yang X, et al. 2018. Real-world emission factors of gaseous and particulate pollutants from marine fishing boats and their total emissions in China. Environ Sci Technol; doi:10.1021/acs.est.7b04002.

Zhang X, Zhang Y, Liu Y, Zhao J, Zhou Y, Wang X, et al. 2019. Changes in SO_2 level and $PM_{2.5}$ components in Shanghai driven by implementing the Ship Emission Control Policy. Environ Sci Technol 53:11580–11587; doi:10.1021/acs.est.9b03315.

Zhang Y, Deng F, Man H, Fu M, Lv Z, Xiao Q, et al. 2019a. Compliance and port air quality features with respect to ship fuel switching regulation: A field observation campaign, SEISO-Bohai. Atmos Chem Phys 19:4899–4916; doi:10.5194/acp-19-4899-2019.

Zhang Y, Fung JCH, Chan JWM, Lau AKH. 2019b. The significance of incorporating unidentified vessels into AIS-based ship emission inventory. Atmos Environ 203:102–113; doi:10.1016/j.atmosenv.2018.12.055.

Zhang Y, Yang X, Brown R, Yang L, Morawska L, Ristovski Z, et al. 2017. Shipping emissions and their impacts on air quality in China. Sci Tot Environ 581–582:186–198; doi:10.1016/j.scitotenv.2016.12.098.

Zhao B, Zheng H, Wang S, Smith KR, Lu X, Aunan K, et al. 2018. Change in household fuels dominates the decrease in $PM_{2.5}$ exposure and premature mortality in China in 2005–2015. Proc Natl Acad Sci U S A 115:12401–12406; doi:10.1073/pnas.1812955115.

Zhao M, Zhang Y, Ma W, Fu Q, Yang X, Li C, et al. 2013. Characteristics and ship traffic source identification of air pollutants in China's largest port. Atmos Environ 64:277–286; doi:10.1016/j.atmosenv.2012.10.007.

Zheng H, Cai S, Wang S, Zhao B, Chang X, Hao J. 2019. Development of a unit-based industrial emission inventory in the Beijing–Tianjin–Hebei region and resulting improvement in air quality modeling. Atmos Chem Phys 19:3447–3462; doi:10.5194/acp-19-3447-2019.

MATERIALS AVAILABLE ON THE HEI WEBSITE

Appendices A through F and the Additional Materials contain supplemental material. They are available on the HEI website at *www.healtheffects.org/publications.*

Appendix A. Methods

Appendix B. Emissions Results

Appendix C. Air Quality Results

Appendix D. Health Analysis Results

Appendix E. Evaluation Results

Appendix F. 2030 Results

Additional Materials. China Workshop on Concentration–Response Functions, Tsinghua University, School of Environment, 1 December 2017

ABOUT THE AUTHORS

Yan Zhang received her Ph.D. in environmental science and engineering from Fudan University, where she is currently an associate professor in the Institute of Atmospheric Sciences. Her research interests include numerical simulation of meteorology and air quality and analysis of atmospheric pollution sources.

Junlan Feng received her M.S. in environmental sciences at Fudan University. Feng was an M.S. student during this study.

Cong Liu received his B.S. from Fudan University, where he is currently a Ph.D. student in the Department of Environmental Health.

Junri Zhao received his M.S. degree in environmental science at the China University of Mining and Technology. He is currently a Ph.D. student in the Department of Environmental Science and Engineering at Fudan University.

Weichun Ma received his Ph.D. in geographic science from East China Normal University. He is currently a full professor in the Department of Environmental Science & Engineering at Fudan University.

Cheng Huang received his Ph.D. from Tongji University. He is currently the director of the Atmospheric Environment department at the Shanghai Academy of Environmental Science.

Jingyu An received his M.S. degree from Donghua University. He is currently an engineer in the Atmospheric Environment department at the Shanghai Academy of Environmental Science.

Yin Shen received his M.S. degree from Tongji University. He is currently an engineer in the Vehicle Pollution Monitoring Department at the Shanghai Environmental Monitoring Center.

Qingyan Fu received her Ph.D from Fudan University. She is currently a director of the Atmospheric Environment Department at the Shanghai Environmental Monitoring Center.

Shuxiao Wang received her Ph.D. in environmental engineering from Tsinghua University. She is currently a distinguished professor in the Department of Environmental Engineering at Tsinghua University.

Dian Ding received her M.S. in environmental engineering from South China University of Technology. She is currently a Ph.D. student in the Division of Air Pollution Control in the School of Environment at Tsinghua University.

Wangqi Ge received his M.S. degree from Northwest University. He was an engineer at the Shanghai Urban-Rural Construction and Transportation Development Research Institute during this study. He currently works in the Urban Development Department at the Shanghai Municipal Development and Reform Commission.

Freda Fung received her master's in environmental policy and management from Lund University and an M.Phil. in economics from the Chinese University of Hong Kong. She is currently a consultant researcher at the Natural Resources Defense Council.

Kethural Manokaran received her B.A. in neuroscience and South Asian studies from Wellesley College. At the time of the study, Manokaran was a research assistant at the Health Effects Institute. She is currently pursuing graduate studies in biology and public health.

Allison P. Patton received her Ph.D. in environmental engineering from Tufts University. She is currently a staff scientist at the Health Effects Institute.

Katherine D. Walker received her Sc.D. in environmental health sciences/biostatistics and decisions sciences from the Harvard School of Public Health. She is currently a principal scientist at the Health Effects Institute.

Haidong Kan received his Ph.D. in environmental epidemiology from Fudan University. He is currently a distinguished professor of environmental health sciences in the School of Public Health at Fudan University.

OTHER PUBLICATIONS RESULTING FROM THIS RESEARCH

Feng J, Zhang Y, Li S, Mao J, Patton AP, Zhou Y, et al. 2019. The influence of spatiality on shipping emissions, air quality and potential human exposure in the Yangtze River Delta/Shanghai, China. Atmos Chem Phys 19:6167–6183; 10.5194/acp-19-6167-2019.

ABBREVIATIONS AND OTHER TERMS

AIS	Automatic Identification System
BenMAP-CE	Environmental Benefits Mapping and Analysis Program-Community Edition (software)
China CDC	China Center for Disease Control
CMAQ	Community Multiscale Air Quality (model)
CNG	compressed natural gas
CO	carbon monoxide
COPD	chronic obstructive pulmonary disease
DECA	domestic emissions control area (China)
DPM	diesel particulate matter
EC	elemental carbon
ECA	emission control areas
GBD MAPS	Global Burden of Disease from Major Air Pollution Sources (initiative)
GDP	gross domestic product
GEMM	Global Exposure Mortality Model
ICD-10	International Classification of Diseases codes, 10th version
IER	integrated exposure response
IHD	ischemic heart disease
IIASA	International Institute for Applied Systems Analysis
IMO	International Maritime Organization
INV	International Vehicle Emission
LNG	liquefied natural gas
MARPOL	International Convention for the Prevention of Pollution from Ships
NH_3	ammonia
Ni	nickel

NM	nautical miles
NMB	normalized mean bias
NME	normalized mean error
NMVOCs	non-methane volatile organic compounds
NO_2	nitrogen dioxide
NO_x	nitrogen oxides
NRDC	Natural Resources Defense Council
O_3	ozone
OC	organic carbon
PM	particulate matter
PM_{10}	particulate matter ≤ 10 µm in aerodynamic diameter
$PM_{2.5}$	particulate matter ≤ 2.5 µm in aerodynamic diameter
RMSE	root mean-square error
SAES	Shanghai Academy of Environmental Sciences
SEMC	Shanghai Environmental Monitoring Center
SO_2	sulfur dioxide
SO_x	sulfur oxide
UNCTAD	United Nations Conference on Trade and Development
U.S. EPA	U.S. Environmental Protection Agency
V	vanadium
WRF-CMAQ	Weather Research and Forecasting–Community Multiscale Air Quality modeling system
VECC	Vehicle Emission Control Center (China)
VOCs	volatile organic compounds
WHO	World Health Organization
YRD	Yangtze River Delta

RELATED HEI PUBLICATIONS

Number	Title	Principal Investigator	Date

Research Reports

199	Real-World Vehicle Emissions Characterization for the Shing Mun Tunnel in Hong Kong and Fort McHenry Tunnel in the United States	X.L.Wang	2019
195	Impacts of Regulations on Air Quality and Emergency Department Visits in the Atlanta Metropolitan Area, 1999–2013	A.G. Russell	2018
194	A Dynamic Three-Dimensional Air Pollution Exposure Model for Hong Kong	B. Barratt	2018
190	The Effects of Policy-Driven Air Quality Improvements on Children's Respiratory Health	F. Gilliland	2017
189	Ambient Air Pollution and Adverse Pregnancy Outcomes in Wuhan, China	Z. Qian	2016
154	Public Health and Air Pollution in Asia (PAPA): Coordinated Studies of Short-Term Exposure to Air Pollution and Daily Mortality in Four Cities	HEI Public Health and Air Pollution in Asia Program	2010

Special Reports

21	Burden of Disease Attributable to Major Air Pollution Sources in India	GBD MAPS Working Group	2018
20	Burden of Disease Attributable to Coal-Burning and Other Air Pollution Sources in China	GBD MAPS Working Group	2016
18	Outdoor Air Pollution and Health in the Developing Countries of Asia: A Comprehensive Review	Health Effects Institute	2010

HEI Website

	State of Global Air (report and website; *www.stateofglobalair.org*)	Health Effects Institute	Updated annually

Copies of these reports can be obtained from HEI; PDFs are available for free downloading at www.healtheffects.org/publications.

HEI BOARD, COMMITTEES, and STAFF

Board of Directors

Richard F. Celeste, Chair *President Emeritus, Colorado College*

Enriqueta Bond *President Emerita, Burroughs Wellcome Fund*

Jo Ivey Boufford *President, International Society for Urban Health*

Homer Boushey *Emeritus Professor of Medicine, University of California, San Francisco*

Michael T. Clegg *Professor of Biological Sciences, University of California, Irvine*

Jared L. Cohon *President Emeritus and Professor, Civil and Environmental Engineering and Engineering and Public Policy, Carnegie Mellon University*

Stephen Corman *President, Corman Enterprises*

Martha J. Crawford *Dean, Jack Welch College of Business and Technology, Sacred Heart University*

Michael J. Klag *Dean Emeritus and Second Century Distinguished Professor, Johns Hopkins Bloomberg School of Public Health*

Alan I. Leshner *CEO Emeritus, American Association for the Advancement of Science*

Henry Schacht *Managing Director, Warburg Pincus; Former Chairman and Chief Executive Officer, Lucent Technologies*

Research Committee

David A. Savitz, Chair *Professor of Epidemiology, School of Public Health, and Professor of Obstetrics and Gynecology, Alpert Medical School, Brown University*

Jeffrey R. Brook *Senior Research Scientist, Air Quality Research Division, Environment Canada, and Assistant Professor, University of Toronto, Canada*

Francesca Dominici *Professor of Biostatistics and Senior Associate Dean for Research, Harvard T.H. Chan School of Public Health*

David E. Foster *Phil and Jean Myers Professor Emeritus, Department of Mechanical Engineering, Engine Research Center, University of Wisconsin, Madison*

Amy H. Herring *Sara & Charles Ayres Professor of Statistical Science and Global Health, Duke University, Durham, North Carolina*

Barbara Hoffmann *Professor of Environmental Epidemiology, Institute of Occupational, Social, and Environmental Medicine, University of Düsseldorf, Germany*

Allen L. Robinson *Raymond J. Lane Distinguished Professor and Head, Department of Mechanical Engineering, and Professor, Department of Engineering and Public Policy, Carnegie Mellon University*

Ivan Rusyn *Professor, Department of Veterinary Integrative Biosciences, Texas A&M University*

Review Committee

James A. Merchant, Chair *Professor and Founding Dean Emeritus, College of Public Health, University of Iowa*

Kiros Berhane *Professor of Biostatistics and Director of Graduate Programs in Biostatistics and Epidemiology, Department of Preventive Medicine, Keck School of Medicine, University of Southern California*

Michael Jerrett *Professor and Chair, Department of Environmental Health Sciences, Fielding School of Public Health, University of California, Los Angeles*

Frank Kelly *Professor of Environmental Health and Director of the Environmental Research Group, King's College London*

Jana B. Milford *Professor, Department of Mechanical Engineering and Environmental Engineering Program, University of Colorado, Boulder*

Jennifer L. Peel *Professor of Epidemiology, Colorado School of Public Health and Department of Environmental and Radiological Health Sciences, Colorado State University*

Roger D. Peng *Professor of Biostatistics, Johns Hopkins Bloomberg School of Public Health*

HEALTH EFFECTS INSTITUTE

75 Federal Street, Suite 1400
Boston, MA 02110, USA
+1-617-488-2300
www.healtheffects.org

SPECIAL REPORT 22

December 2019